Electronic Theses and Dissertations   Theses, Dissertations, and Major Papers

Winter 2014

Dent behaviour of steel pipes under pressure load

Jandark Oshana Jajo
University of Windsor

Dent Behaviour of Steel Pipes under Pressure Load

By

Jandark Oshana Jajo

A Thesis

Submitted to the Faculty of Graduate Studies

through the Department of Civil and Environmental Engineering

in Partial Fulfillment of the Requirements for

the Degree of Master of Applied Science

at the University of Windsor

Windsor, Ontario, Canada

2013

Canadä

Dent Behaviour of Steel Pipes under Pressure Load

by

Jandark Oshana Jajo

APPROVED BY:

_____

Dr. N. Kar, External Reader

Department of Electrical and Computer Engineering

_____

Dr. M. Madugula, Internal Reader

Department of Civil and Environmental Engineering

_____

Dr. S. Das, Advisor

Department of Civil and Environmental Engineering

December 16th 2013

DECLARATION OF ORIGINALITY

I hereby certify that I am the sole author of this thesis and that no part of this thesis has been published or submitted for publication.

I certify that, to the best of my knowledge, my thesis does not infringe upon anyone's copyright nor violate any proprietary rights and that any ideas, techniques, quotations, or any other material from the work of other people included in my thesis, published or otherwise, are fully acknowledged in accordance with the standard referencing practices. Furthermore, to the extent that I have included copyrighted material that surpasses the bounds of fair dealing within the meaning of the Canada Copyright Act, I certify that I have obtained a written permission from the copyright owner(s) to include such material(s) in my thesis and have included copies of such copyright clearances to my appendix.

I declare that this is a true copy of my thesis, including any final revisions, as approved by my thesis committee and the Graduate Studies office, and that this thesis has not been submitted for a higher degree to any other University or Institution.

ABSTRACT

Formation of dent defects in steel pipelines is not uncommon. A dent is a plastic deformation causing strains in the pipe wall which can be a threat to the structural integrity of the pipeline. This study investigated the effect of dent shapes, dent depths, and internal pressures on the strain distribution of the pipe. The work was completed using full-scale tests and numerical method. The study found that as the D/t ratio and the pressure increases so does the maximum strain around the dent. The study found that the location of the maximum strain value does not change with D/t ratio or internal pressure for rectangular dents. The maximum strain occurs at 125 mm away from the dent centre and at the dent centre for the longitudinal and circumferential axes, respectively. For spherical dent the location of the maximum strain in the longitudinal and circumferential axes differs for different pressures.

DEDICATION

I dedicate this thesis first to our Lord and saviour Jesus Christ, and second to all the people that surrounded me throughout my journey including my beloved Christopher Cvetkovski and my loving parents and sisters.

ACKNOWLEDGEMENTS

I would like to sincerely acknowledge my advisor, Dr. Sreekanta Das. His suggestions and continuous support have helped me through my journey.

I would like to acknowledge all my colleagues in Dr. Das' research group especially Hossein Ghaednia and c Zohreh for their continuous help and guidance.

I would like to thank the lab technicians Matt St. Louis and Lucian Pop for aiding me in all the experimental tests that had to be performed in this study.

I would also like to acknowledge my friends and family for all their love and support.

TABLE OF CONTENTS

LIST OF TABLES

LIST OF FIGURES

CHAPTER 1

1.0 INTRODUCTION

1.1 Overview

Steel pipelines are used for the transportation of oil and gas across the nation. Most of these pipelines lie underground, which in turn creates a greater risk for the creation of damages. Because they are underground it is much more difficult to detect any damage existent in the pipeline. If damage exists, it has the capacity to affect the structural integrity of the pipes. This in turn can cause safety and environmental disasters as well as cause operational setbacks. The damages can be due to mechanical damages or construction damages (Cosham and Hopkins 2004).

Mechanical damages are caused from the impact of construction equipment that hits the underground pipes. These impacts can cause dents in the pipeline to form. A dent is an inward plastic deformation in the cross-section of the pipe. Such a deformation causes residual stresses to exist in the deformed pipeline (Cosham and Hopkins 2004).

Construction damages are those that occur when placing the pipeline in the field. They occur due to the fact that the ground has rocks and inconsistencies which can cause the formation of dents to occur in the pipeline. Furthermore, when a pipeline rests on top of a rock, dent can also form. If the rock remains in its position the dent is called a constrained dent. Constrained dents are those that are not free to re-round back after the dent has been formed. However, if the rock is removed after such dent has been found, this type of dent is called unconstrained dent as the dented area can now re-round back as the internal pressure is pushing it outwards.

There are different types of dents that can form in the surface of a pipeline. A dent can be accompanied by additional damages such as gouges or cracks. These dents can cause the pipe to fail before reaching its service life (Rosenfeld 2001). The focus of the study by Rosenfeld (2001) was plain dents. Plain dents are smooth dents having no gouges, cracks, or other inconsistencies in its dented surface. These types of dents are much less dangerous than the previously mentioned, however, they can still cause problems in the long-term due to the fluctuating pressure which can cause fatigue cycling, or from the development of corrosion as well as similar problems (Baker 2004a). Additionally, it was also determined from analytical models for unconstrained dents that the fatigue life of the pipe decreases as the initial dent depth is higher (Alexander and Kiefner 1997). Moreover, the fatigue life also decreases with an increasing D/t ratio, with D being the outer diameter of the pipeline and t being the thickness of the pipe wall, (Fowler 1993).

Furthermore, other studies were carried out in order to determine the burst strength of a pipe containing a plain dent. It was determined by different researchers that the burst strength of a pipeline with a plain dent is not greatly reduced as compared to the burst strength of a dent containing a gouge (Cosham and Hopkins 2001).

1.2 Problem Statement

Dent can cause serious structural integrity problems for field pipelines leading to economic and environmental damages. In order to avoid such problems, it is necessary to determine more efficient and improved ways of determining the safety of a linepipe with dent defect. Dent depth is one of the most studied parameters; however, the dent shape, D/t ratio, and strain distributions around the dented area are also important parameters that also need to be considered to find improved methods for the assessment of the dent severity.

Hence the current study looked into the strain distributions at and near the dented region of a pipeline. Different parameters such as the dent shape, dent depth, D/t ratio, and

internal pressure after denting were considered in this study. The study was completed using full-scale tests and finite element models on dented pipes.

1.3 Objective of the Study

The main objective of this study was to better understand and predict the behaviour of pipelines that are subjected to a plain dent by determining the strains and their locations in and around dent. Monotonically increasing pressure was applied on the dented pipe to determine the strains in and around the dents. The parameters that were considered are the strain distribution around the dented area, the different dent shapes, and the position and location of the maximum strain value for the different types of indenters, internal pressures, and D/t ratios. A specific objective of this work is to create a Finite Element Model (FEM) based on experimental verification and validation. Second, to determine the value and location of the maximum strains in and around the dented region of a pipe for different dent shapes. Third, to develop a parametric study to determine the effect of the D/t ratio, the dent shape, and the internal pressure have on the maximum strain value and location. Lastly, to determine the

1.4 Layout of Thesis

This thesis is divided into seven chapters. The first chapter is the introduction, the second chapter deals with the literature review that was conducted for the purpose of reviewing other similar works as well as determining what is necessary to continue to research. The third chapter looks into the experimental test procedure. This chapter details all the specimens used, their material properties, the parameters, and the methods of testing the pipes as well as the equipment used. Chapter four describes in detail all the experimental tests results obtained for the pipes tested. Chapter five describes the Finite Element Modeling technique used to develop the numerical tool. Chapter six deals with the validation of the FE models and results of the parametric study involving the dent shape, D/t ratio, and internal pressure. Lastly, chapter seven concludes all the findings of this study and recommendations on future research.

CHAPTER 2

2.0 LITERATURE REVIEW

2.1 Research Background

Various studies using different methodologies related to dents in pressurized pipelines were undertaken to understand and assess the severity of such pipelines. Pipelines carrying oil and gas can be subjected to failure due to mechanical damages, natural disasters, as well as corrosion (Ong et al. 1992). Mechanical damages such as dents that occur due to earthmoving equipment striking the pipeline can be in the form of dents along with gouges (Rosenfeld 2002). Other forms of dent damage that arise are those that occur during construction of the pipeline. These damages appear in the form of plain dents along the bottom half of the pipe (Rosenfeld 2002). Dents can also form in buried pipelines if the pipe rests on a rock or sharp hard surface. These failures can be environmentally and economically detrimental. In most studies, mechanical damages in the form of dents were studied and analyzed through the use of experimental and or analytical studies as well as Finite Element method based on numerical study. Dent defect can lead to a leak or rupture in the line pipes. These studies as well as existing standards and codes use the dent depth as the main leading parameter for the determination of pipeline safety (Rosenfeld 2002). Furthermore, other studies used the strain level as another important criterion for the evaluation of the severity of dents (Lancaster and Palmer 1996; Rafi et al. 2012). As discussed in the following chapters, evaluation of the severity of dents requires an understanding of the dent behaviour.

2.2 Dent Overview

A dent in a pipeline is usually defined as the permanent inward indentation or plastic deformation of the cross-section of the pipe, causing distortion to the pipeline cross-

section. This permanent deformation causes residual (locked-in) stresses to remain in the deformed pipeline. The dent depth is measured as the maximum reduction in the pipe's diameter as compared to its original diameter (Cosham and Hopkins 2004). Figure 2.1 shows both a dent in a pipeline as well its dent depth, H.

Buried linepipe develops different types of damages, however only a few of these are discussed in this chapter.

2.2.1 General Defects

Buried linepipe can develop various defects as follows:

- Gouges: Surface damages caused by external object which removes material from the pipe wall and hence surface metal loss occurs (Cosham and Hopkins 2004).
- Cracks: A material discontinuity in which the surfaces are located very closely to each other and the surfaces end in sharp tip (El Sayed 2013).
- Corrosion: Deterioration of the material due to chemical or electrochemical action.
- Wrinkles: A localized deformation of the pipe wall that is frequently characterized by a main outward bulge (Baker 2004).
- Dent: A permanent plastic inward deformation of the cross-section of a linepipe as discussed next. Dents can be further classified into smooth dent, kinked dent, and plain dent.

2.2.2 Dent Defects

- Smooth dent: A dent causing smooth changes on the pipe wall's curvature.
- Kinked dent: A dent with a sharp change in the wall of the pipe.

- Plain dent: A smooth dent having no gouges or cracks or other defect in the dent. It can be either smooth dent or kinked dent depending on dents curvature pattern

This research focuses on the study of plain dent on steel oil and gas pipelines and hence, the literature review is mainly focused on such dent defect.

2.3 Strains in Dents

In previous studies, the strains in dented pipelines was determined in two ways: when dent was being formed and when the dented pipe was being pressurized. The severity of dent can be obtained by determining the strain level of the dent. Strains in the dented region of the pipe can be obtained either numerically using finite element (FE) method or using experimental method. Determining strain values using FE method requires the solution of large plastic deformation shell with large number of nodes (Lukasiewicz et al. 2006). A comparison between the results obtained from the finite element analysis (FEA) and the experimental or analytical results is usually carried out to validate the numerical (FE) model.

2.3.1 Strains after dent formation

Strains formed after the formation of a dent were widely studied by many (Lancaster and Palmer 1996; Ong et al. 1992; Keating and Hoffmann 1997). Most of the studies discussed different methods for calculation of strains in dented pipelines (Rosenfeld et al. 1998). The work by Rosenfeld et al. focused on obtaining the signal from inline inspection tools so that the residual strain due to the indentation of the pipe can be determined. The study determined that there are three different strain components in order to accurately assess the severity of the dent. These components are the longitudinal bending strain, membrane strain, and circumferential bending strains. Once all three strain components were obtained, it was assumed that the strain components occur at the

dent apex which may not be correct and Equations 2.1 and 2.2 were combined to determine the net strain on the outer and inner diameter surfaces.

$$\varepsilon_i = \sqrt{\varepsilon_{ci}^2 - \varepsilon_{ci}\varepsilon_{xi} + \varepsilon_{xi}^2} \tag{2.1}$$

$$\varepsilon_o = \sqrt{\varepsilon_{co}^2 - \varepsilon_{co}\varepsilon_{xo} + \varepsilon_{xo}^2} \tag{2.2}$$

Where ε_i and ε_o are the net strains on inner and outer surface, respectively; ε_{ci} and ε_{co} are net circumferential strains on the inner and outer surfaces, respectively; and ε_{xi} and ε_{xo} are the net longitudinal strains at the inner and outer surfaces, respectively (Rosenfeld et al. 1998).

Furthermore, Noronha et al. (2010) presented a procedure based on B-spline curves that interpolate the dent geometry obtained from the data extracted by in-line inspection (ILI) tools. The results obtained were then validated to those obtained from the non-linear FE analysis carried out for dented pipes with a 323.9 mm nominal outer diameter and 4.78 mm wall thickness. The dent was created by a 219.1 mm diameter dome indenter. The study found a good estimation for both the circumferential and longitudinal bending strains. This method however, is valid if the field data from ILI tools is available (Noronha et al. 2010). The limitations with this method are that the study was carried out on rock dents that have the strain components ε_1, ε_2, and ε_3 in the principal strain directions. This means that the dent is symmetric in both the longitudinal and circumferential directions.

2.3.2 Strains in dented pipelines under internal pressure

Strains in dented pipes subject to monotonically increasing internal pressure have been widely studied by various researchers. One of those researchers was Ong et al. (Ong et al.

7

1992) who performed FE analysis and experimental study on a pipe with a plain dent in order to study the elastic strain distribution. The pipe in the study was 900 mm long with a mean diameter of 160 mm and 2 mm wall thickness. The indenter used was spherical in shape with a 63.5 mm diameter. This indenter left a permanent dent depth of 13.5 mm (8.45% of the pipe diameter). Strain gauges were placed on the exterior surface of the pipe to obtain the elastic strain distributions in the dented region. It was found that the maximum strain occurred in the hoop direction along the longitudinal direction and located at the flank of the pipe (Ong et al. 1992) (See Figure 2.3).

As described by Lancaster and Palmer (Lancaster and Palmer 1996), dent damage to transmission pipelines is a main cause of work-related failures which has serious environmental, economic, and safety consequences. The study undertook a series of tests to measure strains and displacements in previously dented mild steel pipes subjected to increasing internal pressure. The objective was to identify the size, shape, and location of regions of high strains. Small-scale pipes of 100 mm diameter, 1.85 mm thickness, and 338 mm length were chosen in this study. The material chosen was aluminum alloy 6063-TB with a yield stress of 163 MN/m^2 and a yield strain of 2090 μe. The Poisson's ratio of the pipes was 0.32. The model pipe material and geometry was chosen to ensure that strains in the models would be identical to strains in the full-size pipes. Some of the specimens were dented under no pressure while others contained internal pressure. The indenter used to make the short dents was a steel sphere with a diameter of 50.8 mm. The total dent depth reached up to 16% of the diameter. Linear variable differential transformers and a traverse system were used to monitor the dent displacement and surface profile throughout the pressure tests (Lancaster and Palmer 1996). Furthermore, strain gauges and a photoelastic coating were used to determine the changes in surface strain in three specimens with identical small (short) plain dent depths of 0.16D. The photoelastic coating's purpose was to measure the difference in the principal strains on the surface. Although the strains in a plain dent were observed on the longitudinal and circumferential axes, it was found that the maximum strains occur at the flanks (See Figure 2.3) of the axial extremities of the dented pipe. The high strain concentration values along with a larger reduction in the dent depth were observed in pipes dented at

zero pressure as compared to those dented under non-zero internal pressure (two pipe specimens of $0.23p_y$ and $0.57p_y$). The study found that to observe a significant amount of plastic deformation on the pipes dented with internal pressure, the indentation pressure, pressure used to indent the pipe, must be exceeded. It was recommended that further research on pipes dented under internal pressure is needed to understand this phenomenon better.

Another research conducted by Rosenfeld (2002), found that having the combination of a dent with a gouge can have serious effects due to the existence of the gouge and the re-rounding internal pressure that is constantly existent throughout the pipeline. Such combination is dangerous because as the damage has occurred, plastic flow or even re-melting, which could happen due to the heat from the contact between the material and the pipe, might have occurred within the gouge. When this happens, the local ductility and toughness of the pipe decreases and hence, a local rupture can occur. The study also found that as the dent is being pushed out by the internal pressure of the pipe this produces high tensile strains at the root of the gouged area which can in turn cause cracks due to the low ductility and toughness in the dented region. The study concluded that for such damage there are no reliable methods for determining whether a dent with a gouge in a pipeline is safe at operating pressures. However, some repair options were recommended such as using steel sleeves to contain pressure. Furthermore, the study also recommended a composite wrap as long as the gouge is first grounded down to have a smooth contour, no cracks exist after grounding the gouge, and finally the dented region is filled with a hard filler (hardenable materials) under the sleeve. If the damage, however, is light, the study suggested that by simply grinding the damage out and repairing the coating, the pipeline will be safe for the operating pressures. The study recommended the following relationship for the safe length of grinding out the damage region:

$$L \leq 1.12 \left[(Dt) \left[\left(\frac{\frac{a}{t}}{1.1 \left(\frac{a}{t} \right) - 0.11} \right)^2 - 1 \right] \right]^{1/2} \qquad (2.3)$$

Where L is the safe length of grinding, a is the grinding depth, t is the pipe's wall thickness, and D is the pipe's diameter. Furthermore, the safest grinding depth is suggested as 0.40t. Although the previous relationship contains parameters that can be simply obtained from the geometry of the pipe, the study did not specify what characterizes a light damage in order to just grind the damage out. An educated guess would have to be taken to determine if the damaged region is light.

The study also discussed another form of damage that occurs when the pipeline is poorly installed. These damages occur mostly in the bottom half of the pipe and are usually not accompanied damages such as gouges or cracks; however, scratches could exist. As the pipeline is improperly installed, dents occur which are caused by rocks located in the bottom of the ditch (Rosenfeld 2002). Although this other type of damage does not pose an immediate danger to the integrity of the pipeline due to the restrain from being pushed out, long-term problems can still occur such as corrosion, punctures, and even stress-corrosion cracking, or even hydrogen cracking. As it was mentioned, the best way to prevent such long-term problems is to remove the rocks from the bottom of the ditch. Although this maybe be complicated to do as there could be large amount of rocks, a padding of sand can be laid in the ditch before placing the pipe. This can provide some form of protection against the sharpness of the rocks (Rosenfeld 2002). If the damage has already been created, there are ways to repair them as suggested by the authors such as by adding steel sleeves or a composite wrap with a filler in the dent area. The study recommended that only hardenable filler materials are to be utilized.

2.3.3 Determination of Strains with the use of In-line Caliper Data

In-line calipers provide accurate data from which the dent shape can be obtained with the use of Finite Element Models (FEM) (Lukasiewicz et al. 2006). Strains in pipe walls have two major components; longitudinal and circumferential strains. Each of these can be split into bending and membrane components. The main difficulty arises when determining the membrane component as it stays constant through the pipe wall. The bending component of the strain changes linearly from inner to outer surface (Lukasiewicz et al. 2006). Based on the findings, most of the existing techniques focus on finding only the longitudinal membrane strains. The study by Lukasiewicz et al. recommended a method for determining both the longitudinal and circumferential membrane strains in dented pipes. The radial displacements of a pipe obtained from the high resolution in-line caliper were used to obtain an effective mathematical algorithm to calculate the bending and membrane strains. Equation 2.4 shows the final equation that combines the membrane and bending strains to obtain the effective strain. The derivation of this equation is detailed in the authors' paper. This algorithm called the Dent Strain Analysis (DSA) program which was used to calculate these two strain components. The results from the DSA were compared with the results from two FEM models (one with a simulated dent and another with a sample dent measured from the in-line caliper). The results from the DSA and the FEM models showed a good agreement validating that the algorithm developed can be used for the assessment of all the strains in dents. This assessment can evaluate whether the strain in dents are within an acceptable range. The study recommended a strain of 6% to be the acceptable limit for strains which is adopted by the B31.8 code for gas transmission and distribution piping systems (ASME 2007). It is important to find such strains as it helps in assessing the severity (risk associated with failure) of a dent in order to repair mechanical damages to the pipe.

$$\epsilon_{ef} = \frac{2}{\sqrt{3}} \sqrt{\epsilon_x^2 + \epsilon_x \epsilon_y + \epsilon_y^2} \qquad (2.4)$$

Where ε_{ef} is the effective strain, ε_x is the strain in the longitudinal direction, and ε_y is the strain in the circumferential direction.

2.3.4 Review of ASME B31.8 Code

A few studies reviewed the ASME B31.8 code which looks at the strain-based criteria to determine whether a pipe with a dent is safe (Noronha et al. 2010). Furthermore, the equations used to determine the strains were reviewed by the authors. Appendix R of the ASME B31.8 code (2003 and 2007) recommends equations for determining the total strain acting on the inside and outside of the pipe surface. Such equations are compared to the allowable strain limit in order to determine whether the dent in the pipe is considered safe. After reviewing the equations, it was found that there was an error in the derivation of those equations as they were derived using the assumption of plane strain. The use of such incorrect assumption can lead to inaccurate results. It was stated that the strains in the dent region were mostly within the plastic range.

Additionally, another error found in the 2003 ASME B31.8 code was that the circumferential and longitudinal bending strain equations which missed a factor of 2 (see Equations 2.5 and 2.6) which divides the pipe wall thickness as seen in. This error leads to conservative estimates of strain components. Such error was corrected in the 2007 revision of the code as shown in Equations 2.6 and 2.7:

$$\epsilon_1 = t \left(\frac{1}{R_o} - \frac{1}{R_1} \right) \tag{2.5}$$

$$\epsilon_2 = -t \left(\frac{1}{R_2} \right) \tag{2.6}$$

$$\epsilon_1 = \frac{t}{2} \left(\frac{1}{R_o} - \frac{1}{R_1} \right) \tag{2.7}$$

$$\epsilon_2 = -\left(\frac{t}{2}\right)\left(\frac{1}{R_2}\right) \qquad\qquad (2.8)$$

In addition, interpolation of dent geometry data to develop the contour shape of dent surface and determine the strain levels was also reviewed (Noronha et al. 2010). The data was obtained from in-line inspection (ILI) tools. The use of fourth-order B-spline curves were used to interpolate the dent contour (Noronha et al. 2010). The use of ILI tools was studied to determine if there are any differences in the resolution. The study found that using more sensors would render better estimations of strains in the dent region and hence, a better contour shapes of the dented region. Finally, this study also reviewed the equations used for determination of longitudinal membrane strains. It was found that the evaluation of such strains is extremely dependent on the definition of the dent length (Noronha et al. 2010). Two different dent lengths used in Appendix R of the ASME B31.8 2007 code were compared to the FE results and the result indicated that a much better agreement exists with the FE results when measuring the length at the dent half-depth (Noronha et al. 2010). These findings can help improve the code for future use.

Later, another study recommended that neglecting the effect of the circumferential membrane strain to determine the critical strain values in a dent as recommended by the ASME B31.8 code (2003, 2007) is not reasonable (Rafi et al. 2012). It was also determined that membrane strains are sensitive to the internal pressure applied aside from the dent depth and dent shape and hence it was recommended that the internal pressure should be taken into account (Rafi et al. 2012).

2.3.5 Strains in Unconstrained and Constrained Dents

Unconstrained dents by definition tend to rebound elastically and re-round inelastically due to the increasing internal pressure (Alexander and Kiefner 1997). Constrained dents are those dents that are not allowed to re-round back after they occur (Alexander 1999).

13

The main finding associated with unconstrained dents is that if dent depth is 2% or less it would not likely fail during the useful life of a pipeline, and therefore, it would not be necessary to repair them.

Rock (constrained) dents that have the rock stay in the same position in the vicinity of the existing dent are of main concern if the rock is sharp enough. If this occurs, it could lead to a puncture in the pipeline and therefore, a failure could occur under increasing internal pressure. The authors conducted three different types of tests on unconstrained smooth dents. The first one had a dome-shaped dent, the next ones had a bar-shaped dent, finally a pyramid-shaped dent. For the dome-shaped dents, a 219 mm (8.625 inch) diameter indenter was used to produce dents that vary between 6% to 18% depth of the pipe's diameter. The dents were made with no internal pressure in the pipe (Alexander and Kiefner 1997). Aside from many findings, it was concluded that the unconstrained dents developed longitudinally-oriented cracks that spread from the outer pipe surface towards the inner pipe surface. It was also found by the comparison of fatigue lives, that constrained dents (with depths of 6% or less) would have longer lives than those of unconstrained dents (Alexander and Kiefner 1997). No conclusion was made by the study for dent depths greater than 6%.

The next tests were completed with two different types of bar indenters: a 305 mm (12 inch) long by a 25 mm (1 inch) in diameter bar-shaped indenter and a 457 mm (18 inch) long by 102 mm (4 inch) in diameter bar-shaped indenter. All dents were formed without internal pressure in the pipes. The bar indenter was oriented in two different positions within the pipe: for six pipes, the bar was placed parallel to the axis of the pipe, and in the last two pipes it was placed transverse to the axis of the pipe (Alexander and Kiefner 1997). It was found that the cracks that occurred were longitudinally oriented and started at the outer diameter surface of the pipe.

The pyramid-shaped indenter had a 324 mm (12.75 inch) outer diameter by 5 mm (0.188 inch) wall thickness. It was concluded by the authors that the pyramid dents exhibited less total rerounding as compared to the other two dent shapes.

The authors concluded that the pipeline operators do not need to be concerned about the short-term consequences of smooth unconstrained dents. The only concern comes when the dent is subjected to severe service pressure if and only if, the dent is subjected to aggressive service pressure over a long period of time. Another finding was that smooth, unconstrained dents that have depths of 2% or more can be left without repairing if the analyses run on the pressure cycles in the pipe show that the dent would not fail within its useful life (Alexander and Kiefner 1997), however, this does not mean that the 6% limit is unsound.

2.3.6 Strain Concentrations in Dented Pipelines with Internal Pressure

As determined by Lancaster and Palmer (1996), high elastic hoop strain concentration factors occurs at the rim of the dent as seen in Figure 2.2. The strain concentration factors (SF) were determined by dividing the strain measured experimentally in the dent of the pipe by the calculated value of hoop strain away from the dent as shown in Equation 2.9 (Lancaster and Palmer 1996).

$$SF = \frac{pD}{2Et} \qquad (2.9)$$

Where p is the internal pressure of the specimen, D is the outside diameter, E is the modulus of elasticity, and t is the pipe wall thickness.

The study observed high strain concentration factors as well as a reduction of the dent depth after pressurization indicating start of plastic deformation in pipes dented under zero pressure. However, for dents formed under internal pressure, the start of plastic deformation is delayed until after exceeding the indentation pressure (Lancaster and Palmer 1996). This result may cause different residual stress distributions and dent shape which should be studied further.

2.3.7 Stress Concentrations in Dented Pipes with Internal Pressure

As stated by Rinehart and Keating (2007), stress concentrations associated with dent defect can degrade the in-service performance as well as the fatigue life of pipes. This study developed a semi-analytical solution to determine the stress concentration distribution for a two dimensional cross-section dented cylinder pipe subjected to internal pressure. The method used for the semi-analytical approach was the equivalent load method. Such method provides a similar stress effect as that associated with the actual dent. It approximates the effect of geometric imperfections by assuming that the deviation in the shell behavior due to the dent imperfection is equivalent to the imperfection caused by pressure distribution on a perfect shell (Rinehart and Keating 2007). The pipe wall profile and applied equivalent pressure and using this method can be found in Equations 2.10 and 2.11, respectively.

$$r(\phi) = R - \zeta \exp\left[-\frac{1}{2}\left(\frac{\phi}{\phi_0}\right)^2\right] \tag{2.10}$$

Where r is the radius at any angle ϕ of the dent (pipe wall profile), R is the pipe's undeformed nominal radius, ζ is the dent depth, and ϕ_o is the circumferential extent of the dent.

$$P_r^*(\phi) = \frac{N_\phi \zeta}{R^2 \phi_0^2}\left[1 - \left(\frac{\phi}{\phi_0}\right)^2\right]\exp\left(-\frac{1}{2}\left(\frac{\phi}{\phi_0}\right)^2\right) \qquad (2.11)$$

Where $P_r^*(\phi)$ is the applied pressure distribution at any ϕ location of the dent.

The displacement coefficient, N_ϕ, in the equivalent load is calculated through the derivation of the thin-wall, small deformation case, shell equations presented by Flugge (Flügge 1962). Furthermore, the actual stress predicted near the imperfection was determined to be the summation of the stresses present in the perfect cylinder and the change in stress induced by the equivalent load as shown in Equation 2.12:

$$SCF_{outer}^{inner} = \frac{\sigma_{\phi,outer}^{inner}}{\sigma_{\phi,nom}} = 1 + \frac{\frac{\zeta}{R}}{\phi_0^2}\left(1 \pm \frac{6R}{t}\right)f(\phi,\phi_0) \qquad (2.12)$$

Where, $\sigma_{\phi,outer}^{inner}$, is the inner wall hoop stress, $\sigma_{\phi,nom}$ is the nominal hoop stress, and t is the pipe wall thickness.

$$f(\phi,\phi_0) = \left[\frac{1+2k}{1+k}I_0 + \sum_{m=1}^{M}\frac{I_M(1-m^2)}{m^4 + 2m^2 + 1}\cos(m\phi)\right] \qquad (2.13)$$

Where, m and n are Fourier series modes, l defines the periodicity in the axial direction, I_o defines the Fourier expansion where m is zero, I_m defines the Fourier expansion when $\phi = \phi_o$, and k is a material and specimen constant.

The semi analytical results were compared with the FEM results to study their agreement. The pipe geometry used in such FE models was the same as the semi analytical solution. A more simplified formula was deduced from such models for calculating the stress concentrations. The simplification of such formula as seen in Equation 2.14.

$$SCF^{outer} \approx 1 + \frac{5.22d}{t}$$
(2.14)

Where d is the dent depth and t is the pipe wall thickness.

This equation takes into consideration that fatigue cracks in dents normally develop on the outer surface of the dent center and therefore, the inner surface component was ignored (Rinehart and Keating 2007). It was also observed from parametric studies that long dents have a greater dependency on the dent depth to pipe thickness ratio (d/t) and hence, the relationship was simplified to include only that specific geometry. Such relationships provides conservative solutions (Rinehart and Keating 2007). This study determines the stress concentration factors for dents that have a longer length compared to the depth (L>50d). This study did not take into account the effects of gouges in dents as well as the effects of residual stresses that can influence the behavior of dent fatigue (Rinehart and Keating 2007).

Furthermore, a study compared by Pinheiro and Pasqualino (2008) evaluates the stress concentration factors for longitudinal and transverse plain dents. The objective was to evaluate the fatigue failure of pipes with such dents that occurs due to stress concentrations in the dented region. High cycle fatigue theory was used to modify the S-N curves for metallic structures undergoing high cycle fatigue loadings (Pinheiro and Pasqualino 2008). The S-N curves demonstrate the stress required to cause a fatigue failure in the pipe due to a number of cycles. This was done to propose a new method to calculate the fatigue life. Stress concentration factors for longitudinal and transverse plain

dents were obtained from a previously developed FE model for a spherical dent (Pinheiro and Pasqualino 2008). Stress concentration factors for spherical dents were previously determined from another parametric study (Pinheiro and Pasqualino 2008). FE models were used to perform a parametric study to asses stress concentration factors for longitudinal and transverse dents. It uses a non-linear elastic-plastic simulation of the denting process and generation of deformed shape, followed by an elastic determination of the stress concentration factors (Pinheiro and Pasqualino 2008). It used a nonlinear 3D elastic-plastic shell model. The mesh was set to be S8R5 second-order quadrilateral thin shell elements that include five degrees of freedom per node (Pinheiro and Pasqualino 2008). From the parametric results, analytical expressions were also carried out to estimate stress concentration factors for longitudinal, transverse, and spherical dents as function of pipe and dent geometries. The FE model results were validated with experimental results of small-scale fatigue test on steel pipe with spherical dents under cyclic internal pressure (Pinheiro and Pasqualino 2008). Both, the experimental tests and FE models were conducted with the same dimensions, boundary conditions, and material properties. The study found a good agreement between the experimental and numerical strain results. The study also determined that the numerical model can accurately calculate the stress concentration factors. As suggested in the study, the analytical expressions developed in this study can be also used to evaluate the fatigue life of dented steel pipes with the use of modified S-N curves.

2.4 Effect of Dent on Fatigue Behaviour

As stated by Cosham and Hopkins (2004), strains and stress concentrations occur from the formation of a dent. Furthermore, a reduction in the pipe's diameter is also observed. The dent depth is a very important factor which influences the fatigue life of pipelines (Cosham and Hopkins 2004). Additionally, the dent width and length play an important role in the distribution of strains and stresses which can also influence the fatigue life of pipes. Furthermore, Baker (2004) found from analytical models that for the fatigue life of unconstrained dents:

- Decrease with an increase in dent depth (Alexander and Kiefner 1997)
- Decrease with increasing local strain (Alexander and Kiefner 1997)
- Decrease with increasing pipe D/t ratio (Fowler 1993)

2.4.1 Long and Short Dents Overview

The following section provides an overview of the differences in the fatigue behavior between long and short dents. Long dents are dents that span a significant portion of the total pipe length and short dents are much smaller.

For long dents, the maximum strain and stress occurs at the root of the dent. Furthermore, for long dents it is observed that fatigue cracking usually occurs at the center of the root of the dent and it is oriented longitudinally (Cosham and Hopkins 2004). For short dents, the maximum strain and stress occurs on the flanks of the dent (See Figure 2.2). A similar finding from another study found that the maximum hoop strain in short dents is located at the flanks of the dent and for long dents it is located at the root of the dent (Ong et al. 1992). The nomenclature of a typical dent can be found in Figure 2.2. Additionally, fatigue cracking for short dents usually occurs around the flanks of the dent (Cosham and Hopkins 2004). A subsequent study researched by Keating and Hoffman (1997), concluded that long dents developed fatigue cracks in the root (See Figure 2.2) of the dent and for short dents, it occurs at the rim (See Figure 2.2) of the dent. In their study, dents were developed using three types of indenters. The specimen's diameter ranged from 305 mm (12 inches) to 914 mm (36 inches) and the D/t ratio ranged from 34 to 96.

As also mentioned by Cosham and Hopkins (2004), the fatigue life of plain dents is much less than that of a perfect pipe based on experimental tests. However, the fatigue life of s dents is much higher than those of kinked dents or plain dents containing gouges. A study done by Beller et al. (1991) which investigated the effect of dent depth and shape on pipeline stress distributions states that the largest local stresses for a semi-spherical indentation are located along the rim (See Figure 2.2) of the dent while those of a

cylindrical indentation are located at the root of the dent (See Figure 2.2). It was suggested from the results that it is possible that a critical ratio of length to width exists for a dent such that the location of the largest stresses changes from the root to the rim of the dent (Beller et al. 1991).

2.4.2 Importance of Fatigue

Pipeline operation is an important factor in the determination of the life of pipes. It is an important issue as the pressure in the field oil pipelines changes constantly which in turn can lead to fatigue failure. As stated by Wu et al. (2011), if a dent defect exists on a pipeline, the undented shape will be recovered by the pressure wave circulating through the pipe (Wu et al. 2011). The study conducted tests using a FE model. This will in turn cause a movement of bending stresses. In addition to that, if there are other mechanical damages in the pipe such as a gouge or a weld, then the movement of bending stresses increases which can cause the pipeline to fail due to fatigue fracture. It was also found that, actual pipe pressures can be obtained from the daily reports of each pump along the pipeline. Such data can be beneficial in the prediction of pipeline failure if such mechanical damages exist within the body.

2.5 Summary

Overall, pipelines are widely used in the industry to carry and transport oil or pressurized gas. Having a dent defect in a pipeline introduces strain and stress concentrations that must be examined in order to determine the structural integrity and safety of the linepipe. The determination of strains in dents has been a major topic for research for a long period of time. Different methods were developed to determine the strains in different type of dents as there is no specific method of determining strains for all types of dents. It was found from the literature review that plain dents, which are the focus of this research project, are the least dangerous types of dents encountered in pipelines. It has also been determined that for short dents, the maximum strain and stress occurs at the flanks of the dent. This project deals with the determination of the strain distributions in short dents of

various shapes and dent depths in order to determine the stress concentration locations and values. This was done as it is important for the fatigue life assessment as well as other pipeline structural integrity issues.
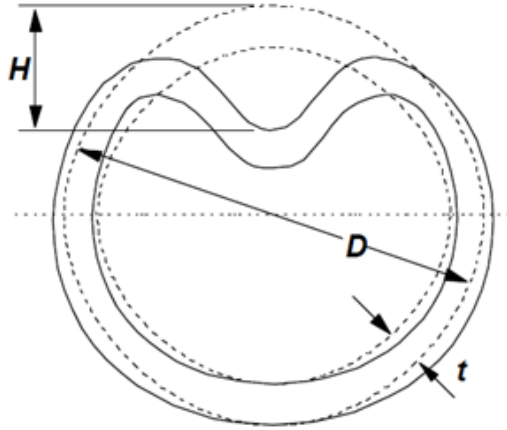
Figure 2.1: Cross Section of Dented Pipeline (Cosham and Hopkins 2004)
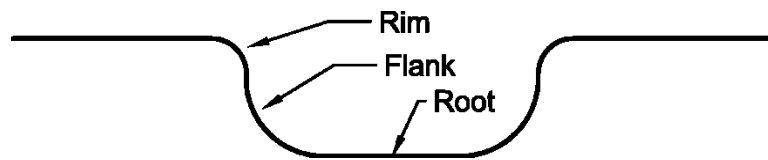
Figure 2.2: Nomenclature of Typical Dent
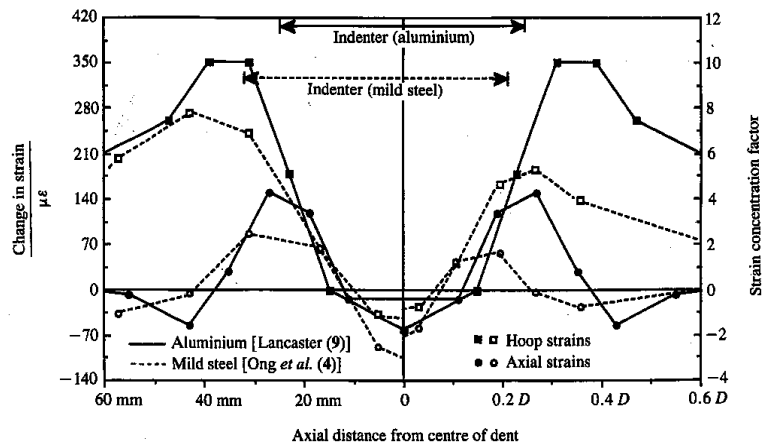
Figure 2.3: External Strains along the Axial Line of Symmetry

(Lancaster and Palmer 1996)

CHAPTER 3

3.0 TEST PROCEDURE

3.1 Overview

Previous research conducted on dented pipelines looked into the effect that dents have on the strain distribution around the dented area. Furthermore, the fatigue behaviour of dented pipes was also studied by different researches. From the many previous studies, it was determined that the main parameters that have an effect on the strength as well as fatigue life of the pipe are the dent depth and its shape.

Most experimental studies focused on one or two different parameters, however, the current study investigates the effect that different parameters such as the dent depth, dent shape, and internal pressures have on the strain distribution around the dented area. There are a range of different parameters that can affect pipelines in the field; however in this study not all parameters were tested. The different dent shapes as well as dent depths and internal pressures were considered in this study and the results provided good general overview of the expected outcome of dented field pipelines. Additionally, the results obtained from the experimental work were then used to validate numerical models that could in turn provide results for many more different parameters.

3.2 Specimens

Full-scale tests were previously carried out by Centre for Engineering Research in Pipelines (CERP) led by Dr. S. Das at the University of Windsor, to determine the behaviour of a dented pipe under constant internal pressure (Rafi 2011). The strain distributions of were extracted to determine such behaviour. In order to do so, the

specimens chosen for testing represent the properties of gas and oil field pipes used in the industries.

The pipelines were manufactured with an outer diameter of 274 mm, a wall thickness of 8.2 mm, D/t ratio of 34 and a length of 1100 mm. The grade of steel conformed to API 5L X52 steel pipes (American Petroleum Institute 2007). The ends of the pipes were welded to 50 mm thick end plates.

3.3 Material Properties

The pipe specimens chosen in this study were comprised of the same material. In order to obtain the mechanical properties of the steel pipes, tensile coupons were made from the longitudinal direction of the pipes. The tensile coupons were then tested according to the specifications set in ASTM E8/E8M-08 specifications (ASTM E28.04 Subcommittee 2013). All pipe specimens with same diameter-to-thickness ratio of 34 were made from same steel.

The mechanical properties obtained from testing the coupons were then used in the creation of the finite element models. The mechanical properties of the pipelines are shown in Table 3.1. The stress vs. the strain behaviour from such tensile coupons are plotted and shown in Figure 3.1 (Rafi 2011).

3.4 Preparation of Selected Specimens

The dents were created previously by Dr. Das's research group CERP by applying monotonically increasing static load and deformation with constant internal pressure (Rafi 2011). Theses dented pipe specimens are used in the current study again under the leadership of Dr. S. Das of CERP. The dented pipe specimens were cleaned around the dented area in order to provide a smooth surface and to facilitate installation of strain

gauges for a better and more precise reading. Figures 3.2 and 3.3 show the setup of a pipe tested in the current study.

3.5 Parameters

In the experimental work of this study tests, different parameters were considered. The parameters are: i) the internal pressure, ii) the indenter shape, iii) the dent depth. Table 3.2 shows the test matrix of this study. In order to differentiate between the different specimens tested, the pipes were given names to reflect their important characteristics. As can be found in Table 3.2, the test matrix shows the specific names given to each pipe. As an example, for a rectangular indented pipe of name RP20D8, R means that the pipe has a rectangular dent; P20 describes the internal pressure that was maintained in the pipe at the time of indentation and the pressure of this specimen was $0.2p_y$. The internal pressure is in terms of p_y, which is the pressure that causes the stress in the circumferential axis to reach the material's yield pressure as shown by the following equation (3.1). Finally, D8 describes the permanent dent depth as a percentage of the pipe's outer diameter.

A more in-depth study was carried out in the numerical parametric study as it is not possible to test a wide range of pipe specimens.

3.6 Boundary Conditions

The boundary conditions chosen for the experimental study simulate the conditions experienced in the field. This was done in order to be able to accurately simulate the results that can occur in the field as well as report on the parameters of most importance that can affect the integrity and safety of field pipelines. In the field, a pipe buried underground usually rests on the soil. In the experimental testing, the pipes rested on a rigid table in order to provide a similar support system. Furthermore, the internal pressure within the pipe was applied through a hydrostatic pump (Figure 3.3).

3.7 Indenters

Three different indenters used in the experimental study were chosen to produce different dent shapes that can be found in the field pipelines. These indenters were used to produce the different dent shapes in the pipe (Figure 3.4). In a previous study by Centre for Engineering Research in Pipeline (CFRP) as reported by Rafi (Rafi 2011). The dent can form due to the accidental impact of construction equipment such as excavators or sometimes during the construction of the pipe itself. Furthermore, rocks can also create a dent in the field buried linepipe. Figure 3.4 shows the shape of the three indenters used:

- Sphere indenter acting as a sharp indenter
- Rectangular indenter acting as a moderate indenter
- Dome indenter acting as a smooth indenter

3.8 Internal Pressure

Oil and gas pipelines are constantly transporting fluid which needs internal pressure to be existent within the pipe. As the pipeline is setup underground until it serves its lifetime, dents can occur anytime during its lifetime. A dent an pose environmental as well as economic threats since a dent can lead to a rupture or even burst. For this study, the denting of the pipelines was already created previously by CERP (Rafi 2011); however an explanation of such process is described in the following section since the current study is a continuation of the previous study. The internal pressure in the dent tests was applied as a function of p_y, the yield pressure as shown in equation (3.1) and the pressure was kept unchanged during the entire indentation process;

$$p_y = \frac{\sigma_y t}{r} \tag{3.1}$$

Where σ_y is the material's yield stress level, t is the thickness of the pipe wall, and r is the inner radius of the pipe.

3.8.1 Internal Pressure while Denting

The internal water pressure during the indentation process was applied to simulate the indentation process occurring in the field. The internal pressure was varied between 0% and 20% of p_y for different pipes specimens. The value of p_y is 23.5 MPa (3410 psi) calculated using equation (3.1). The objective was to determine the effect of the internal pressure on the load-deformation behaviour of pipes as well as the strain distribution around the dented region (Rafi 2011).

3.8.2 Internal Pressure after Denting

In this study, monotonically increasing internal pressure was applied after the removal of the indenter. The internal pressure of the pipe was increased to 0.90 p_y to determine the effect that the different dents have on the strain distribution in the dented area. The increasing pressure caused re-bounding of the dent and this, releasing locked-in strains created by the denting process.

3.9 Test Process

All specimens were pressurized same way. The pipes were first filled with water and then pressurized with the use of an air-driven hydrostatic pump. The maximum pressure applied was 20.7 MPa (3000 psi) as it was not desired to reach the yield pressure of 23.5 MPa (3410 psi). This yield pressure is obtained from equation 3.1. The main reason for having 20.7 MPa was to push out the dent as much as possible without reaching the yielding pressure. After pressurizing the pipes, the internal pressure was then slowly reduced to zero (de-pressurized).

3.10 Experimental Setup and Instrumentation

The experimental testing was performed in the structural engineering lab at the University of Windsor. The pipes were resting on a strong steel table while being pressurized as seen in Figure 3.2 and 3.3.

Two linear voltage displacement transducers (LVDTs) were used to monitor the dent displacement throughout the test. They were mounted at right angles to each other to record the displacements. Figure 3.2 shows the photo of the test setup and Figure 3.3 shows the schematic. Strain gauges were placed along the longitudinal and circumferential lengths of the dent. This was done to obtain the strain readings as the pipes are being pressurized (Figure 3.3).

3.10.1 Fluid Pump and Pressure Transducer

The internal pressure applied in the test specimens was carried out using an air-driven hydrostatic pump. The capacity of the pump is 10,000 psi (68.9 MPa). A pressure transducer was also used in order to read and obtain the internal pressure applied. A highly accurate pressure dial gauge was also used to monitor pressure at the pump.

3.10.2 Linear Voltage Displacement Transducers (LVDTs)

Two linear voltage displacement transducers (LVDTs) were used during the tests to measure the displacements that occurred when the pressure within the pipe pushed the dent outwards (See Figure 3.3). The first LVDT (LVDT1) was placed at the centre of the dent and the second LVDT (LVDT2) was placed at the side at 90° angle to LVDT1 in order to more accurately capture the displacement caused by the internal pressure.

3.10.3 Strain Gauges

There were a total of 16 strain gauges used for each pipe tested (See Figures 3.5 to 3.7). The strain gauges measure the local strain on the top surface of the pipe. The locations of the strain gauges are shown in Figure 3.5 for the sphere, dome, and rectangular pipe specimens. For all indented pipes, the strain gauges were placed at 25 mm intervals near and around the dent area with the first gauge placed at the midpoint of the dent in the longitudinal direction. The last strain gauges in both directions were placed at 50 mm intervals. This was done to obtain a better understanding of the strain values at the center of the dent.

The gauges used were 5 mm in length and had an electrical resistance of 120 ohms. They were applied at the outer surface of the pipe. Strain gauges were installed in the circumferential axis as well as the longitudinal axis. As the pipes were previously dented, residual strains were existent within the pipeline.

3.10.4 Data Acquisition System

A data acquisition system called CERP-DAQ was used to record and keep all the data that was obtained during the experimental testing. The CERP-DAQ was developed by Jamshid Zohreh of CERP using LabView® code (National Instruments Corporation 1996). The data collected was set to be two readings per second. Nineteen channels were used in order to connect the sixteen strain gauges as well as the two LVDTs and the pressure transducer. By doing so, all the necessary data was saved for later retrieval and analysis. The DAQ-CERP is able to record data from up to 100 channels. The test setup and tests were jointly carried out with the active help and guidance from other CERP members.

Table 3.1: Material Properties of Specimes

Modulas of Elasticity (MPa)	Yield Strength (MPa)	Tensile Strength (MPa)
200	410	498
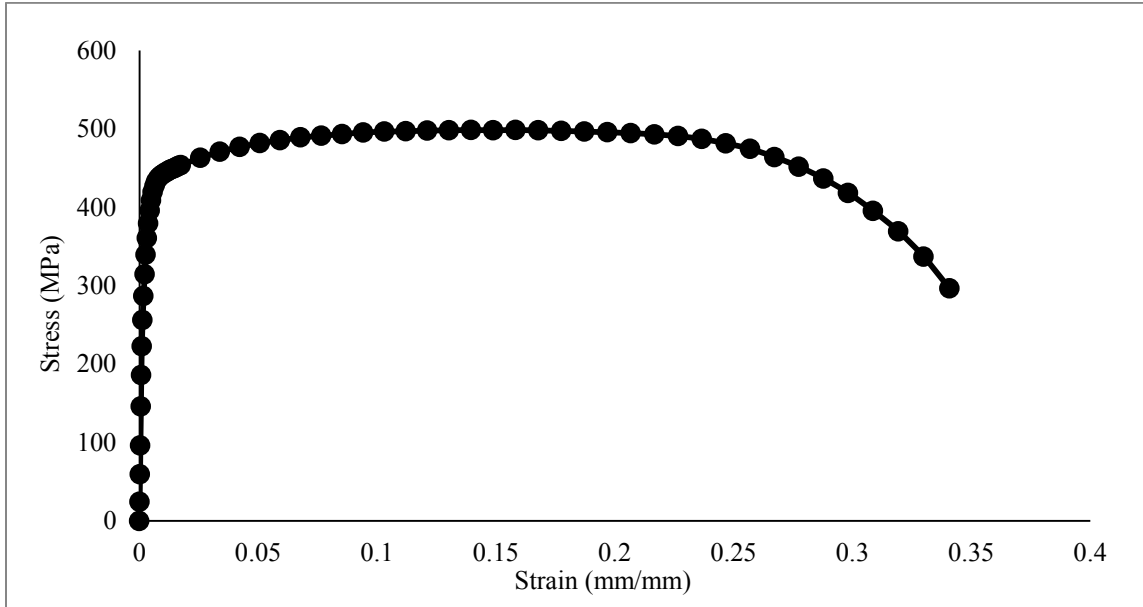
Figure 3.1: Tensile Coupon Stress-Strain Behavior (Rafi 2011)

Table 3.2: Test Matrix

Test #	Specimen	Dent Depth (% of Diameter)	D/t	Denting Internal Pressure (%)	Max. Internal Pressure (MPa)	Indenter Shape
1	RP20D8	8%	34	20%	20.7	Rectangular
2	RP20D12	12%	34	20%	20.7	Rectangular
3	SP20D8	8%	34	20%	20.7	Sphere
4	DP0D8	8%	34	0%	20.7	Dome
5	DP20D8	8%	34	20%	20.7	Dome

Figure 3.2: Photo of Test Setup
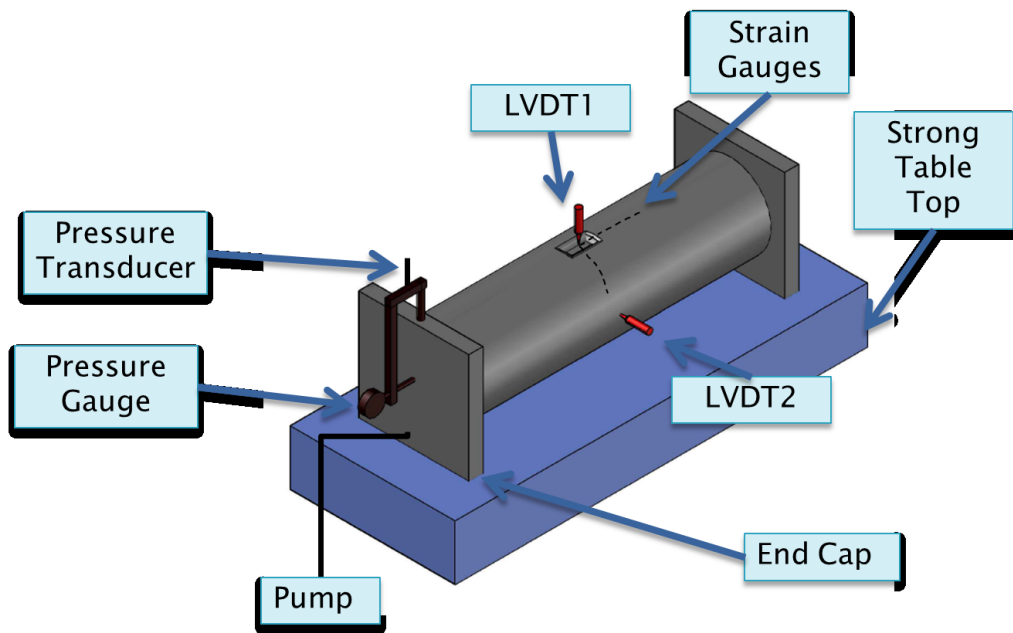
Figure 3.3: Schematic of Test Setup

(a) Rectangular indenter   (b) Sphere indenter   (c) Dome indenter

Figure 3.4: Indenters

Figure 3.5: Strain Gauge Locations for Rectangular, Sphere, and Dome Indented Pipes
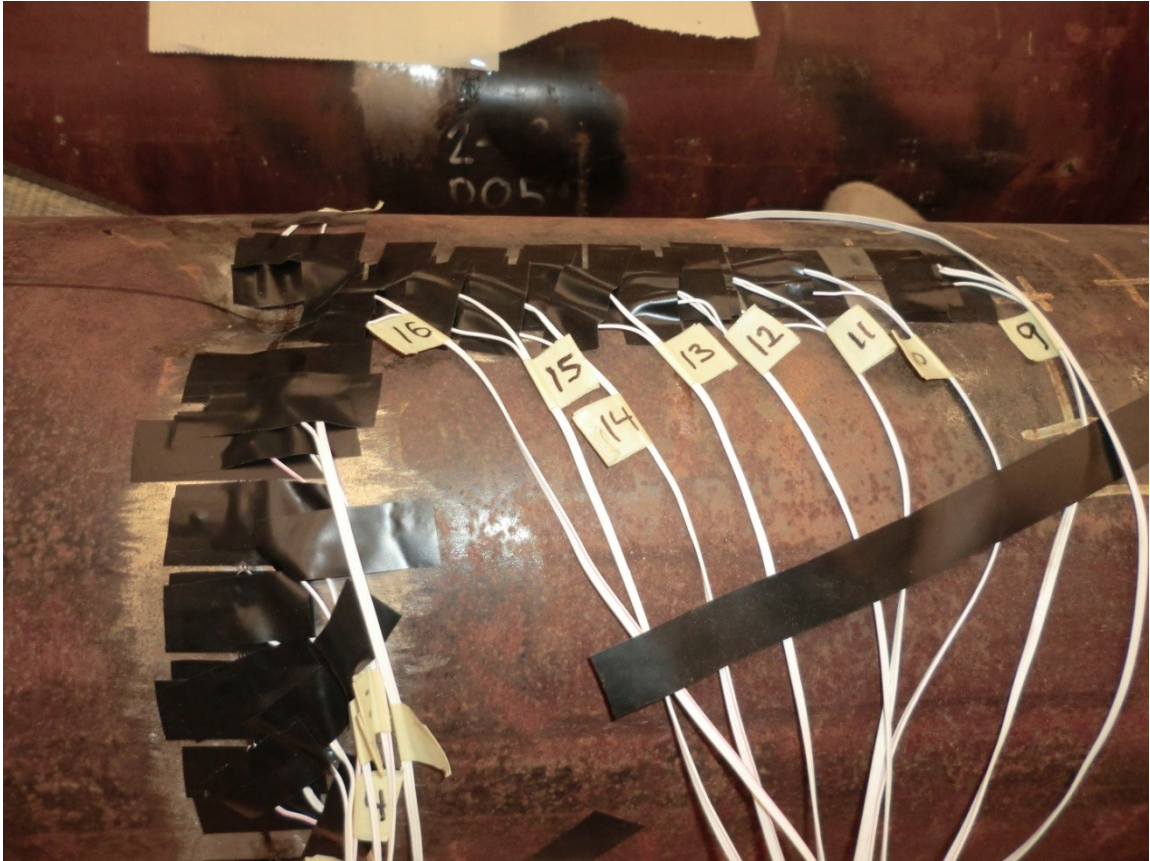
Figure 3.6: Photo of Strain Gauge Locations for Sphere and Dome Indented Pipes

Figure 3.7: Photo of Strain Gauge Locations for Rectangular Indented Pipes

CHAPTER 4

4.0 TEST RESULTS

4.1 Overview

The purpose of this chapter is to present and discuss the results obtained from the tests carried out in the structural engineering laboratory. There are three different types of plots that are shown and explained in this chapter and these are as follows:
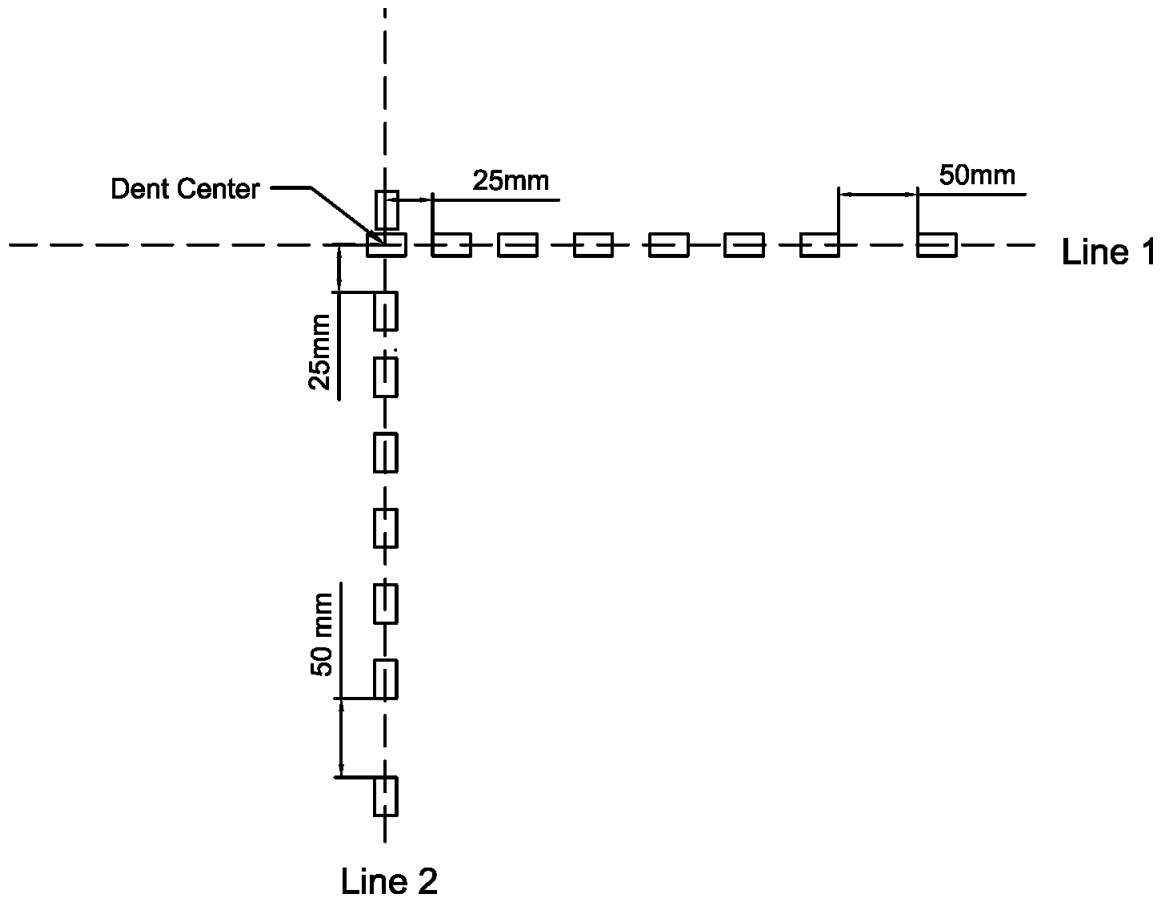
- Load vs. displacement relationship
- Pressure vs. displacement relationship
- Strain distributions

The load vs. displacement relationships were obtained in previous work by CERP (Rafi 2011). This work dealt with the creation of indents on the same pipelines that were used in the current study as well. The pressures vs. displacement relationships were obtained with the use of a pressure transducer and a 25 mm LDVT through a data acquisition system. Finally, for the strain distributions, strain gauges of 5 mm gauge length were placed on the outer surface of the pipe specimens at and around the dent center to acquire the strain caused by the internal pressure applied in the pipe specimens.

The effect of the indenter shape (or dent shape) as well as the dent depth and internal pressure existent within the pipe are explained in the following sections.

4.1.1 Indenter Shape

As explained previously, the following three different types of indenters were used (Figure 3.2).

- •   Rectangular Indenter
- •   Sphere Indenter
- •   Dome Indenter

Each of these indenters can exemplify a broad range of dent defect that can be found in the field pipe specimens. In the experimental work, two pipe specimens were indented with a rectangular indenter but at different dent depths. Furthermore, one pipeline was dented with a spherical indenter, and finally two pipe specimens were dented with a dome indenter but, at different internal pressures.

4.1.2 Dent Depth

For the three different indenter shapes, the dent depth was varied for the two rectangular indented pipes. The reference dent depth (permanent depth) in all pipes was 8% of the pipe's outer diameter. However, the dent depth for the rectangular indented pipes was varied to 8% and 12%. During the test of the 8% dent depth with a rectangular shape (RP20D8), the data acquisition system failed to save the test data when the internal pressure was raised to 1000 psi (6.9 MPa); however; the test data was interpolated as the experiment was carried out for a maximum pressure of 3000 psi (20.7 MPa). All other dent depths were run and the data was extracted. The following sections discuss the relationship between the load-displacement relationship as well as the pressure-displacement relationships and the strain distributions of all the specimens used in this study.

4.1.3 Pressurization

For all the test specimens, the maximum internal pressure applied in the pressurizing process was 3000 psi (20.7 MPa). This is about 90% of the yield pressure of the pipe (0.9p_y). It was decided not to go beyond this pressure limit to avoid any leak or rupture. The data for an internal pressure of 1000 psi (6.9 MPa) and 2000 psi (13.8 MPa) was also obtained before obtaining the test data for 3000 psi (20.7 MPa) which is the desired pressure.

4.2 Load-Displacement Relationship

The load vs. displacement relationship was studied and plotted in order to determine the effect of different types of indenters as well as dent depths. This was carried out in order to have a better understanding of the effect that different dent shapes on the behaviour of pipelines during denting process. The denting tests were completed in the previous study of CERP (Rafi 2011). The indenters used are able to represent most of the dents found in oil and gas field pipelines. Figures 4.1 through 4.5 show the load vs. displacement behaviours for all five specimens tested. It is observed that depending on the shape of indenter, there is a large difference on the amount of load required to obtain the same dent depth if the internal pressure is kept unchanged. As an example, in order to create a permanent dent depth of 8% (22 mm) of the pipe's outer diameter, a higher load is required for a rectangular indenter ($\approx$ 349 kN) rather than a dome ($\approx$ 190 kN) or sphere ($\approx$ 170 kN) indenters which are smaller in shape. This is because a greater area is in contact with the pipe when creating a rectangular dent, which in turn needs a higher force to create the same dent depth.

4.3 Pressure-Displacement

The pressure vs. displacement relationship was studied and plotted to determine the effect of different shapes of indenters and dent depths. As shown in Figures 4.6 through 4.10,

there is a greater bounce-back in the dent depth for dome indented pipes (Figure 4.8 and 4.9) as compared to the rectangular (Figure 4.6) and sphere indented pipelines (Figure 4.10) for equal initial total dent depth. This is due to the fact that a dome indenter has a more evenly circular shape than the sphere and hence, it allows the dent to re-round back to a greater extent. Additionally, the rectangular indenter has four corners which are regions that have localized strain concentrations and hence, it is hard to re-round back, thus there is a smaller displacement than that of the dome shape. However, the displacement for the 12% dent depth (Figure 4.7) is much greater than any of the 8% dent depths. Furthermore, in Figure 4.6, it is observed that the data for 6.9 MPa (1000 psi) had to be interpolated as the computer program failed to save the data for this pressure.

4.4 Strain Distributions

The key objective of this study is to determine the strain distributions around the dented region when the pipe specimen is under constant internal pressure. This study is very important as the safety and structural integrity of the pipe is at risk if dent damage occurs. In the following sub-sections, the relationships between the dent shape and the strain distribution are explained.

4.4.1 Rectangular Indented Specimens RP20D8 and RP20D12

Specimen RP20D8 was indented with a rectangular indenter at the internal pressure of $0.20p_y$. The permanent dent depth was 8% of the pipe's outer diameter. The strain gauge locations for the rectangular indented pipes are shown in Figure 3.5. Figures 4.11(a) and 4.11(b) show the strain distributions along the longitudinal axis, Line 1 for specimen RP20D8, when the maximum pressure of 3000 psi (20.7 MPa) was applied and when all the pressure was released, respectively. It is observed that the maximum strain occurs at approximately 125 mm from the dent center which is outside of the dented region (see Figure 2.2). The value of the maximum strain is 0.19% when a pressure of 3000 psi (20.7 MPa) was reached and 0.13% when the pressure was completely released. The difference between both peeks is about 0.06%.

Figures 4.11(c) and 4.11(d) show the strain distributions along the circumferential axis which is Line 2 for specimen RP20D8, when the maximum pressure of 3000 psi (20.7 MPa) was reached and when such pressure was released to zero, respectively. The maximum strain occurs at the dent center. The value of the maximum strain is 1.26% when a pressure of 3000 psi (20.7 MPa) was reached and 0.95% when the pressure was completely released. The difference between both curves is around 0.31%.

Specimen RP20D12 was dented with a rectangular indenter with an internal pressure of $0.20p_y$. The total permanent dent depth was 12%. The strain gauge locations for the rectangular indented pipes are shown in Figure 3.5. Figures 4.12(a) and 4.12(b) show the strain distributions along the longitudinal axis, Line 1 for specimen RP20D12, when the maximum pressure applied was 3000 psi (20.7 MPa) and then after releasing all the pressure to zero, respectively. It is observed that the maximum strain occurs at approximately 125 mm from the dent center which is outside of the dented region (see Figure 2.2). The value of the maximum strain is 1.51% when a pressure of 3000 psi was reached and 1.33% when the pressure was completely released. The difference between both strains is about 0.18%.

Figures 4.12(c) and 4.12(d) show the strain distributions along the circumferential axis which is Line 2 for the same specimen RP20D12, when the pressure was 3000 psi (20.7 MPa) and when the entire pressure was released, respectively. The maximum strain occurs at the dent center. The value of the maximum strain is 2.43% at 3000 psi pressure (20.7 MPa) and 2.39% when the pressure was completely released. The difference between applying and releasing pressure is about 0.04%.

4.4.3 Dome Indented Specimens DP20D8 and DP0D8

Specimen DP20D8 was indented with a dome indenter with an internal pressure of $0.2p_y$. The dent final permanent depth was 8% of the pipe's outer diameter. The strain gauge locations for the dome indented pipes are shown in Figure 3.5. Figures 4.13(a) and 4.13(b) show the strain distributions along the longitudinal axis, Line 1, when the maximum pressure of 3000 psi (20.7 MPa) was reached and when the pressure was released to zero, respectively. It is observed that the maximum strain occurs at approximately 100 mm from the dent center which is outside of the dented region. The value of the maximum strain is 0.57% when a pressure of 3000 psi (20.7 MPa) was reached and 0.65% when all the pressure was released. The difference between these two strain values is 0.08% which is marginal. However, a higher strain was observed when the pressure was released.

Figures 4.13(c) and 4.13(d) show the strain distributions along the circumferential axis, Line 2 for same specimen DP20D8, at maximum pressure of 3000 psi (20.7 MPa) and after releasing all the pressure, respectively. The maximum strain occurs at the dent center. The value of the maximum strain is 3.7% at a pressure of 3000 psi (20.7 MPa) and 3.1% when the pressure was released to zero. The strain gauge at that location failed during depressurization. Hence the strain at that location was extrapolated at 3.1%. The difference between these two strain values is 0.6%.

Specimen DP0D8 was indented with the same dome indenter with an internal pressure of $0p_y$. The dent depth was 8%. The strain gauge locations for the dome indented pipes were shown in Figure 3.5 (a). Figures 4.14(a) and 4.14(b) show the strain distributions along the longitudinal axis which is Line 1 for specimen DP0D8, when the maximum pressure of 3000 psi (20.7 MPa) was reached and when such pressure was released, respectively. It is observed that the maximum strain occurs at approximately 75 mm from the dent center which is outside of the dented region. The value of the maximum strain is 1.29%

when a pressure of 3000 psi (20.7 MPa) was reached and 1.25% when the pressure was completely released. The difference between both strain values is about 0.04%.

Figures 4.14(c) and 4.14(d) show the strain distributions along the circumferential axis, Line 2 for same specimen DP0D8, at the maximum pressure of 3000 psi (20.7 MPa) and at zero pressure, respectively. The maximum strain occurs at the dent center. The value of the maximum strain is 2.67% at the pressure of 3000 psi (20.7 MPa) and 2.38% when the pressure was completely released. The difference between both curves is around 0.29%.

4.4.3 Spherical Indented Pipe SP20D8

Specimen SP20D8 was indented with a spherical indenter with an internal pressure of $0.2p_y$. The total permanent dent depth was 8% of the pipe's outer diameter. The strain gauge locations for the sphere indented pipes are shown in Figure 3.5. Figures 4.15(a) and 4.15(b) show the strain distributions along the longitudinal axis, Line 1 for specimen SP20D8, when the maximum pressure of 3000 psi (20.7 MPa) was reached and when such pressure was released to zero respectively. It is observed that the maximum strain occurs at approximately 50 mm away from the dent center. The value of the maximum strain is 1.29% when a pressure of 3000 psi (20.7 MPa) was reached and 1.22% when the pressure was completely released. The difference between both curves is around 0.07%.

Figures 4.15(c) and 4.15(d) show the strain distributions along the circumferential axis, Line 2 for the same specimen SP20D8, at the maximum pressure of 3000 psi (20.7 MPa) and when such pressure was released to zero, respectively. The maximum strain occurs at a distance of 25 mm from the dent center, which is near the flank of the dent and within the dented region. The value of the maximum strain is 0.92% when a pressure of 3000 psi (20.7 MPa) was reached and 0.79% when the pressure was completely released. The difference between both peeks is around 0.13%.

4.5 Summary

The following conclusions can be made from the results obtained from the experimental tests conducted:

- The load-displacement relationships of pipelines that are dented with a lateral load are dependent on the amount of contact area between the indenter and the pipe surface. A higher load is required for indenters with a higher contact area. Furthermore, a higher load is required to produce the same amount of dent depth for pipelines such as the DP20D8 pipe that was dented while having pressure versus DP0D8 pipe that was dented under no internal pressure (Rafi 2011).

- The pressure-displacement relationships of pipelines vary depending on the shape of indenter used. A rectangular indenter produces a higher displacement for the same pressure as that of the sphere indenter. However a dome indenter has a higher re-rounding than the rectangular indenter as it does not contain any corners that can restrict the dent reversal to a higher value.

- The strain distribution at and near the dented region are dependent on the shape of the dent and the internal pressure applied during indentation process. The locations of the maximum strain are close to each other for the dome and the rectangular indented pipes. However, this is not true for the sphere indented pipes although the dome and sphere indenters are closer in shape.

- The location of the maximum strain depends on the indenting pressure. For example, the location of the maximum strain for specimen DP20D8 occurs at a distance of 100 mm from the dent center, but that of specimen DP0D8 occurs at a distance of 75 mm from the dent center for the longitudinal axis. The locations of the maximum strains are the same for the circumferential axis for both dome specimens (See Table 4.1 to Table 4.4).

- The maximum strain locations vary between the longitudinal vs. the circumferential locations. For the longitudinal axis it is observed that the

maximum strains occur away from the dent center as for the circumferential axis they occur closer to the dent center.

- The dent shape has a significant influence on the strain values at and near the dented region. For the rectangular and dome dented pipes, the maximum strain occurs in the circumferential axis while for the sphere dented pipes the maximum strain occurs in the longitudinal axis.
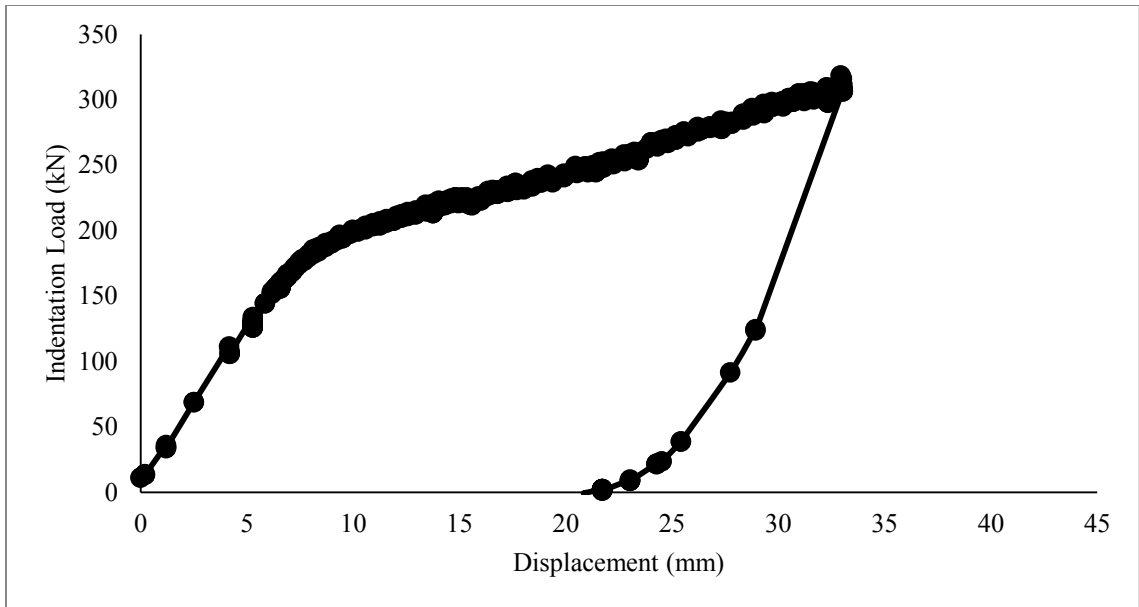
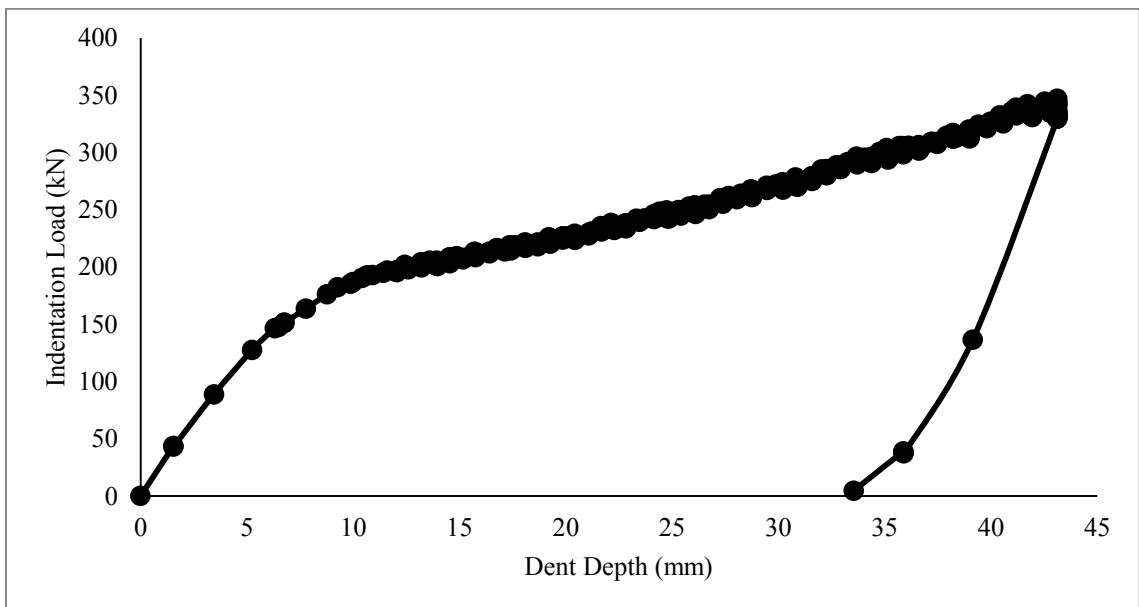Figure 4.1: RP20D8 Experimental Load-Displacement Behaviour (Rafi 2011)

Figure 4.2: RP20D12 Experimental Load-Displacement Behaviour (Rafi 2011)
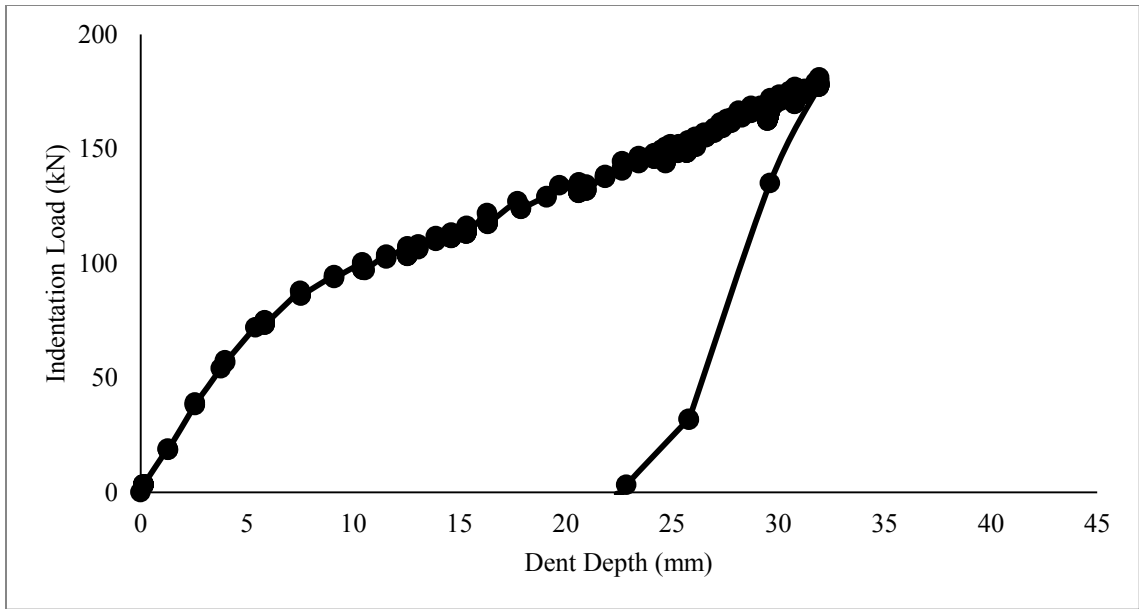
Figure 4.3: DP20D8 Experimental Load-Displacement Behaviour (Rafi 2011)
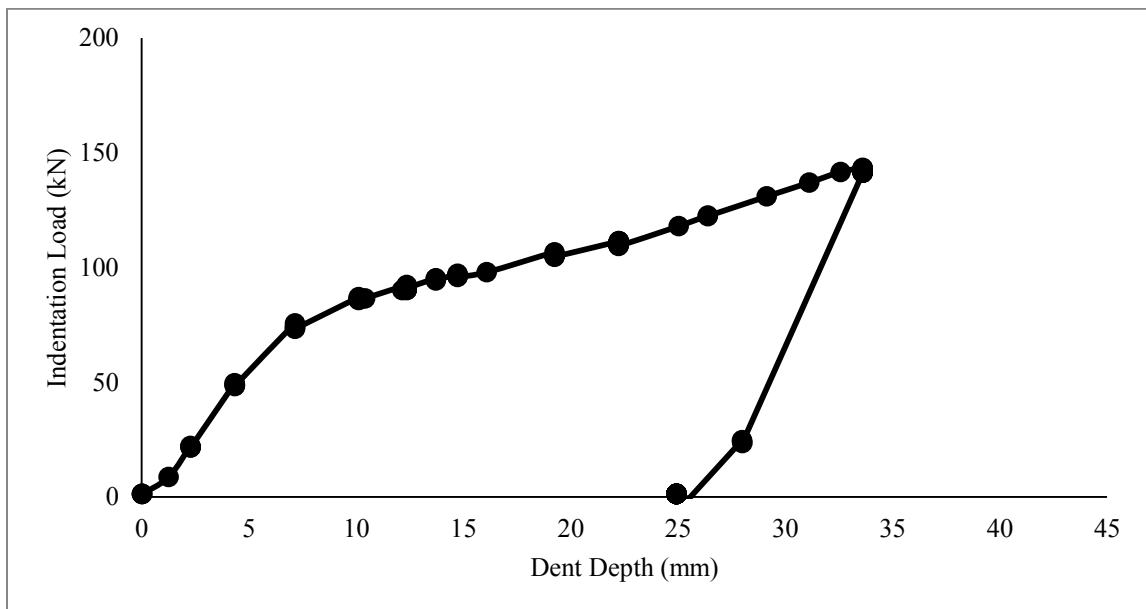

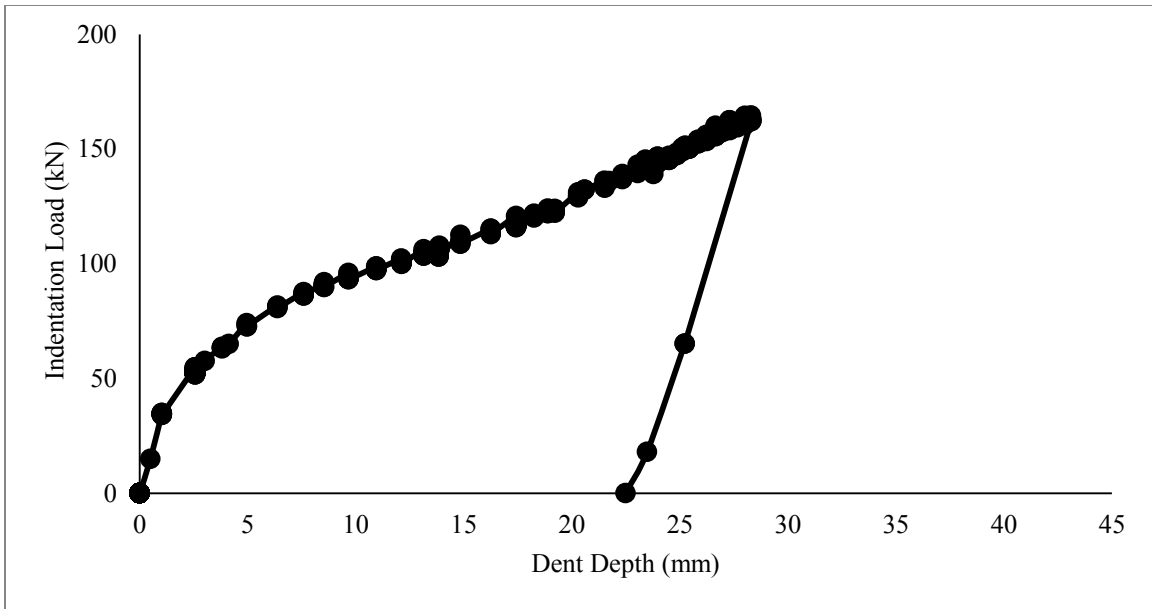Figure 4.4: DP0D8 Experimental Load-Displacement Behaviour (Rafi 2011)

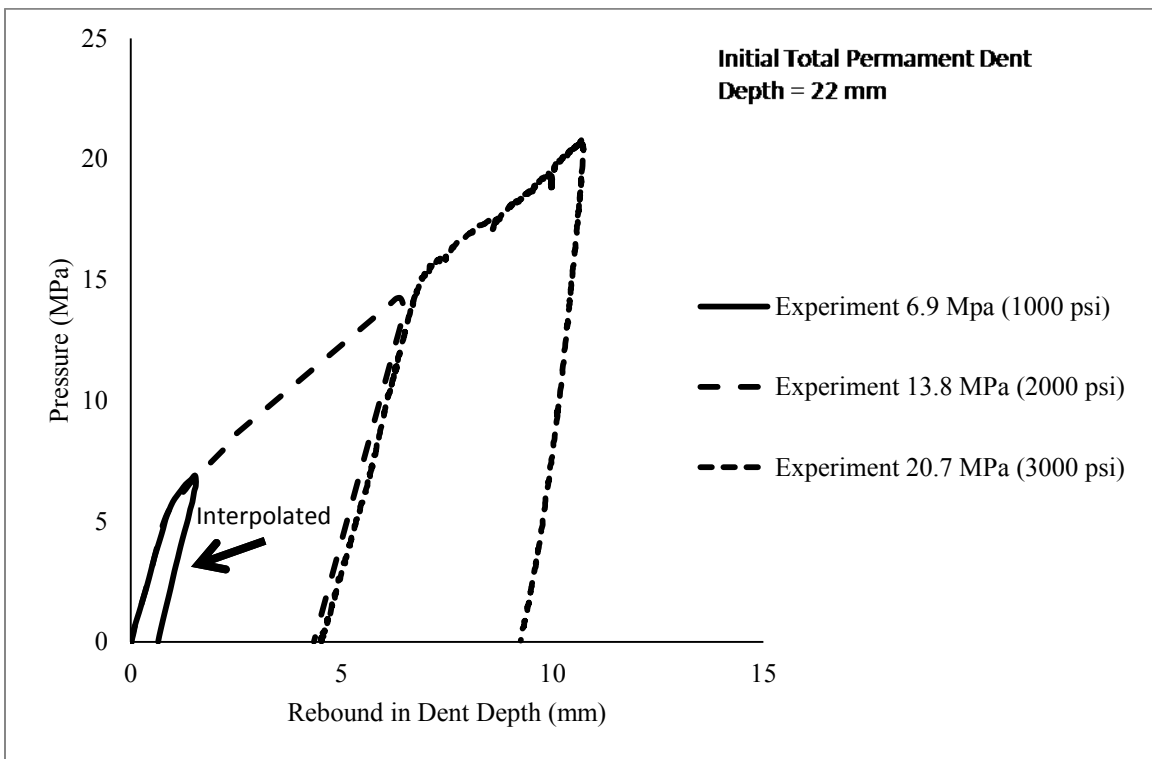Figure 4.5: SP20D8 Experimental Load-Displacement Behaviour (Rafi 2011)

Figure 4.6: RP20D8 Experimental Pressure-Displacement Behaviour
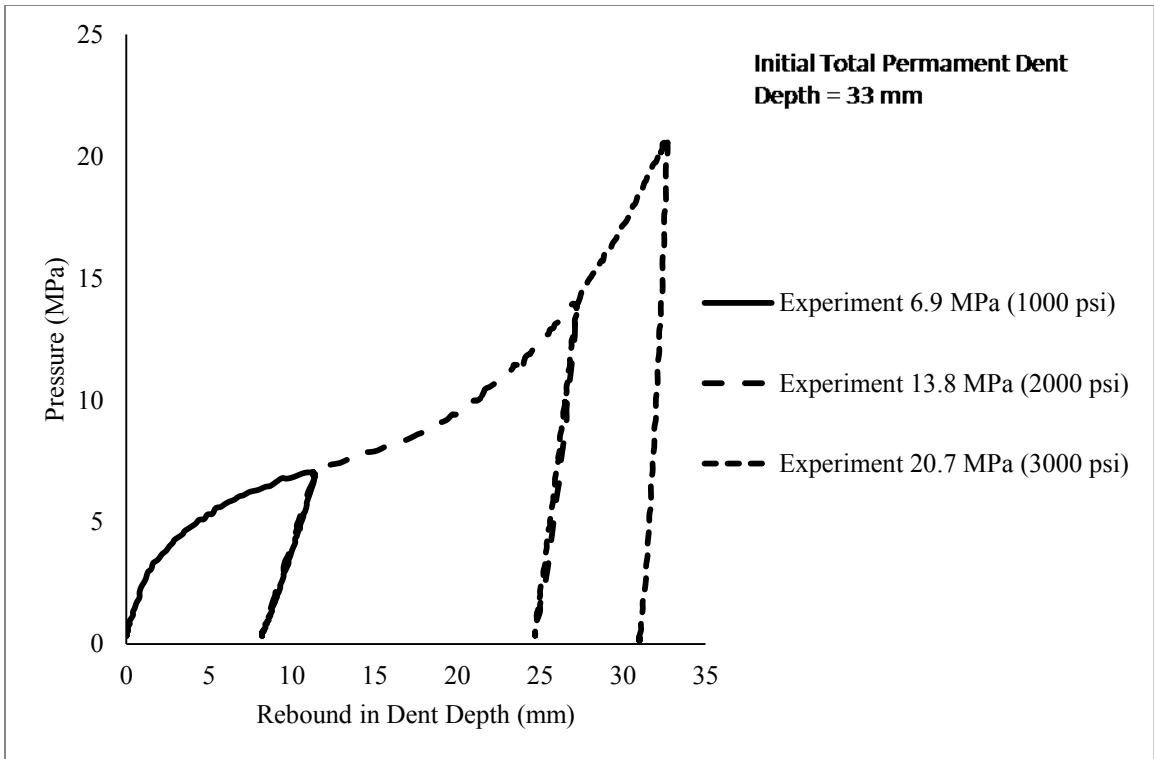
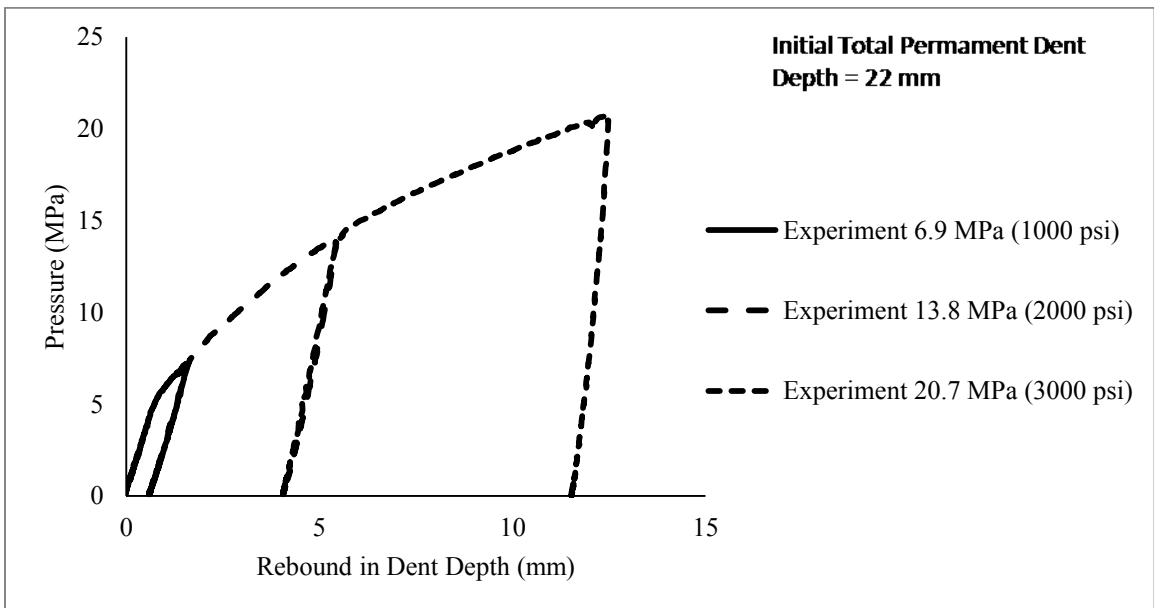Figure 4.7: RP20D12 Experimental Pressure-Displacement Behaviour

Figure 4.8: DP20D8 Experimental Pressure-Displacement Behaviour
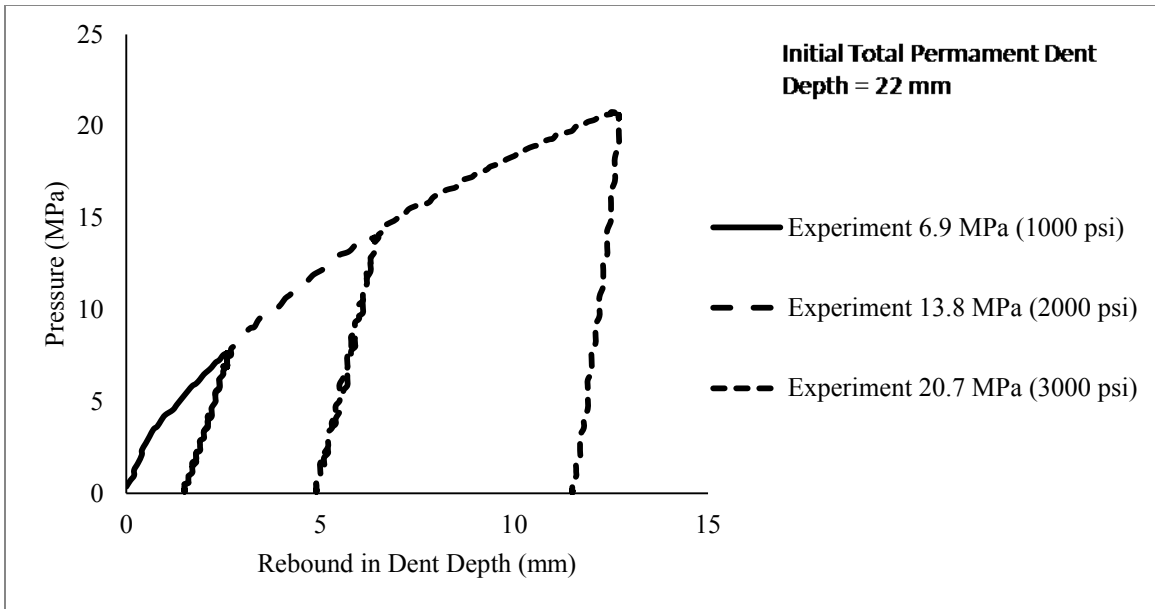
Figure 4.9: DP0D8 Experimental Pressure-Displacement Behaviour
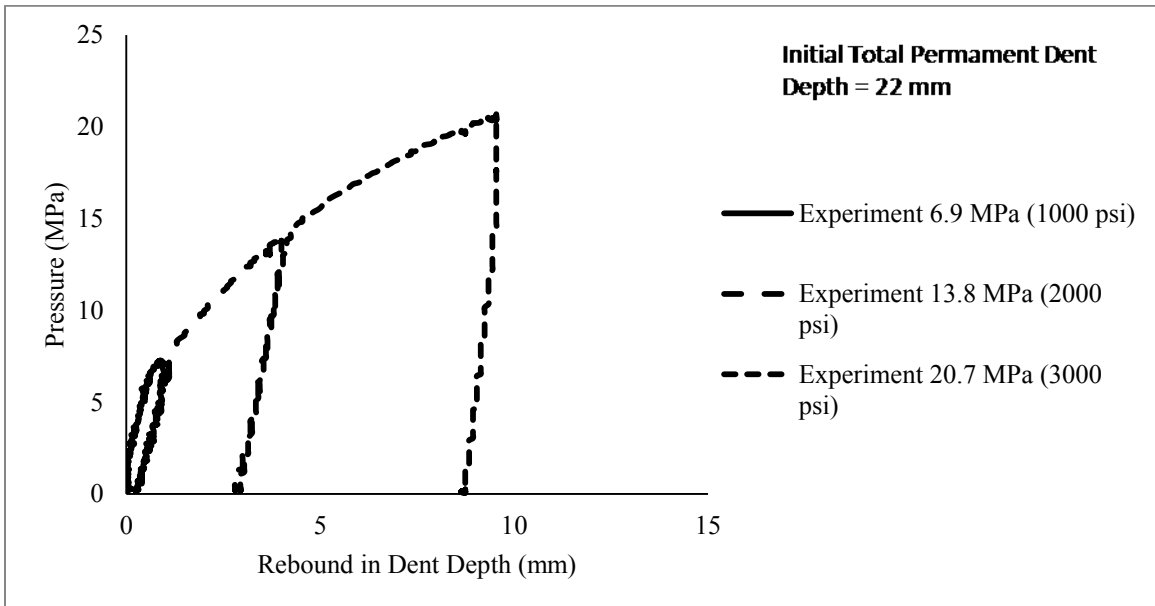

Figure 4.10: SP20D8 Experimental Pressure-Displacement Behaviour

Figure 4.11(a): Longitudinal Strain for RP20D8 Specimen at 20.7 MPa (3000 psi)

Figure 4.11(b): Longitudinal Strain for RP20D8 Specimen at 0 MPa (0 psi)

Figure 4.11(c): Circumferential Strain for RP20D8 Specimen at 20.7 MPa (3000 psi)

Figure 4.11(d): Circumferential Strain for RP20D8 Specimen at 0 MPa (0 psi)
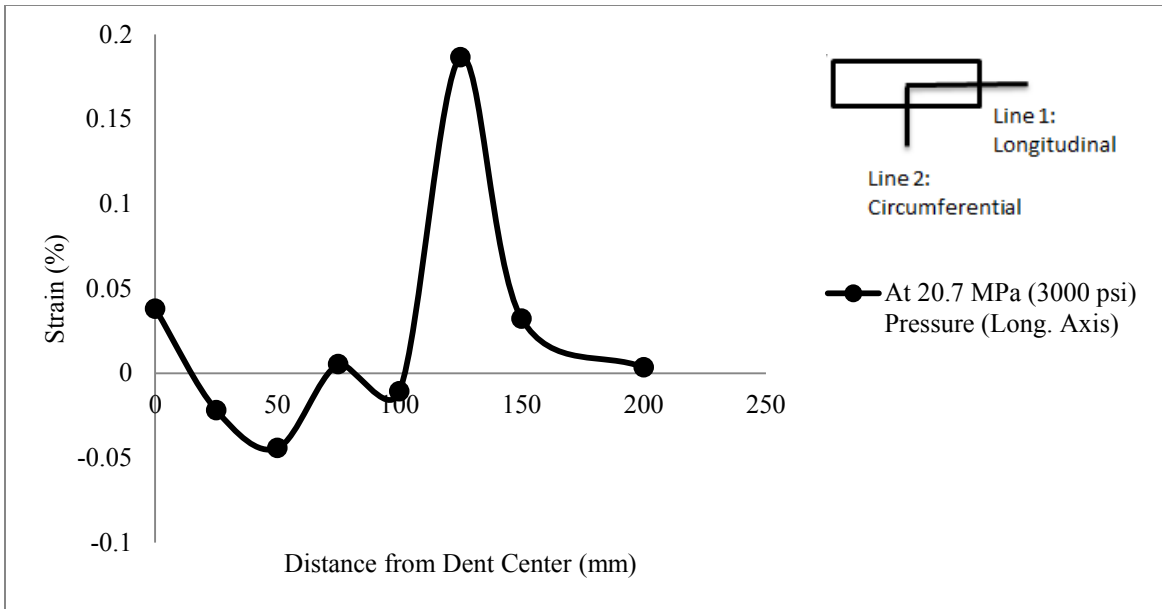
Figure 4.12(a): Longitudinal Strain for RP20D12 Specimen at 20.7 MPa (3000 psi)

Figure 4.12(b): Longitudinal Strain for RP20D12 Specimen at 0 MPa (0 psi)

Figure 4.12(c): Circumferential Strain for RP20D12 Specimen at 20.7 MPa (3000 psi)

Figure 4.12(d): Circumferential Strain for RP20D12 Specimen at 0 MPa (0 psi)

Figure 4.13(a): Longitudinal Strain for DP20D8 Specimen at 20.7 MPa (3000 psi)
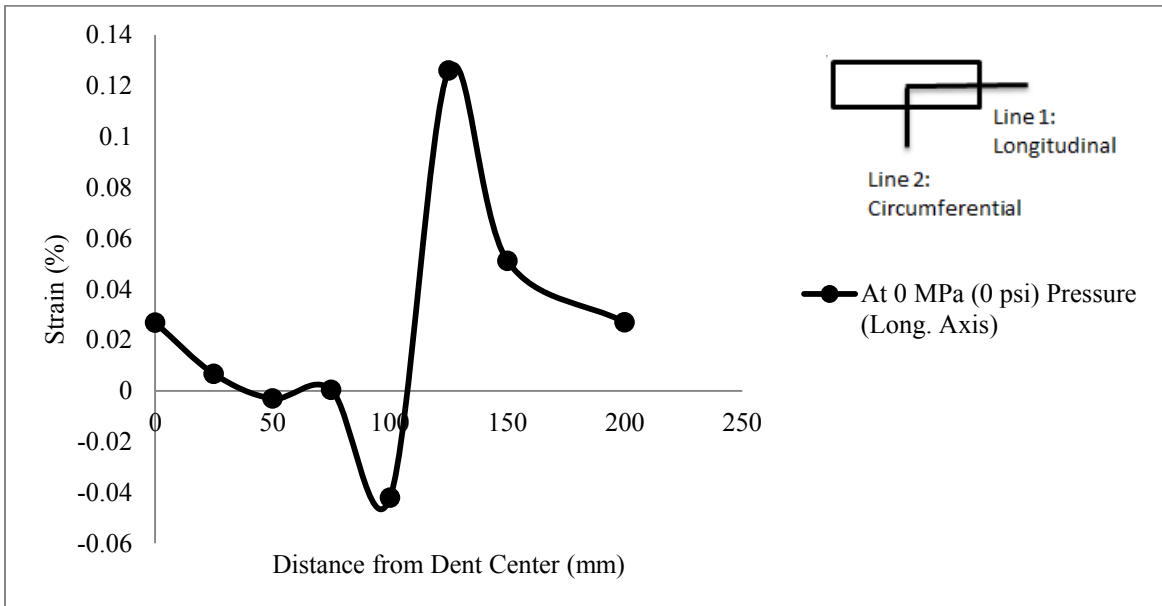

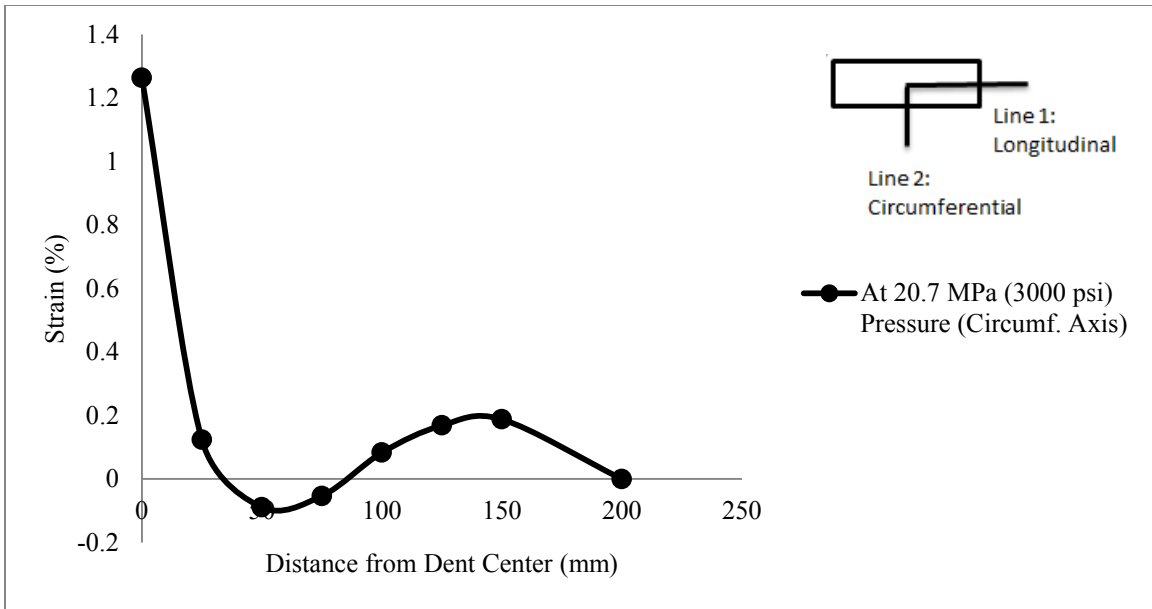Figure 4.13(b): Longitudinal Strain for DP20D8 Specimen at 0 MPa (0 psi)

Figure 4.13(c): Circumferential Strain for DP20D8 Specimen at 20.7 MPa (3000 psi)

Figure 4.13(d): Circumferential Strain for DP20D8 Specimen at 0 MPa (0 psi)
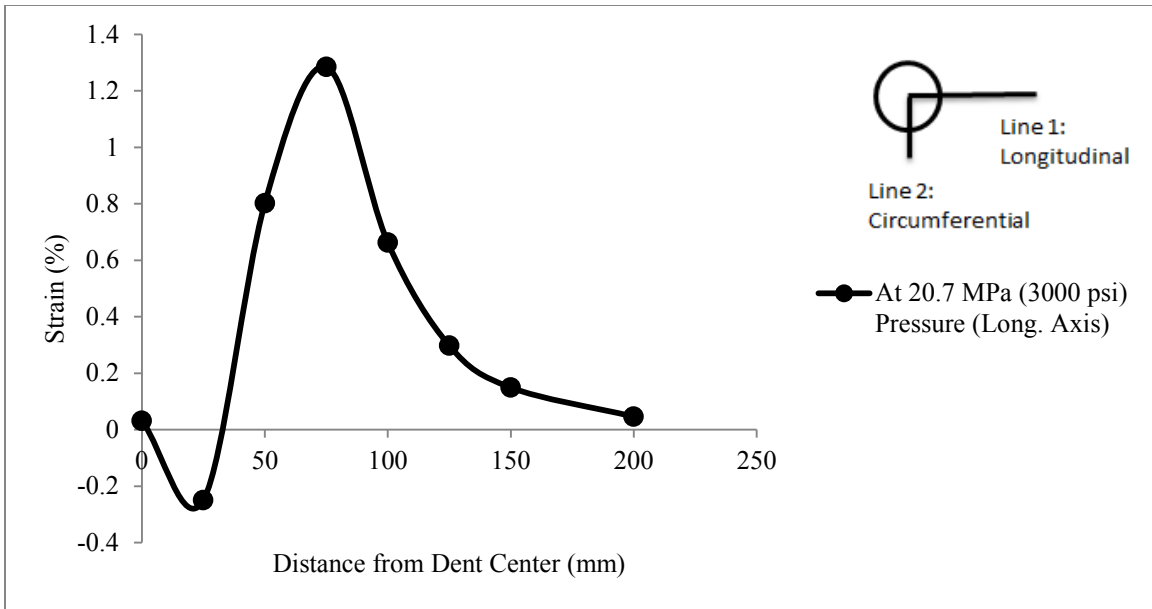
Figure 4.14(a): Longitudinal Strain for DP0D8 Specimen at 20.7 MPa (3000 psi)
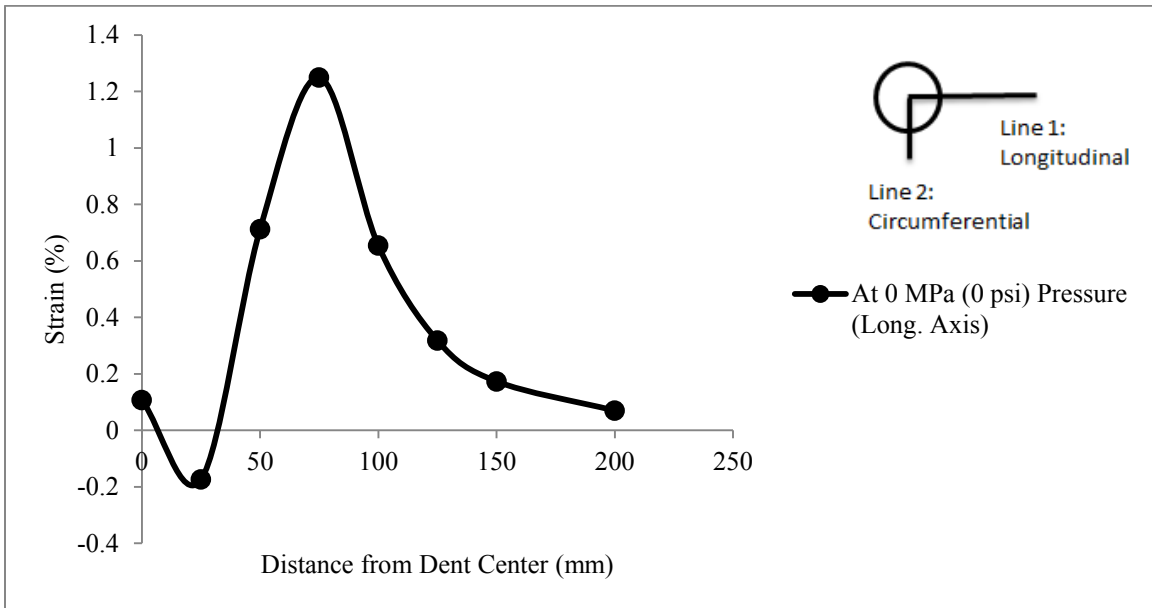
Figure 4.14(b): Longitudinal Strain for DP0D8 Specimen at 0 MPa (0 psi)
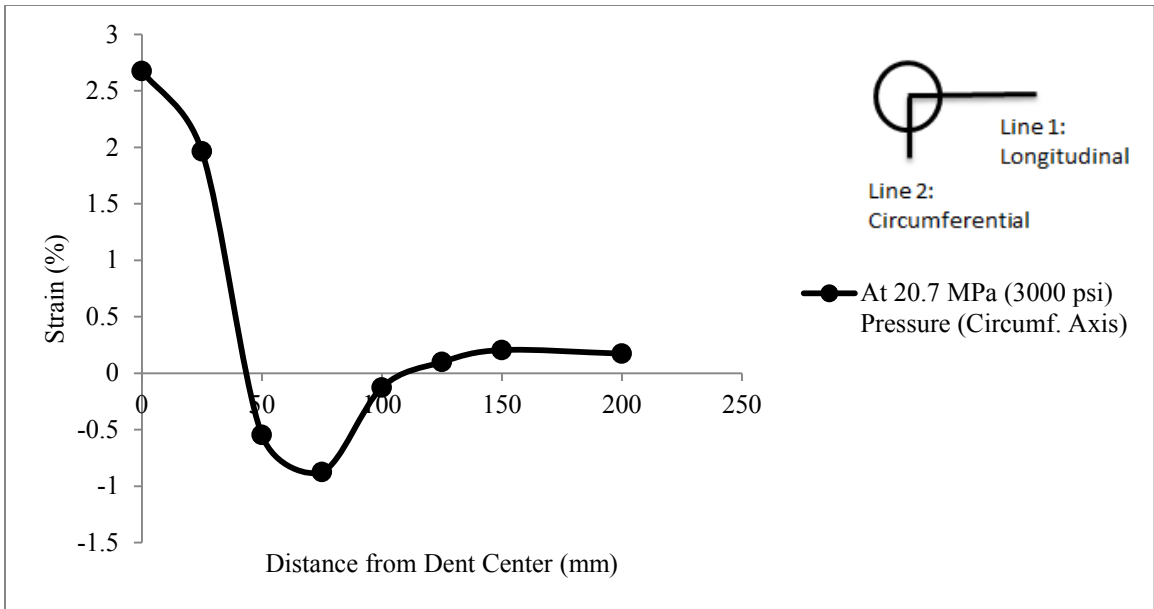
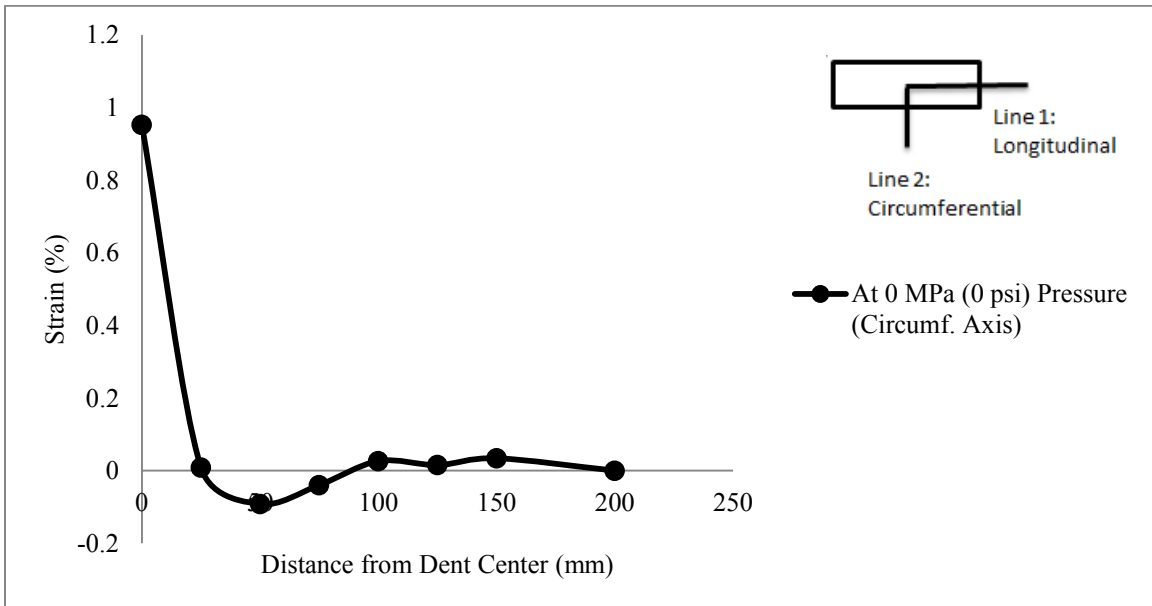Figure 4.14(c): Circumferential Strain for DP0D8 Specimen at 20.7 MPa (3000 psi)
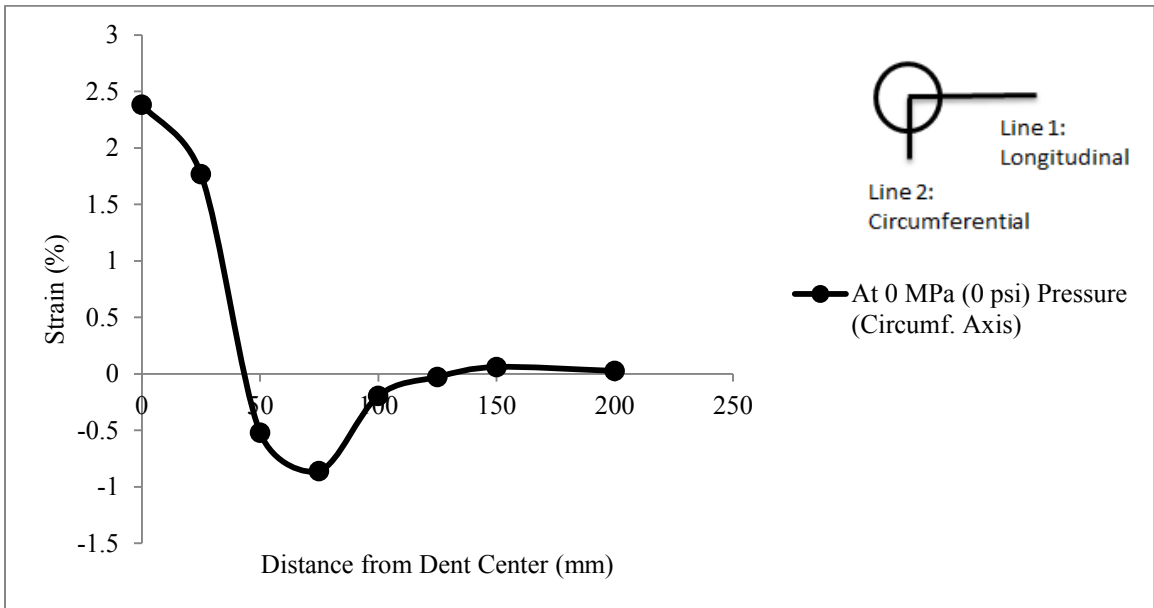
Figure 4.14(d): Circumferential Strain for DP0D8 Specimen at 0 MPa (0 psi)
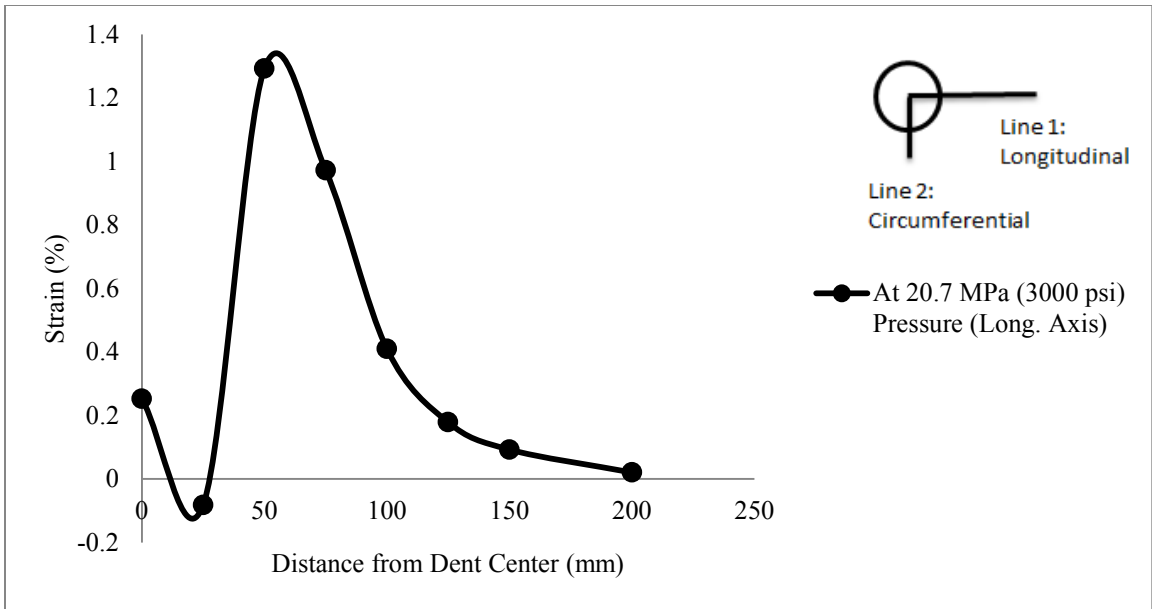
Figure 4.15(a): Longitudinal Strain for SP20D8 Specimen at 20.7 MPa (3000 psi)
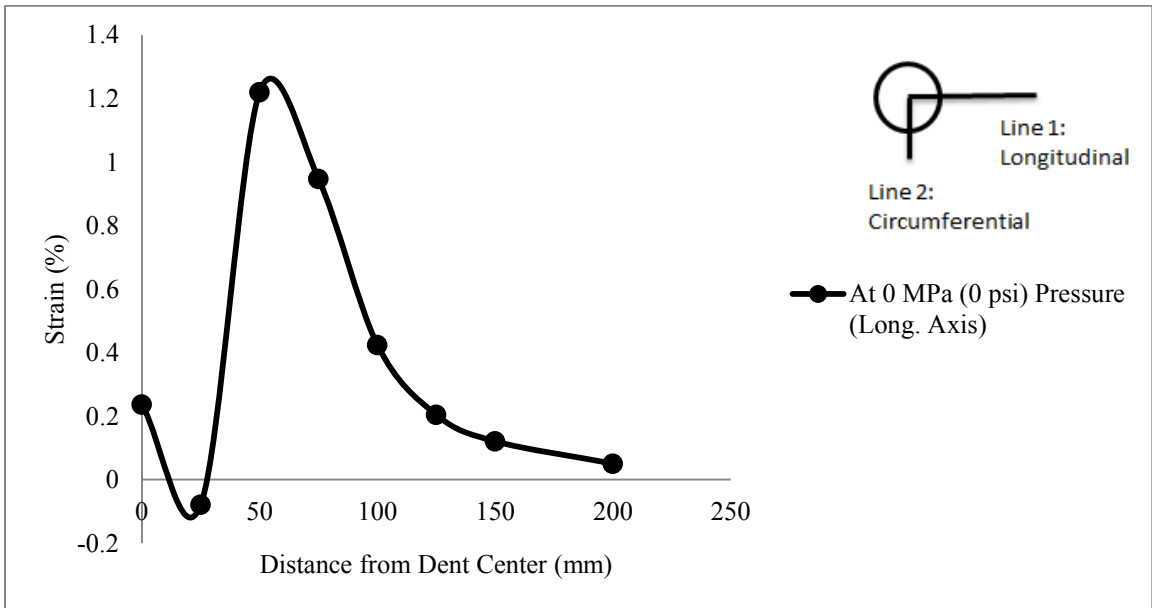
Figure 4.15(b): Longitudinal Strain for SP20D8 Specimen at 0 MPa (0 psi)
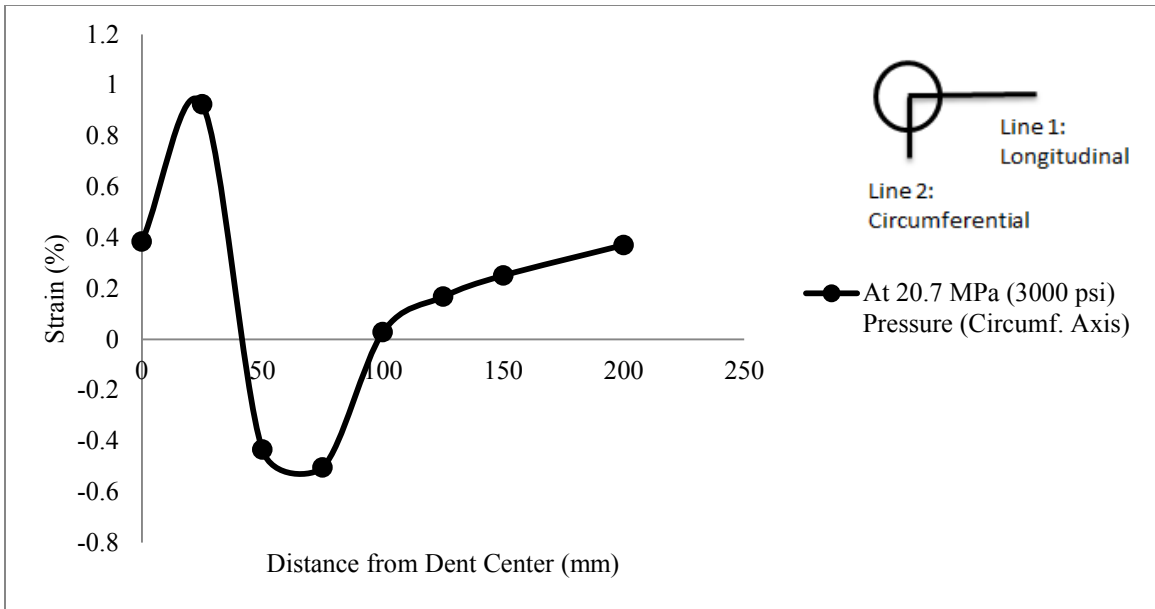
Figure 4.15(c): Circumferential Strain for SP20D8 Specimen at 20.7 MPa (3000 psi)

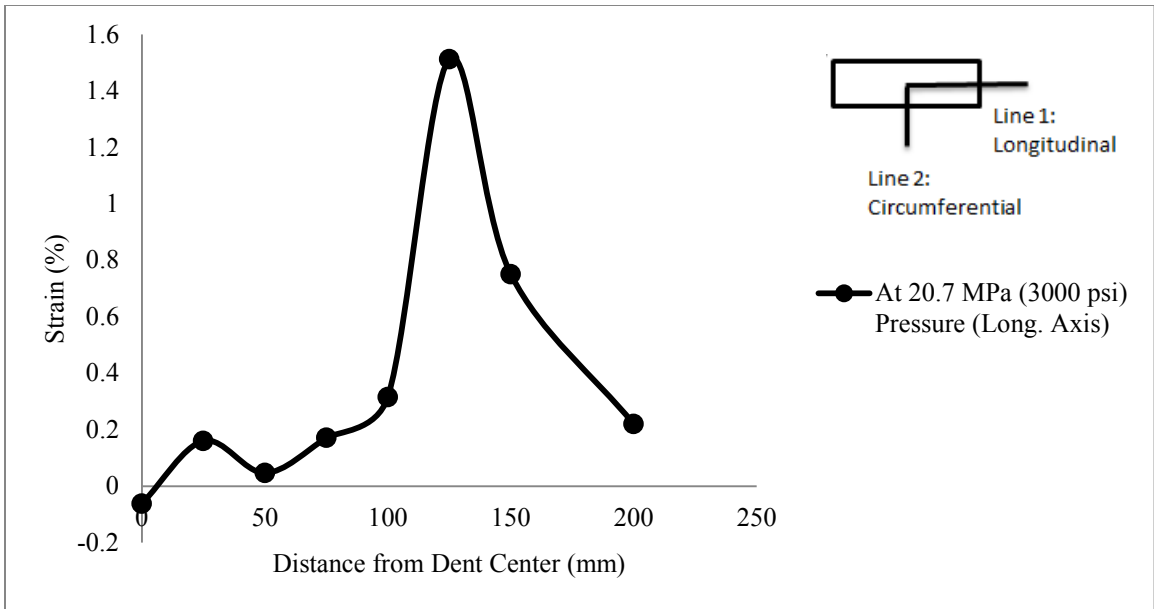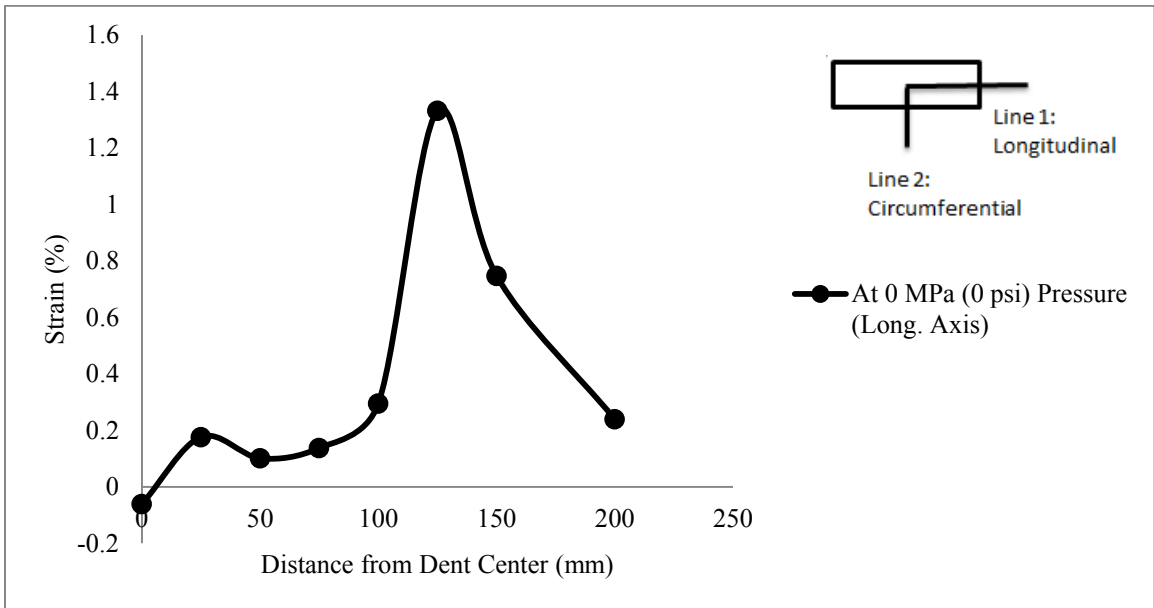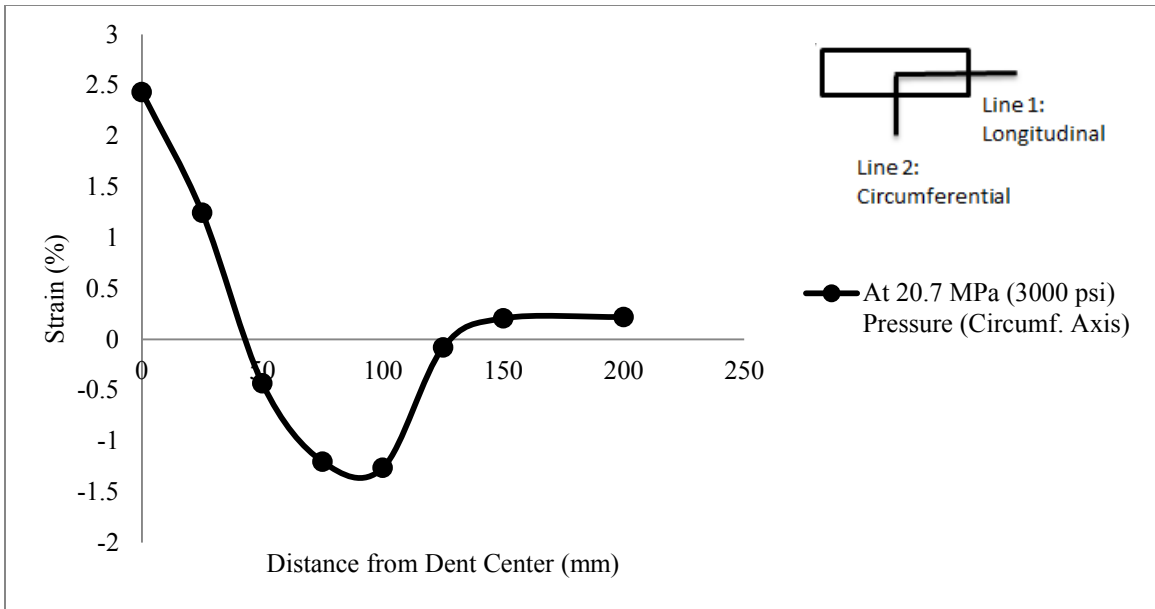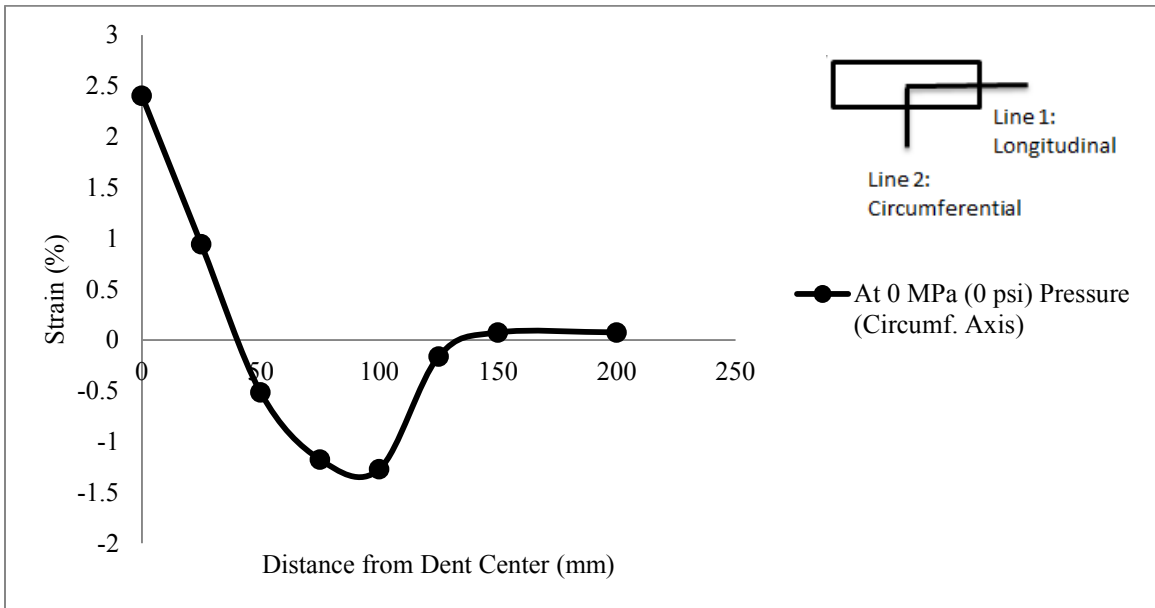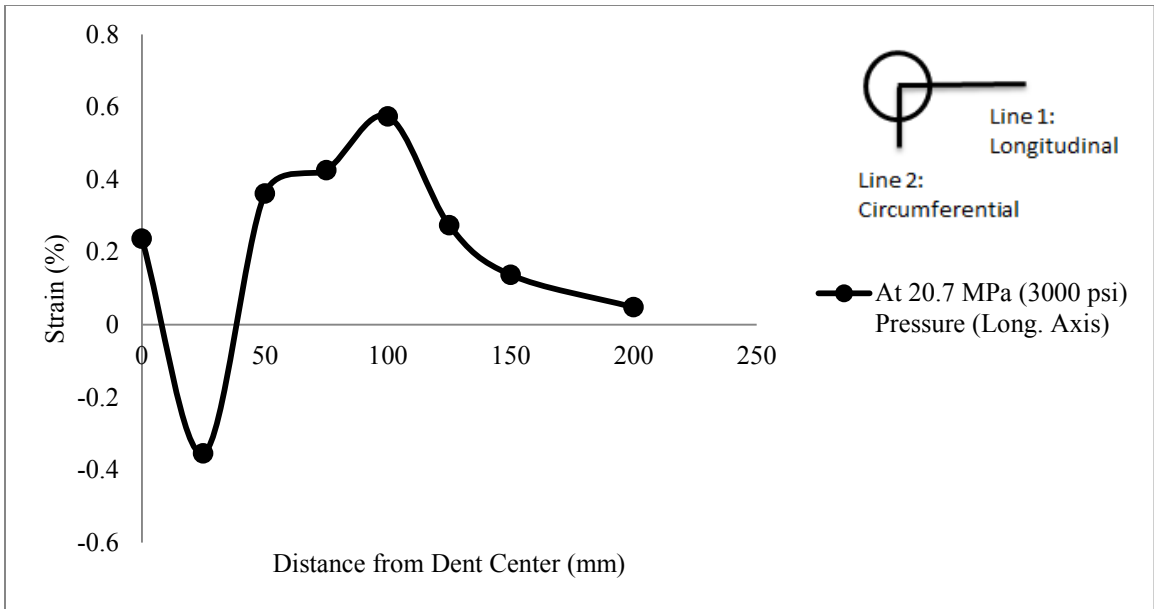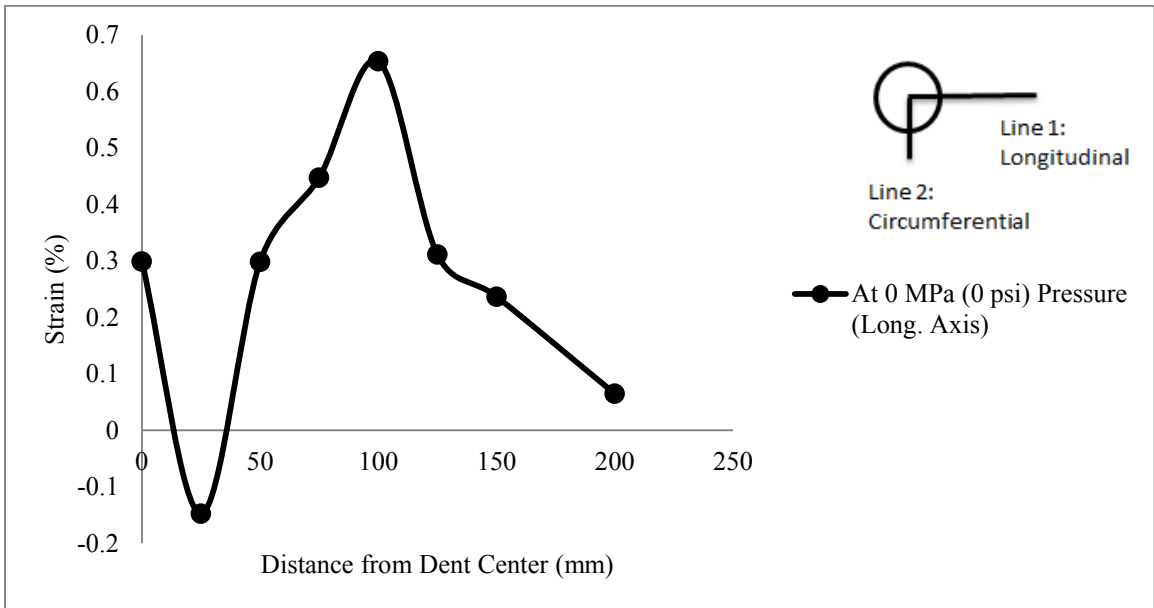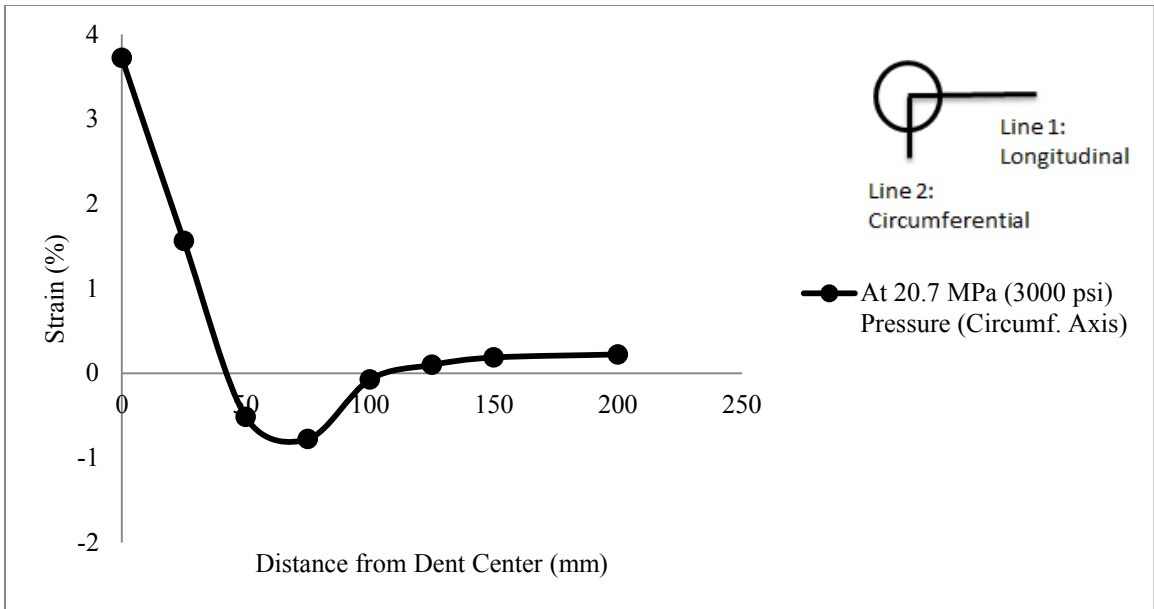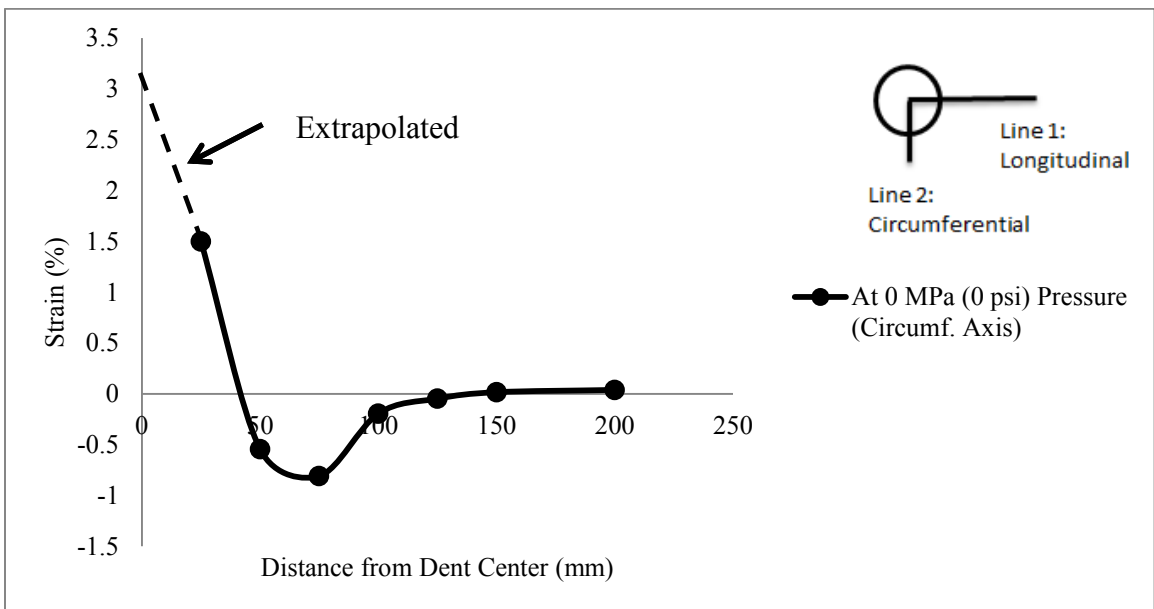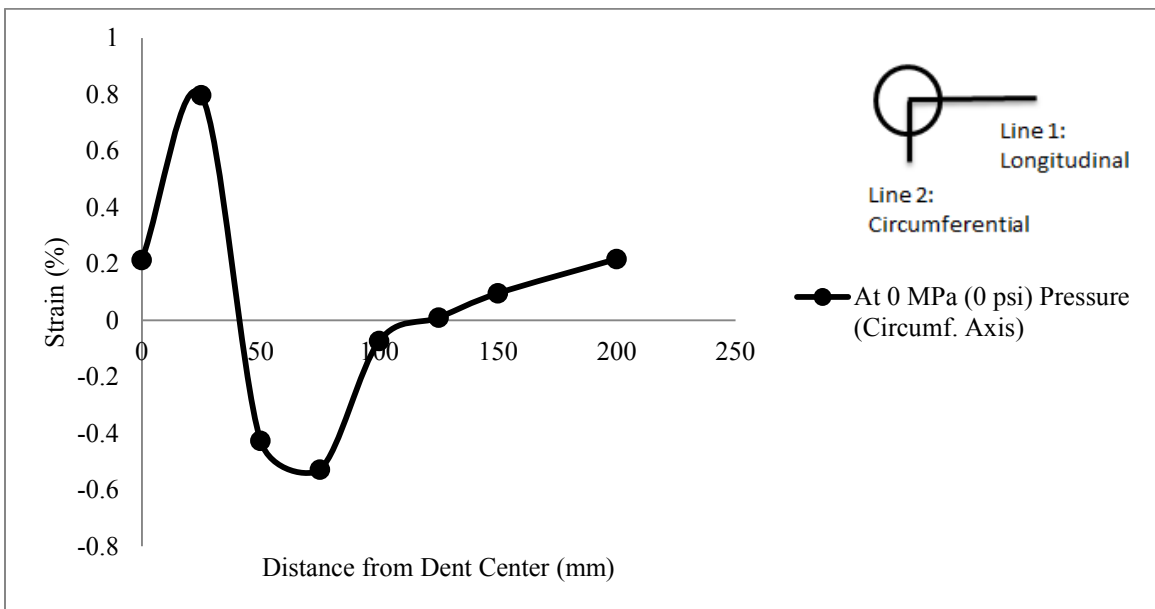Figure 4.15(d): Circumferential Strain for SP20D8 Specimen at 0 MPa (0 psi)

59

Table 4.1: Effect of Indenter Shape, Dent Depth, and Indenting Pressure on Maximum Strain at Maximum Pressure (Tension)

Indenter	Dent Depth (d/D) %	Indenting Pressure (MPa)	Max. Pressurizing Pressure (MPa)	Max. Longit. Strain %	Location (mm)	Max. Circumf. Strain %	Location (mm)
Rectangle	8	20		0.19	125	1.26	0
Rectangle	12	20		1.51	125	2.43	0
Dome	8	20	20.7	0.57	100	3.72	0
Dome	8	0		1.29	75	2.67	0
Sphere	8	20		1.29	50	0.92	25

Table 4.2: Effect of Indenter Shape, Dent Depth, and Indenting Pressure on Maximum Values at Zero Pressure (Tension)

Indenter	Dent Depth (d/D) %	Indenting Pressure (MPa)	Max. Pressurizing Pressure (MPa)	Max. Longit. Strain %	Location (mm)	Max. Circumf. Strain %	Location (mm)
Rectangle	8	20		0.13	125	0.95	0
Rectangle	12	20		1.33	125	2.39	0
Dome	8	20	0	0.65	100	* 3.1	* 0
Dome	8	0		1.25	75	2.38	0
Sphere	8	20		1.22	50	0.79	25

* Educated guess was made as strain gauge failed during de-pressurization process

Table 4.3: Effect of Indenter Shape, Dent Depth, and Indenting Pressure on Maximum
Values at Maximum Pressure (Compression)

Indenter	Dent Depth (d/D) %	Indenting Pressure (MPa)	Max. Pressurizing Pressure (MPa)	Max. Longit. Strain %	Location (mm)	Max. Circumf. Strain %	Location (mm)
Rectangle	8	20		0.044	50	0.089	50
Rectangle	12	20		0.062	0	1.27	100
Dome	8	20	20.7	0.35	25	0.78	75
Dome	8	0		0.25	25	0.88	75
Sphere	8	20		0.082	25	0.50	75

Table 4.4: Effect of Indenter Shape, Dent Depth, and Indenting Pressure on Maximum
Values at Zero Pressure (Compression)

Indenter	Dent Depth (d/D) %	Indenting Pressure (MPa)	Max. Pressurizing Pressure (MPa)	Max. Longit. Strain %	Location (mm)	Max. Circumf. Strain %	Location (mm)
Rectangle	8	20		0.042	100	0.092	50
Rectangle	12	20		0.062	0	1.27	100
Dome	8	20	0	0.15	25	0.81	75
Dome	8	0		0.17	25	0.86	75
Sphere	8	20		0.078	25	0.53	75

CHAPTER 5

5.0 FEA

5.1 Overview

Finite element model (FEM) was used to obtain the necessary information needed to achieve a better understanding of the experimental data and behaviour of dent subject to monotonically increasing internal pressure. This chapter emphasizes how the use of FEM was carried out to develop the numerical model. Validating the FE model with experimental test results is also necessary in order to have similar characteristics and to obtain comparable results with the experimental data. FE modeling was carried out to simulate the behavior of the experimental specimens by adopting similar geometry and material properties. The FEM tool ABAQUS/Standard version 6.11 distributed by SIMULIA was used to carry out the numerical modeling analysis. This tool was chosen as it is able to model pipelines with elasto-plastic isotropic and hardening material properties that are comparable to those from the experimental pipe specimens. Another reason to use such modeling tool is because it is one of the most popular and effective tools used to develop pipeline models that have a comparable denting load. This is demonstrated in other research such as the one conducted by Karamanos and Andreadakis (Karamanos and Andreadakis 2006). Furthermore, ABAQUS/Standard has also options for contact interaction that can simulate the experimental boundary conditions more precisely. The purpose of generating a pipeline model with ABAQUS/Standard is to be able to more precisely predict the behaviour of a dented pipeline when it is being pressurized. Another reason is to obtain the strains within such dent in order to determine if a pipe is within the safe region. Lastly, a parametric study can also be conducted with the help of such modeling tool to develop a guideline that can be used to determine if a dented pipeline is safe. Such guideline will include different types of indenters, internal pressures, and D/t ratios. With this finite element program the

pipe specimens were developed and tested under similar experimental conditions. The development of FE models was done with the support from other students of CERP.

5.2 Modeling

The indentation tests were completed in a previous study (Rafi 2011). However FE simulations are undertaken in the current study. The finite element (FE) model for the pipelines was comprised of an S4R four-node linear doubly curved general purpose shell elements with reduced integration, hourglass control, and finite membrane strain formulation. Each node has three rotational and three translational degrees of freedom. Five integration points were chosen through the thickness of the element. Two flat shaped end caps were used in the model with less than 3000 shell elements. The end caps had a shell thickness of 50 mm which resemble those used in the experiment. The shell elements for the end caps were also S4R. The indenter was composed of 511 R3D4 four-node 3-D bilinear rigid quadrilateral shell elements. The side support conditions were merged into the pipe and the middle support was imbedded into the pipe. Figures 5.1 to 5.3 show the different pipelines that were modeled with end caps and supports in place. More information on each separate part is provided in the following sections.

5.3 Mesh Sensitivity Analysis

A mesh study was needed in order to come up with an efficient way of meshing the pipelines to produce comparable results with the least time possible. Different mesh sizes were compared to determine an optimal solution. The mesh sizes used were 3 mm, 4 mm, 5 mm, 6 mm, 8 mm, and 15 mm. As shown in Figure 5.4 it is observed that there is a small difference between the different mesh sizes. When comparing the discrepancy between the results to the computational time, it was found that an optimal solution was reached when using 5 mm mesh.

Furthermore, the effect of changing the size of the mesh at and near the dented region of the pipe was studied. The mesh size was varied from the mid-length of the pipe to its ends. A finer mesh was used at the mid-length and it increased at the ends as the middle portion of the pipeline suffered the dent (See Figure 5.5). Different mesh sizes were used in this study starting with 5mm square elements at the mid-length covering a length of 100 mm and 20 mm square elements towards the ends of the pipeline. Another size used was 3 mm square elements at the center and 20 mm square elements at the ends. The effect of such change resulted in similar results compared to having the same mesh all around the pipe (See Figure 5.6). The total solution time required on a Dell XPS 8300 with an Intel® Core™ i5-2320 with 8GB of system RAM is 420 min, 300 min, 120 min, 75 min, 55 min, and 10 min respectively. Hence, it was decided to use a uniform mesh of 5 mm x 5 mm throughout the pipe (See Figure 5.7). The total number of elements used in each pipe specimen was 110,815 for the 3 mm mesh, 63, 027 for the 4 mm mesh, 40,645 for the 5 mm mesh, 28,404 for the 6 mm mesh, 16,255 for the 8 mm mesh, and 4,570 for the 15 mm mesh.

The indenters however, were meshed using a bigger element size. The optimal size of the indenters was also chosen in order to obtain a balance between the accuracy of data and the solution time of ABAQUS/Standard. The optimal size used when meshing the rectangular, dome and sphere indenters was 8.5 mm x 8.5 mm. The total number of elements in each indenter was 2,476, 511, and 212 for the rectangular, dome, and spherical indenters, respectively.

5.4 Pipe

Each pipe specimen used was 1100 mm long with an outer radius of 137 mm and an inner radius of 129 mm. The meshing technique was free meshing with quad-dominated element shape and S4R element. The meshing selected was a uniform mesh of 5 mm x 5 mm as seen in Figure 5.7.

5.5 End Caps

The end caps were meshed using a quad-dominated element shape with a free technique. The element type used was also S4R. The shape of the end caps used was shown in Figures 5.1 to 5.3. The end caps were modeled with a 50 mm thick section with an elastic isotropic material behaviour since the plasticity did not occur in these plates. Furthermore, the end caps have a Young's modulus (E) of 200 GPa, and a Poisson's ratio of 0.3. Such properties closely model those obtained from the experiment. The material properties are seen in Table 3.1, and the Tensile Coupon curve is seen in Figure 3.1.

5.6 Contact Formulation between Surfaces

In the denting tests (Rafi 2011), the indenters came into contact with the pipes, introducing an inward deformation on the pipe wall. In order to model this in ABAQUS, a contact algorithm was introduced. This contact acts between the indenter and the outer surface of the pipe. In ABAQUS/Standard, there are two different ways of modeling the contacts needs. They are finite sliding and small sliding. For small sliding, only a small amount of sliding can occur relative to the surfaces that are being contacted. However, for finite sliding, there is an arbitrary range of sliding that can be allowed. This type is sliding is most commonly used due to its versatility. Additionally, a surface-to-surface (SS) discretization method was used for this FE model. This method is the standard discretization method provided in ABAQUS/Standard. With this approach, the surfaces having contact are required to be defined. A master surface and a slave surface must be defined in order to create a SS contact. ABAQUS/Standard provides guidelines regarding the selection of such surfaces. The indenters were chosen as the master surface as their surface is stiffer than that of the pipelines. The pipeline was then chosen as the slave surface.

Different contact formulations were used for the support contacts at the sides and at the mid-length of the pipe specimen. As it is described in the next section, the optimal balance between the results and the solution time was obtained for the chosen supports.

5.7 Supports

Various support conditions were simulated in the FE model to determine the most efficient way of implementing the supports onto the pipelines. This was done to be able to simulate the supports used in the experiments (See Figure 3.2 and 3.3). The supports used in the experiments were blocks of 305 mm length, 171 mm width, and a thickness of 50 mm with a 185 mm groove centered along the length of the support. The supports used in the FE model resembled the ones used in the experiment. The supports were used at three different points along the length of the pipes: these are at the two ends and at the mid-length of the pipe (See Figure 5.1 to 5.3).

For the FEM, four different types of support arrangements were simulated to determine a better fit. The first arrangement was comprised of contact interaction at the ends of the pipe and an imbedded (considered a regular type of BC) for the mid-support. The second arrangement was where all three supports were imbedded. The third arrangement was contact interaction in the middle and the side supports were imbedded. The last arrangement was to use merged contacts at the sides and imbedding the middle support. Imbedded contacts are contacts that are sections of the pipe designated as supports, rather than a new part, independent of the pipe itself, being designated as the support. A merged contact is an independent part, separate from the pipe, acting as the support but rather than using a contact interaction to connect the two parts ABAQUS allows for a merge to take place between the two parts.

The first arrangement was to keep the middle support imbedded into the pipeline. When using contacts for side supports, the boundary conditions used restricted all movement between the base of the support and the surrounding area in order to prevent the contacts

from moving out of place. The dimensions of the contact supports used in the model resembled those in the experiment; however, the thickness and hence the contact surface was changed after many different trials in order to achieve realistic simulation of the supports.

The second arrangement was to keep the middle and side supports imbedded. The boundary conditions used restricted all translational degrees of freedom as well as the torsional degree of freedom (U1, U2, U3 and UR2). The surface used when imbedding the supports onto the pipes was developed after many trials in order to simulate similar results to those from the experiment. The load-deformation behaviour when using contacts or imbedding the side supports is shown in Figure 5.8. This Figure shows very similar results when comparing the use of imbedding the side supports (second arrangement) to that of using contact interaction at the sides (first arrangement).

The third arrangement was to keep the side supports imbedded into the pipelines while changing the mid-support with a contact interaction. When using a contact for the mid-support, the BC used restricted the movement of the support away from the pipelines. When imbedding the side supports onto the pipelines, the BCs used restricted all translational degrees of freedom as well as the torsional degree of freedom (U1, U2, U3, and UR2). The load-displacement behaviour of the mid-support when using a contact algorithm is shown in Figure 5.9. This figure shows similar results when comparing the use of a middle contact interaction (third arrangement) to that of using an imbedded mid-support (second arrangement).

The fourth arrangement was to merge the supports at the sides and keep the mid-support imbedded. ABAQUS/Standard allows for merging to take place so that two different parts can become one. The BCs used for the merged supports at the sides restricted all translational degrees of freedom as well as all the rotational degrees of freedom (U1, U2 U3, UR1, UR2 and UR3). The BCs used for the mid-support, which was imbedded, restricted all translational degrees of freedom as well as the torsional degree of freedom (U1, U2, U3 and UR2).

As can be seen in Figure 5.10, it was concluded to use the fourth arrangement as it proved to be the more efficient type of supports as compared to the experimental test.

5.8 Indenter

For the FEM three different indenter shapes were used: 80 cm diameter dome indenter, 50 cm diameter sphere indenter, and a rectangular indenter. The rectangular indenter is a rectangular prism with bottom dimensions 100 mm by 20 mm and top dimensions 164 mm by 87 mm. The dome, sphere and rectangular indenters were all modeled using R3D4 four-node 3-D bilinear rigid quadrilateral shell elements. The sizes and shapes of all three indenters were modeled according to the size and shape of those used in the experiments to obtain similar results.

5.9 Material Properties

In order to determine the material properties to be used when modeling the pipelines, coupon specimens were tested in accordance with ASTM E E 8/E 8M-08 specification (ASTM E28.04 Subcommittee 2013) to obtain the uniaxial engineering stress-strain behavior of the pipe material (Rafi 2011). Since the section of the pipe specimen under the indenter experienced plastic deformation, a non-linear elastic-plastic material modeling technique was used along with von Mises yield criterion and isotropic hardening was used for numerical modeling. Since ABAQUS/Standard requires the total stress and the plastic strains, the following equations were used in order to obtain such values.

$$\sigma_{\text{true}} = \sigma_{\text{nom}}(1 + \varepsilon_{\text{nom}}) \qquad\qquad (5.1)$$

$$\varepsilon_{\text{ln}}^{\text{pl}} = \ln(1 + \varepsilon_{\text{nom}}) - \frac{\sigma_{\text{true}}}{E} \qquad\qquad (5.2)$$

Where σ_{true} is the true stress, ε_{ln}^{pl} is the true or logarithmic plastic strain, σ_{nom} is the nominal stress or engineering stress, ε_{nom} is the nominal strain, and E is Young's modulus.

Since the end caps do not experience plastic deformation, it was modeled as an elastic material.

5.10 Denting Process

Though the denting was conducted in the previous study of CERP (Rafi 2011). The numerical study was developed and validated in the current study. Support and guidance was provided by other members of CERP.

The load was applied in the FEM in various load steps that resembled the procedure used in the experimental loading procedure. The first step was to apply the internal pressure within the pipe. This was applied as a distributed load. The pressure was varied between 0 to $0.40p_y$, where p_y is the internal pressure that causes circumferential yielding. Such pressure was calculated using the following relationship.

$$p_y = \frac{\sigma_y t}{r} \tag{5.3}$$

Where σ_y is the yield stress of the pipe material, t is the thickness of the pipe wall, and r is the outer radius of the pipe.

Next, the indenter was applied using the displacement central method. The stroke applied to the indenter in the FEM was the same as that applied in the test specimens. For the tests, during the application of the indenter the internal pressure remained unchanged. The next step was to remove the indenter gradually while continuing to have same internal pressure. ABAQUS/Standard is able to set up the necessary number of increments needed to reach convergence in the solution. Lastly, the internal pressure was reduced to zero as done in the experiments.

5.11 Pressurization Process

Both experimental and numerical simulations for pressurization and de-pressurization of dented pipe specimens were completed in the current study. However, other students of CERP were also involved in these activities.

Following the last step of the denting processes, the pipe was gradually pressurized to $0.90p_y$. This was done by adding a step that increases the internal pressure from zero to $0.90p_y$. During the next step, the internal pressure was slowly reduced to zero (de-pressurized). The purpose of doing this is to be able to determine the strain distribution around the dented region when the pipe is subjected to internal pressure.

5.12 Validation of FE Model

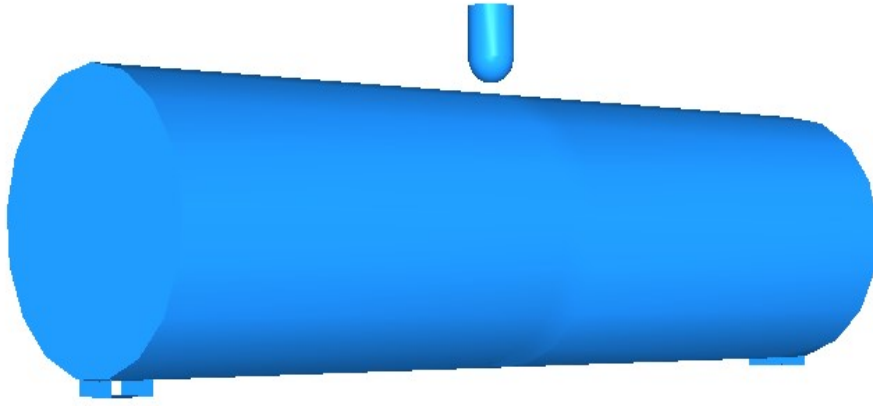All the validation is done in the next chapter along with the parametric study.
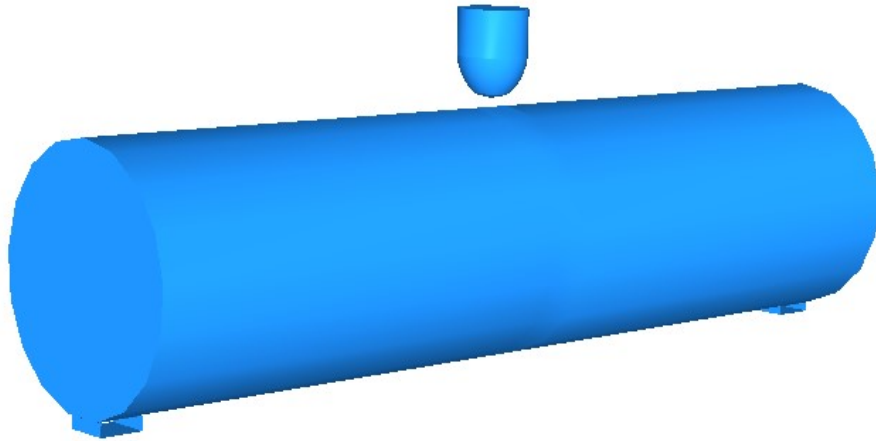
Figure 5.1: Sphere Indented Pipe FEA
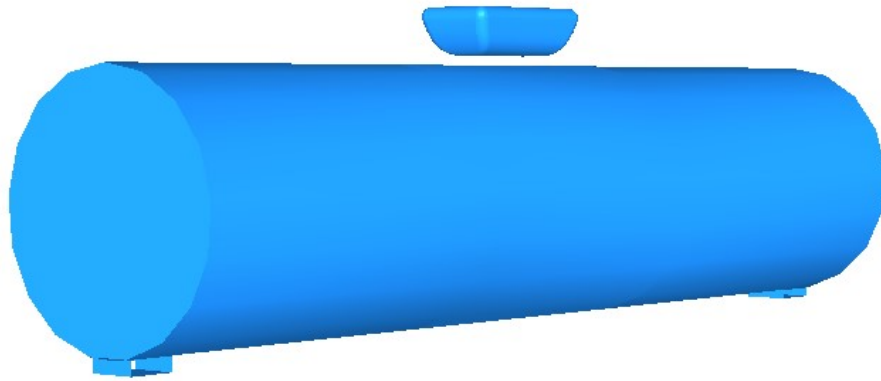

Figure 5.2: Dome Indented Pipe FEA

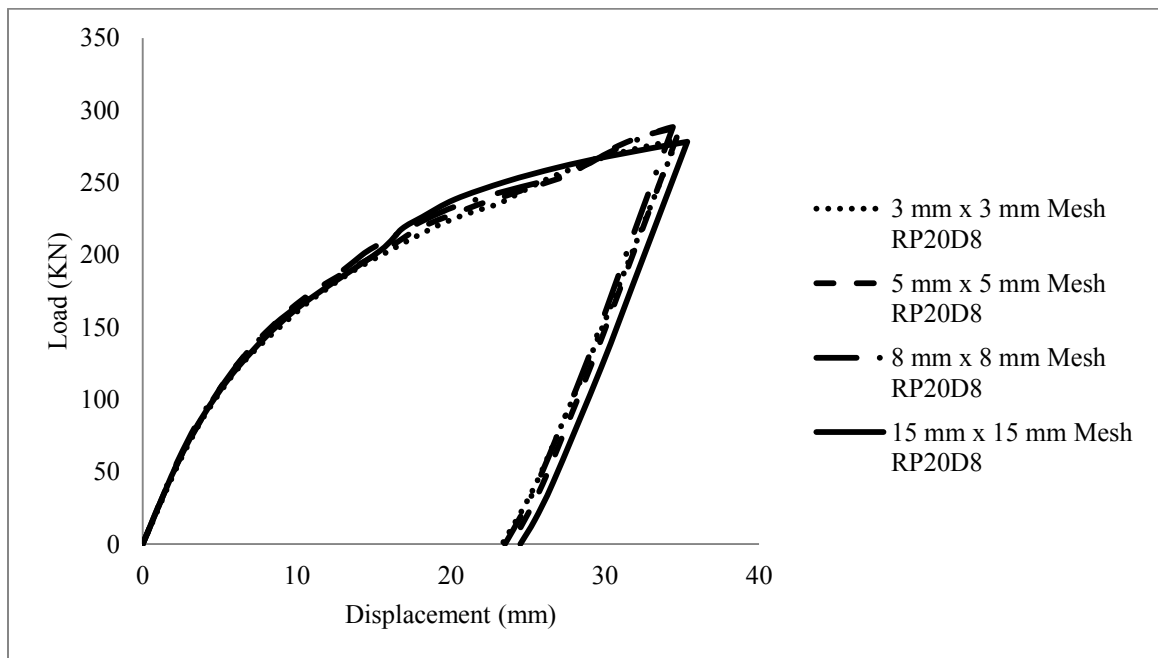Figure 5.3: Rectangular Indented Pipe FEA

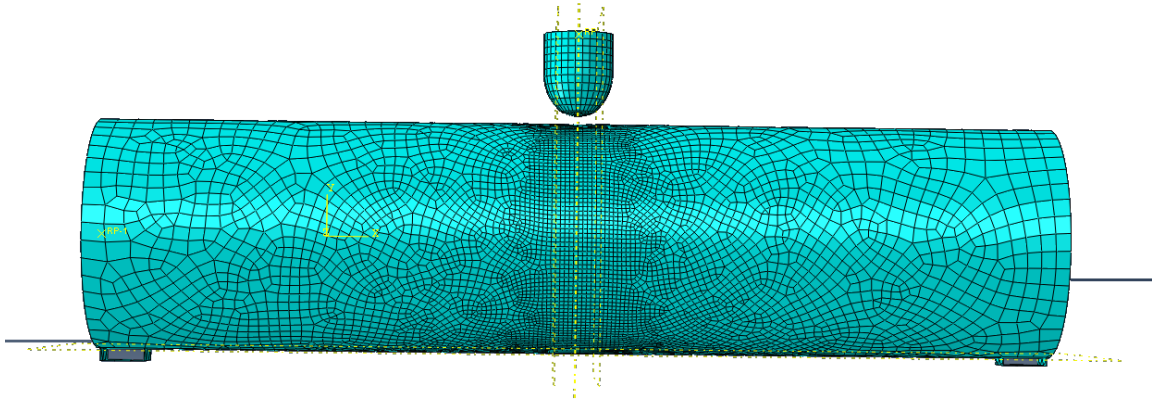Figure 5.4: Mesh Sensitivity Analysis

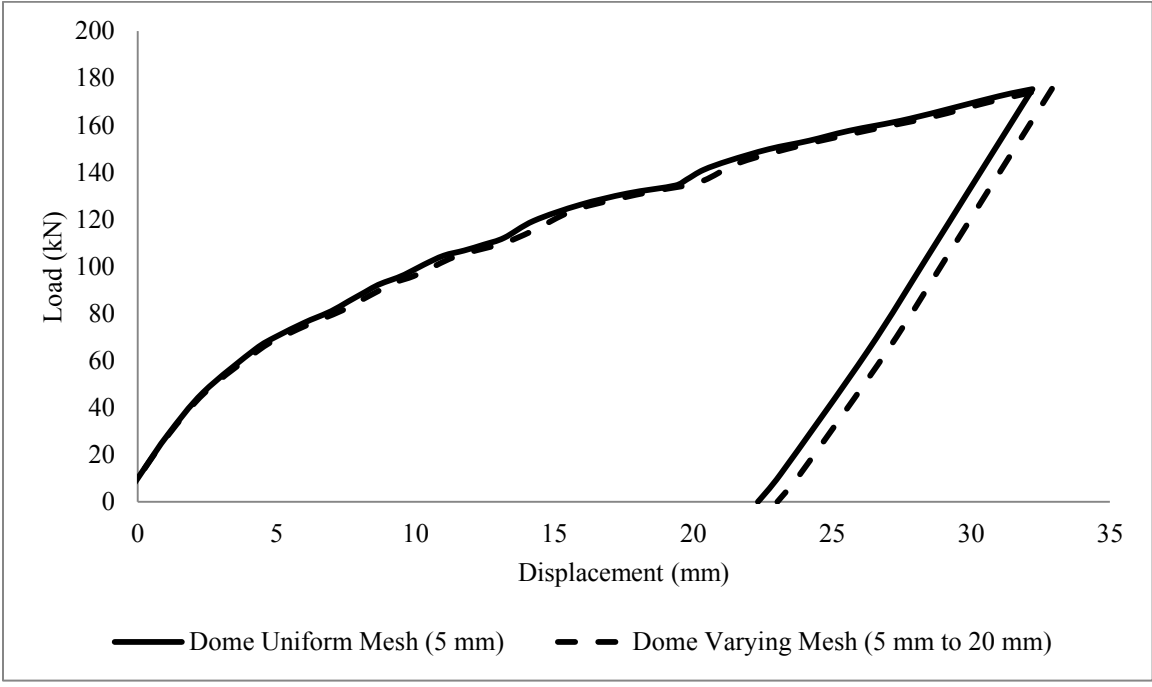Figure 5.5: Varying Size Mesh

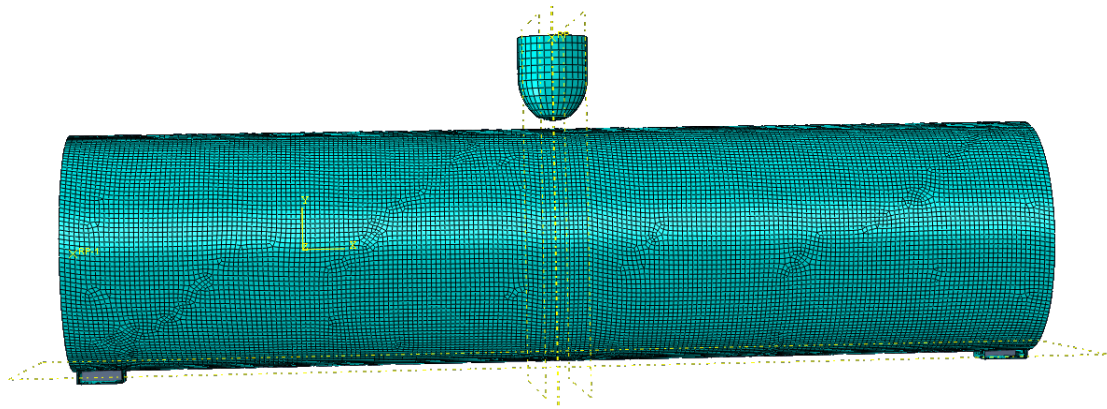Figure 5.6: Mesh Analysis for Uniform and Varying Size Mesh

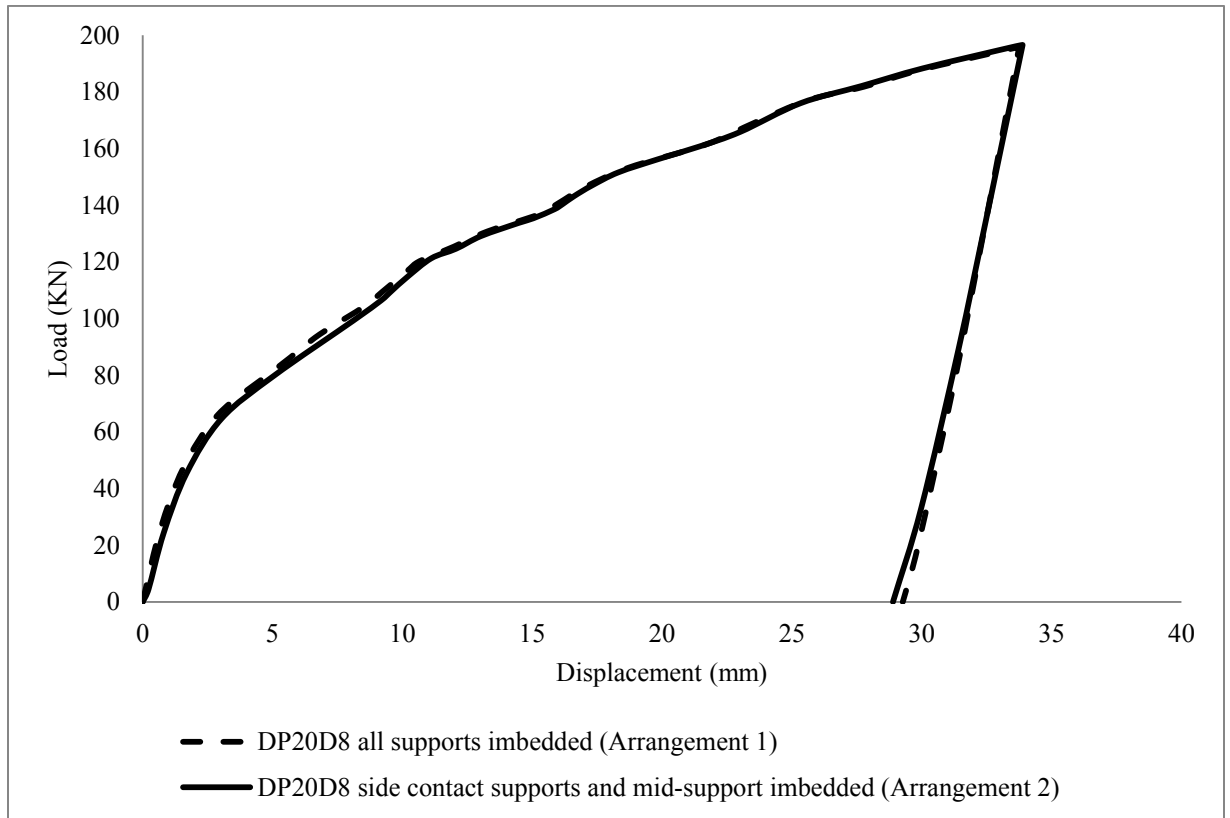Figure 5.7: 5 mm Mesh Selection for all Pipes Tested

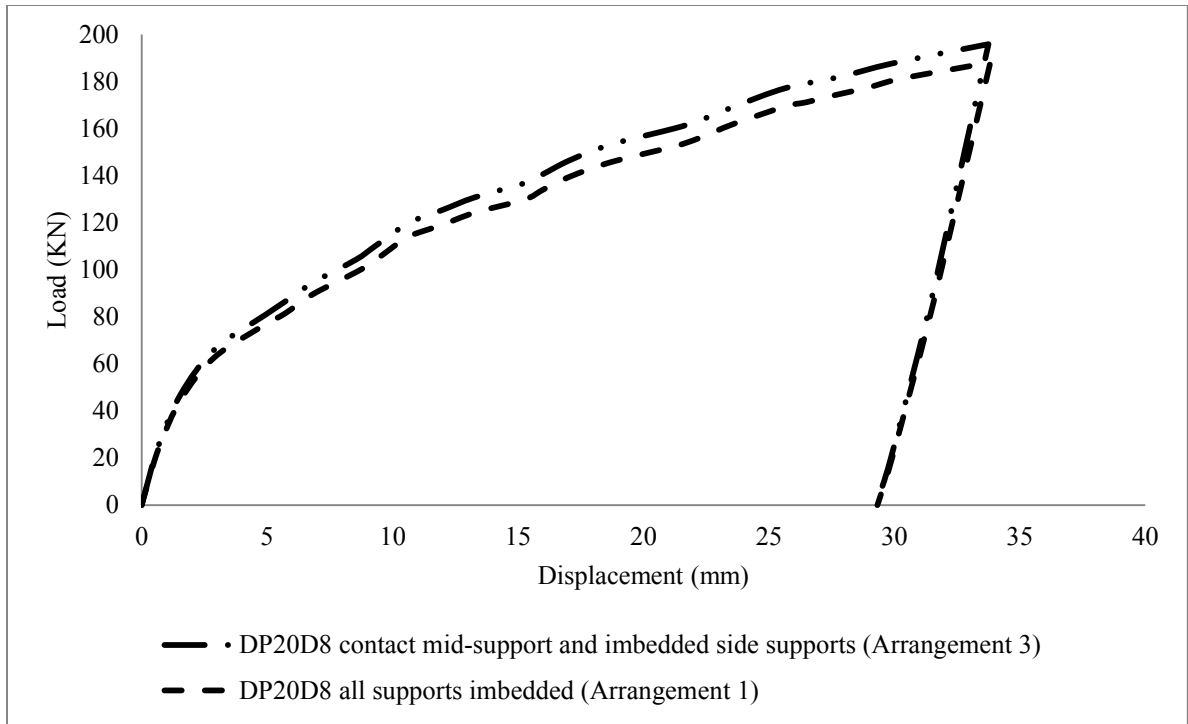Figure 5.8: Comparison between All Contacts Imbedded vs. Side Contacts and Middle
Imbedded

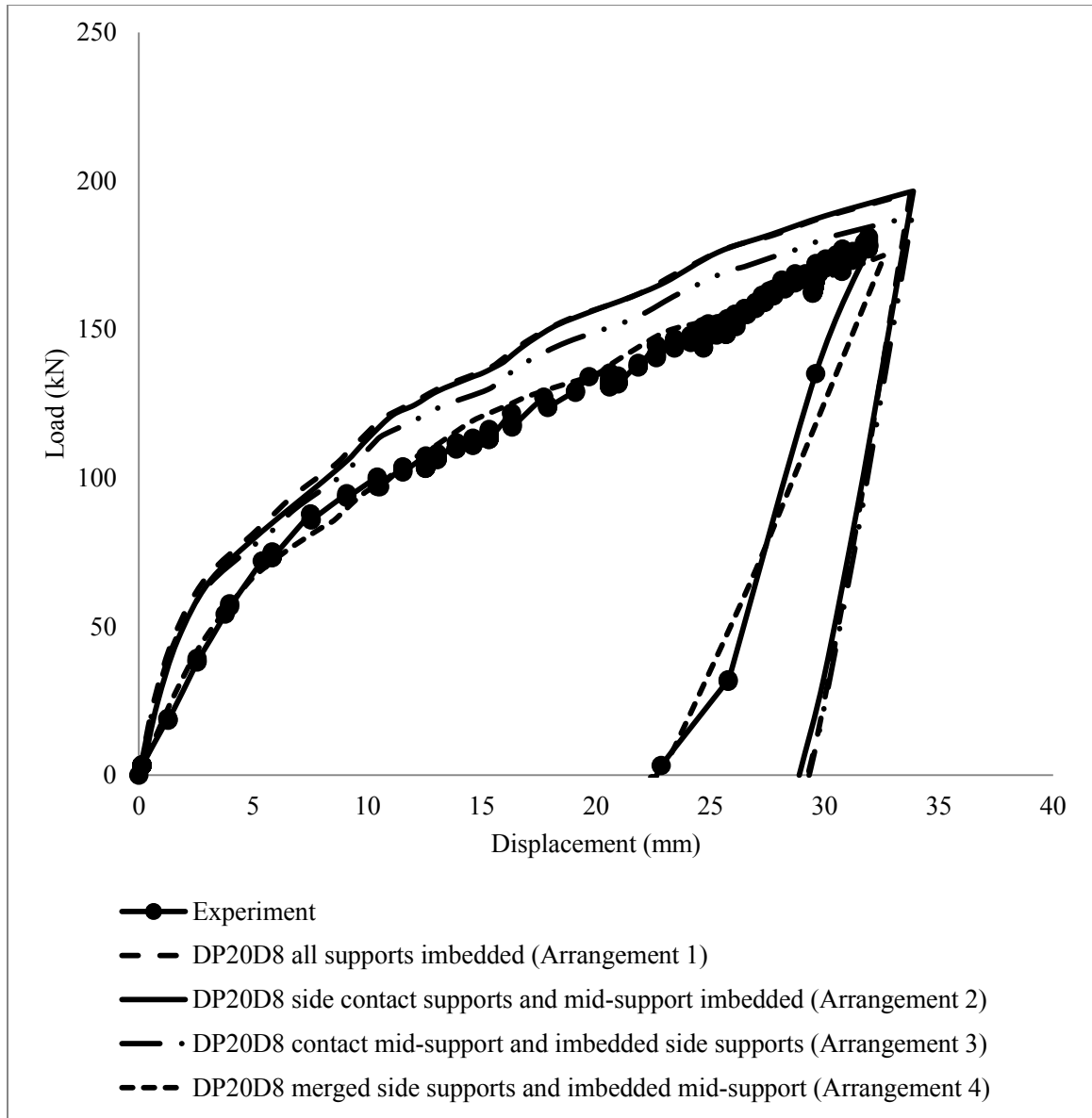Figure 5.9: Comparison between All Contacts Imbedded vs. Sides Imbedded and Middle
Contact

Figure 5.10: Comparison between all Arrangements vs. Experimental Results

CHAPTER 6

6.0 VALIDATION AND PARAMETRIC STUDY

6.1 Overview

As presented in the previous chapters, finite element modeling (FEM) as well as full scale tests were carried out in order to compare and validate the FE models. The FE models were then used to predict the results which could not otherwise be determined from the tests. A validation process must be completed to be able to create a FEM that can be accepted as an alternative to expensive and time consuming full-scale tests. As previously discussed in the Finite Element Modeling chapter, all models were created using the same properties, materials, and geometric parameters as those from the experimental tests. By doing so, the results of both methods can be compared and conclusions can be reached.

Furthermore, another purpose of creating a FEM is to be able to undertake a parametric study in which different parameters are changed and the results for each are obtained. This method is much more economically and time efficient as no real experiments are to be conducted once the model has been validated. For the purpose of the current research, the parameters considered are: the D/t, the internal pressure, the dent, and the dent shape. The D/t varied from 20 to 80 that are typically found in the field. The internal pressure varied from 1000 psi (6.9 MPa) to 3000 psi (20.7 MPa), and the dent shapes were the rectangular and spherical indenters as discussed in more detail in the following sections.

6.2 Assessment between FEA and Experimental results

The purpose of developing a FEM is to compare and validate the results from the experimental tests to have an acceptable numerical model. This model can then be used to undertake a parametric study and determine the effect that different parameters have on the dented pipe. The FEM was validated against the test data for three different parameters. The first one was the load-displacement behaviour from the denting process. As described in the test procedure chapter, an indenting load was applied to the pipelines with the use of different indenters (Rafi 2011). Linear Voltage Displacement Transducers (LVDTs) were used to obtain the displacement of the indenters (indentation depth). For the FEA data, the displacement was obtained from the nodal displacement of the node located at the centre (root) of the dent (maximum displacement), and the magnitude of the load was obtained from the force of the indenter.

The second behaviour checked was the pressure-displacement graphs obtained from the pressurization process. The description of the pressure application process was described in the test procedure chapter.

The third behaviour checked against the test data was the strain distributions around the dented area. For the tests, strain gauges were placed at and near the dented region to accurately determine the behaviour of a dent. For the finite element analysis (FEA), the strain data was obtained from the integration points of the elements within and around the dented area. In the tests, no strain data could be collected from underneath the indenter, however, these strains were obtained from FEA.

Three different indented specimens were tested in the experimental work: rectangular indented specimens, dome indented specimens, and sphere indented specimens. All five pipe specimens had the same outer diameter of 274 mm and thickness of 8.2 mm as well as the same length of 1100 mm. Two rectangular indented pipes were tested. The main

difference between these two pipes is the dent depth used. The first rectangular pipe specimen, RP20D8, had a permanent dent depth of 8% of the outer diameter and the second specimen had a dent depth of 12%. The load-displacement plots showing the comparison between the experimental and FEA data for the 8% dent depth is shown in Figure 6.1. Furthermore, the pressure-displacement relationship is shown in Figure 6.2. Finally, the strain distribution for the longitudinal and circumferential axes around the dented area are shown in Figures 6.3(a), 6.3(b), 6.3(c) and 6.3(d).There is a good agreement between the load-displacement, pressure-displacement, as well as the strain distribution graphs. The FEA data for load-displacement and pressure-displacement agree well with test behaviour as they are compared on a global level. However, the strain values do not always agree well, especially at maximum values. Strain data is very hard to match, even among two physical tests on the same specimen at different times, as it is a very localized behaviour that is very sensitive to environmental influences. Hence, further improvement in FE model is recommended.

Two dome indented pipes were tested. The main difference between these two specimens was the internal pressure applied during the indentation process. The first dome indented pipe (DP0D8) had no internal pressure during denting process, while the second pipe (DP20D8) had a $0.20p_y$ (20%) internal pressure during the denting process. However, both specimens had the permanent dent depth of 8% of the outer diameter of the pipe. The load-deformation plots for the comparison between the experimental and FEA for the DP20D8 is shown in Figure 6.4 and the pressure-displacement plot is shown in Figure 6.5. The strain distributions for the longitudinal and circumferential axes around the dented area are shown in Figures 6.6(a), 6.6(b), 6.6(c), and 6.6(d). The value for the strain at the 0 mm position in Figure 6.6(d) for specimen DP20D8 could not be obtained since this strain gauge failed during the pressurization process. There is a good agreement between the load-deformation plots. However, the agreement between the test and the FEA are reasonable with discrepancies in the maximum values. DP0D8 was not included in the FE model generation because only one specimen for each dent shape was included for validation purposes.

Lastly, one spherical indented pipe was modelled, specimen SP20D8. The internal pressure was $0.20p_y$ and the dent depth was 8% of the outer diameter of the pipe. The load-displacement plot showing the comparison between the experimental and a FEA is shown in Figure 6.7. The pressure-displacement graph is shown in Figure 6.8. The strain distributions for the longitudinal and circumferential axes around the dented area are also shown in Figures 6.9(a), 6.9(b), 6.9(c), and 6.9(d). There is a good agreement between the load-deformation and pressure-displacement relationships. However, agreement in the maximum strain values in the longitudinal and the circumferential axes have differences up to 40% and further research is required.

6.3 Parametric Study

A parametric study was performed to determine the effect that different parameters on the strain distributions of a dented pipeline. Three different parameters were chosen in this parametric study and they are shown below along with their ranges:

- D/t Ratio: 20 to 80
- Internal Pressure: 6.9 MPa (1000 psi) to 20.7 MPa (3000 psi)
- Dent Shape: Rectangular, and Sphere

In order to change the D/t ratio, the thickness of the pipe wall was varied between 3.4 mm to 13.9 mm. This resulted in a range of D/t ratios in between 20 to 80. Next, the internal pressure for pressurization process was varied between 1000 psi (6.9 MPa) to 3000 psi (20.7 MPa) at an increment of 1000 psi (6.9 MPa). Lastly, the dent shape was varied between a rectangular dent shape and a spherical dent shape. The parametric study includes two dent shapes, rectangular, and sphere. Due to time constraint, it was decided not to include the dome shape dented pipes in the parametric study.

The names provided for each pipeline created for the parametric study uses the specific parameters changed for that specific run. As an example, for the specimen RP20D6-3000, R means that it was dented with a rectangular indenter and hence, the dent shape is rectangular, P20 describes the internal pressure at which the pipe was dented is $0.2p_y$ (20%), D6 shows the permanent (plastic) dent depth of the pipe was 6% of the outer diameter, and finally 3000 is the maximum internal pressure reached during the pressurizing process of the pipe after the indenter was removed.

The main purpose of a parametric study was to determine the locations where the maximum strain occurs when changing the D/t ratio, dent shape, and internal pressures. The strain values obtained from the parametric study are the true strain values.

6.3.1 Effect of D/t ratio and Internal Pressure on Strain Distributions

The effect of the D/t ratio on the longitudinal and circumferential strain distribution was determined. Different ranges of D/t ratios were used in the parametric study and depended on the internal pressure applied after the indenter was removed. With a higher internal pressure of around 3000 psi (20.7 MPa), the maximum D/t ratio applied in FE model for a rectangular indented pipe was 65 and minimum was 20. The highest D/t ratio the FE model successfully ran with was 65. A large D/t means very thin pipe wall thickness. The pipe with a very large D/t ratio becomes numerically unstable and the solution process terminates. For a D/t ratio of 65, the thickness of the pipe was around 4.2 mm. However, for the medium internal pressure of 2000 psi (13.8 MPa), the maximum D/t ratio modeled for a rectangular indented pipe was 80 and minimum was 20. With a lower internal pressure of 1000 psi, the maximum D/t ratio modeled was 80 and minimum was 20, since no numerical difficulties were faced at this pressure

For an internal pressure of 3000 psi (20.7 MPa), the maximum D/t ratio that was successfully modeled and solved for a spherical indented pipe was 70 and minimum was 20. The highest ratio reached was 70 due to the same numerical problem as discussed for

the rectangular dented pipe specimen. For a D/t ratio of 70, the thickness of the pipe was around 3.9 mm.

However, for medium internal pressure of 2000 psi (13.8 MPa), the maximum D/t ratio modelled which was successfully run was 80 and minimum was 20.

6.3.1.1 Rectangular Dent

The strain distribution plots for the 8% dent depth rectangular indented specimen for 3000 (20.7 MPa) and after pressurizing along the longitudinal and circumferential axes are shown in Figures 6.3(a), 6.3(b), 6.3(c), and 6.3(d). The maximum strain for the longitudinal axis vs. the different D/t ratios for the internal pressures of 3000 psi (20.7 MPa), 2000 psi (13.8 MPa), and 1000 psi (6.9 MPa) are shown in Figure 6.10. The maximum strain for the circumferential axis vs. the different D/t ratios for the internal pressures of 3000 psi (20.7 MPa), 2000 psi (13.8 MPa), and 1000 psi (6.9 MPa) are shown in Figure 6.11. In these figures the distance of these maximum strains from the dent centre are indicated.

The results show that for increasing D/t ratios the maximum strain in the pipe increase. Furthermore, as the internal pressure in the pipe increases the maximum strain in the pipe increases. It was found that as the internal pressure increases the strain also increases. Furthermore, as the D/t ratio increases, so does the strain. The results obtained follow a pattern which details that the smaller the pipe's wall thickness and the higher internal pressure a higher strain exist. The location of the maximum strain in the longitudinal direction remains unchanged for each pressure with changing D/t ratios. The location of the maximum strain stays constant at 125 mm for all three pressures. The location of the maximum strain in the circumferential direction remains constant for a constant pressure with changing D/t ratios. The location of the maximum stays constant at 0 mm for all three pressures.

6.3.1.2 Spherical Dent

The strain distributions graphs for the spherical indented pipe specimen along the longitudinal and circumferential axes are shown in Figures 6.9(a), 6.9(b), 6.9(c), and 6.9(d). The maximum strain for the longitudinal axis vs. the different D/t ratios at the internal pressures of 3000 psi (20.7 MPa), 2000 psi (13.8 MPa), and 1000 psi (6.9 MPa) are shown in Figure 6.12. The maximum strain for the circumferential axis vs. the different D/t ratios for the same internal pressures of 3000 psi (20.7 MPa), 2000 psi (13.8 MPa), and 1000 psi (6.9 MPa) are shown in Figure 6.13. It can be found that the same pattern of strains as that of the rectangular dent was observed; as the internal pressure increases the strain also increases. Additionally, as the D/t ratio increases, so does the strain. The location of the maximum strain in the longitudinal direction does not change if pressure is unchanged with changing D/t ratios. The location of the maximum strain for the longitudinal axis varies as pressure changes. For example, at a pressure of 13.8 MPa (2000 psi) the maximum strain occurs at 25 mm away from the dent center, while for 20.7 MPa (3000 psi) it occurs at 50 mm away from the dent center. The location of the maximum strain in the circumferential axis does not follow any pattern.

6.4 Summary

The summary is as follows

- Having a large D/t ratio means that the pipe's wall thickness is very small. When this happens, the FE model becomes numerically unstable and the solution process terminates. However, further research is recommended to overcome this issue.
- As the D/t ratio increases, so do the strain values. This increase is much larger when the internal pressure is higher. This phenomenon occurs for both rectangular and spherical indented pipe specimens.

- The strain values increase as the internal pressure increases. This occurs for the rectangular and sphere indented specimens as shown in Figures 6.10 to 6.13.

- The location of the maximum strain for the rectangular dent in the longitudinal axis occurs away from the dent centre while the location of the maximum strain for the circumferential axis occur at the dent center for all internal pressures.

- The location of the maximum strain for the spherical dent in the longitudinal axis increases by 25 mm as the internal pressure increases while the location of the maximum strain for the circumferential axis has no apparent pattern.

- For the rectangular dented pipes, maximum strain values are observed in the circumferential axis while for the spherical dent, the maximum values occur in the longitudinal axis.

Figure 6.1: FEA vs. Experimental Load-Displacement Behaviour of RP20D8
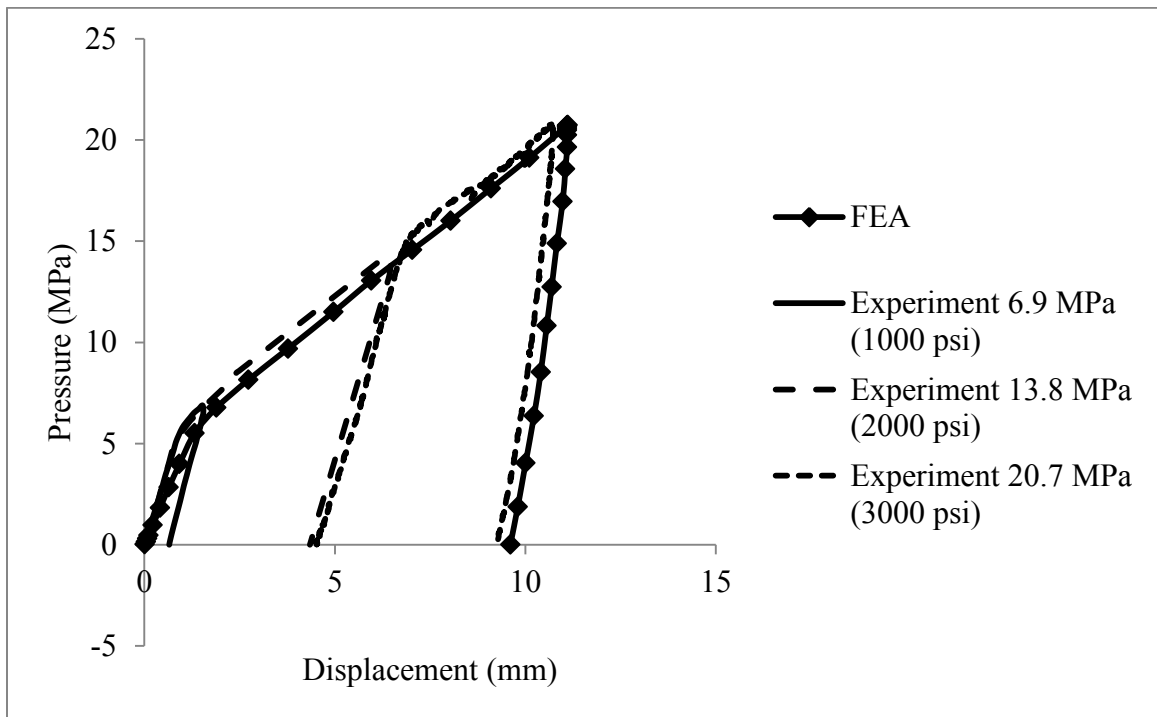
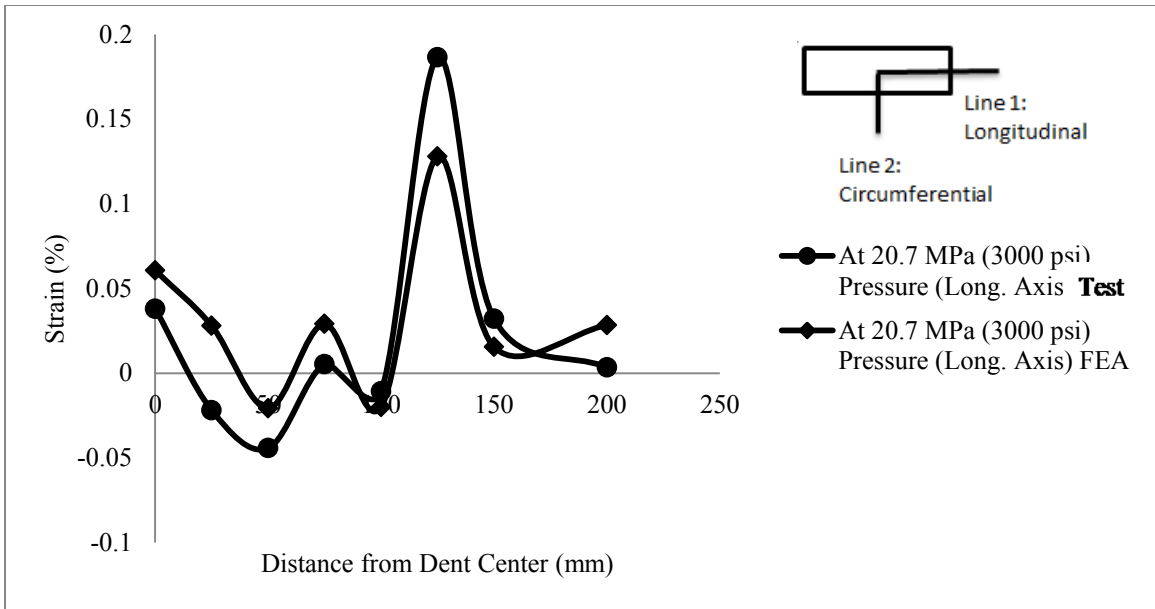Figure 6.2: FEA vs. Experimental Pressure-Displacement Behaviour of RP20D8

Figure 6.3(a): Longitudinal Strains for RP20D8 at 20.7 MPa (3000 psi)
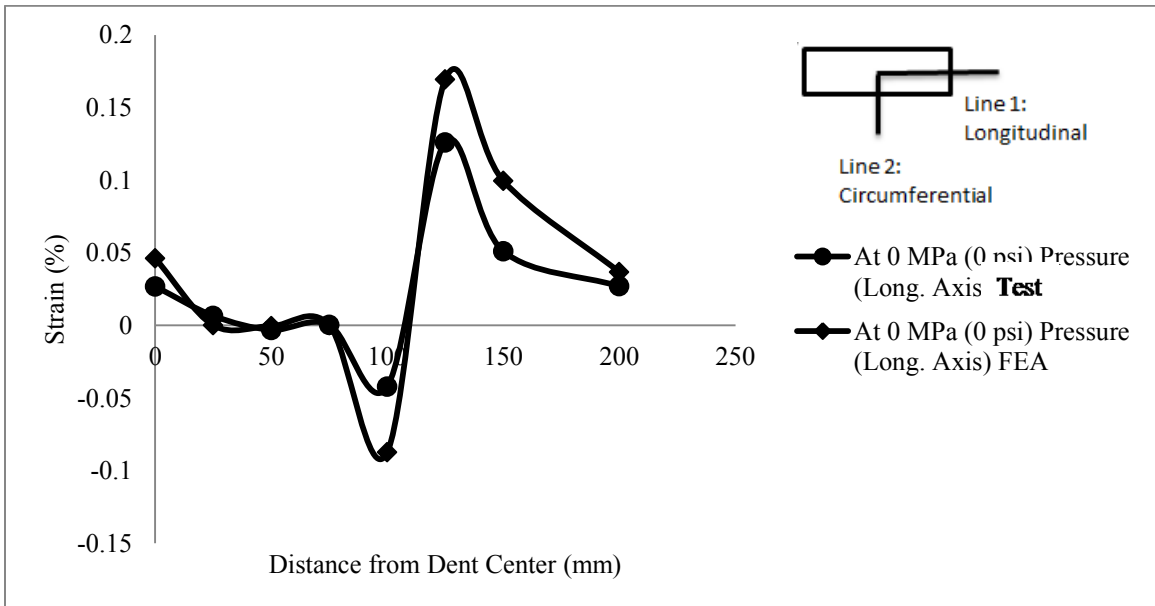

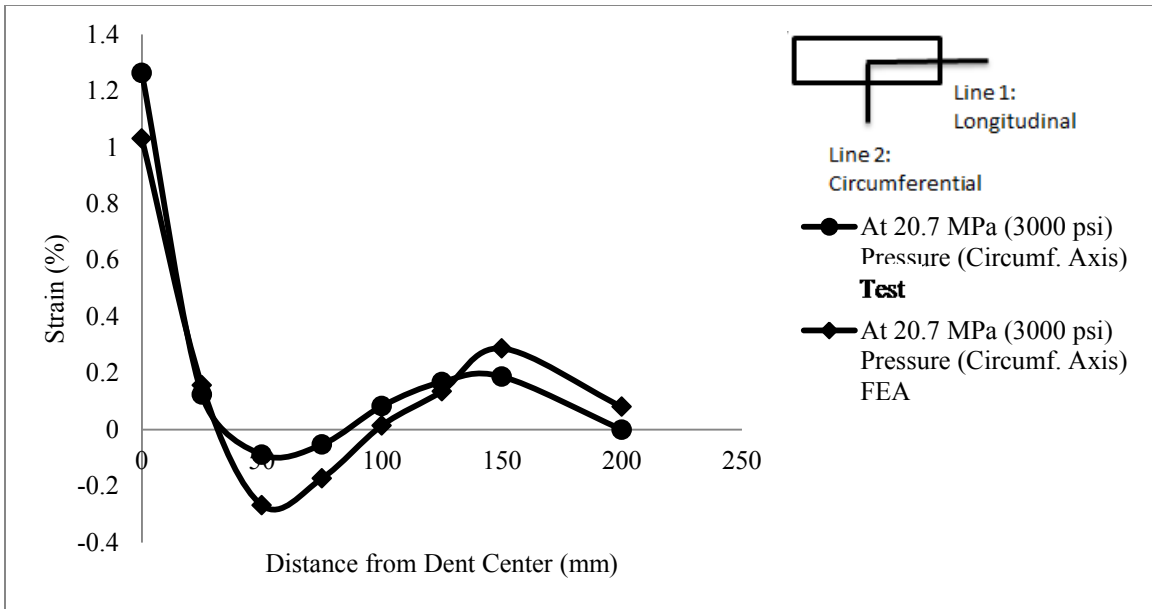Figure 6.3(b): Longitudinal Strains for RP20D8 at 0 MPa (0 psi)

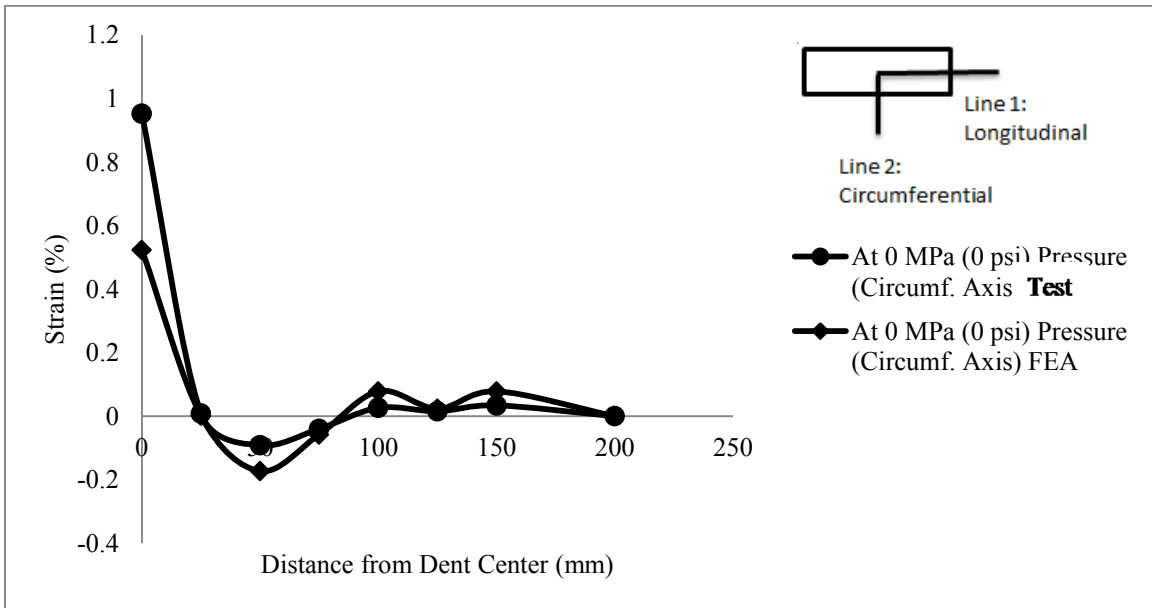Figure 6.3(c): Circumferential Strains for RP20D8 at 20.7 MPa (3000 psi)

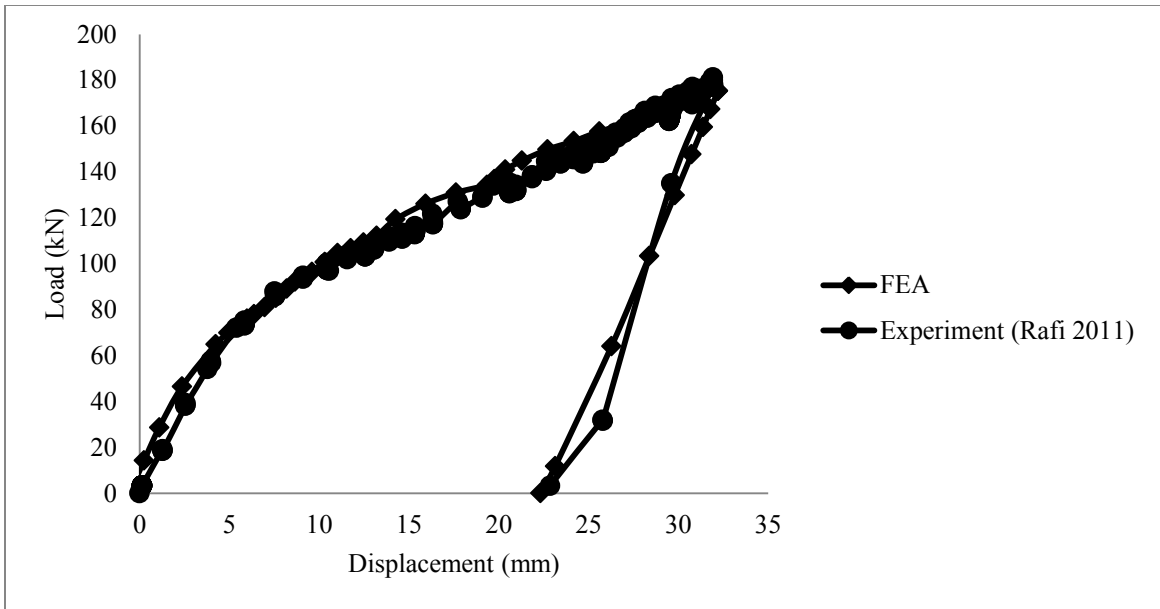Figure 6.3(d): Circumferential Strains for RP20D8 at 0 MPa (0 psi)

Figure 6.4: FEA vs. Experimental Load-Displacement Behaviour for DP20D8
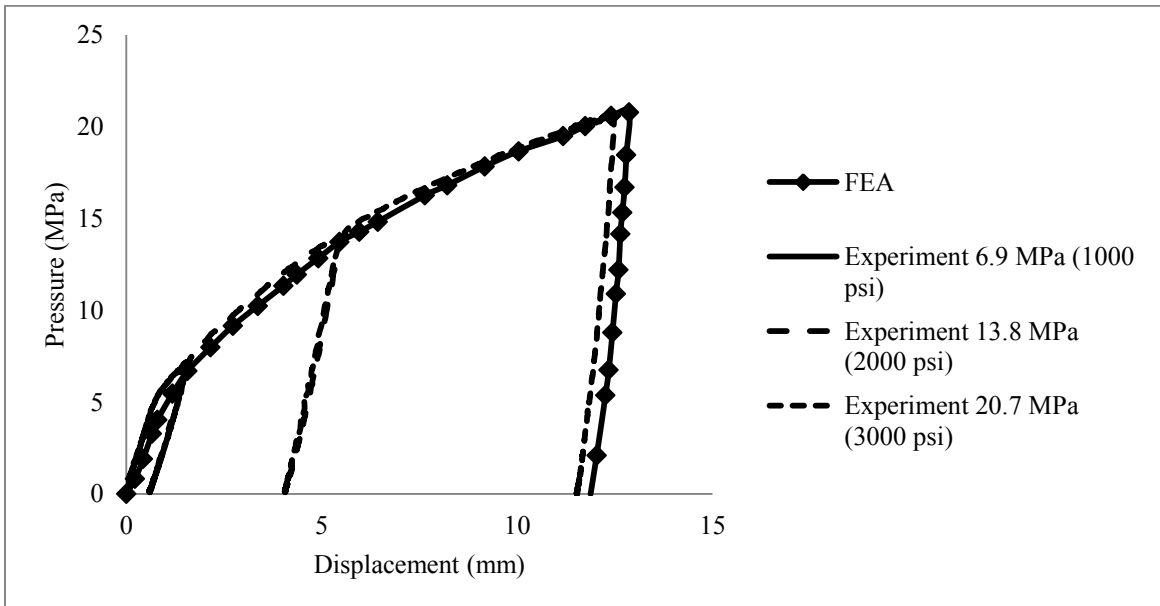

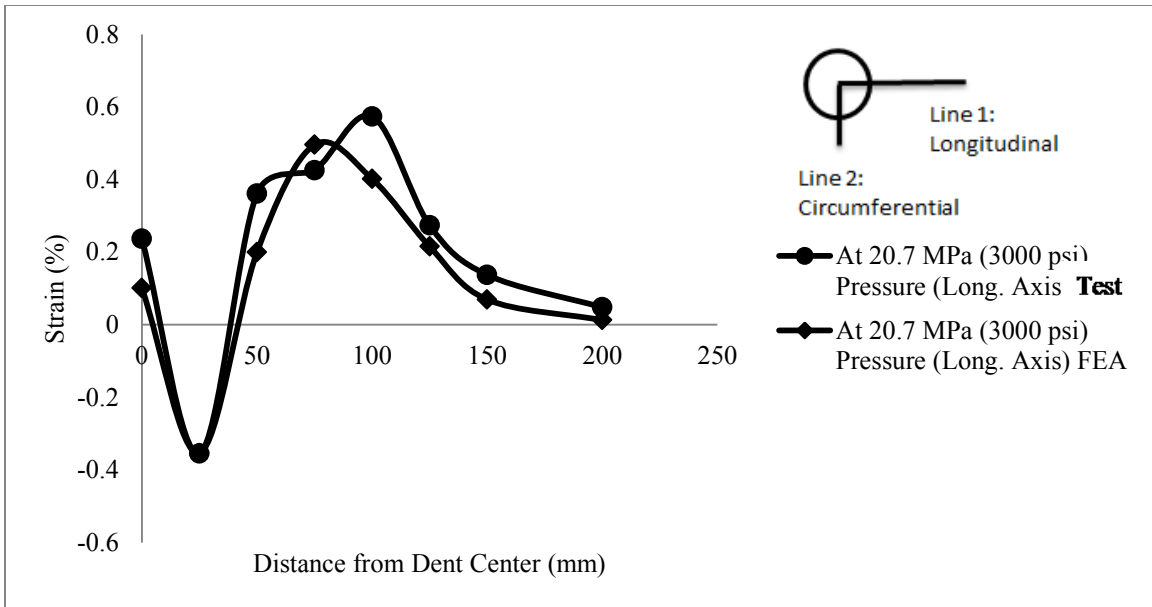Figure 6.5: FEA vs. Experimental Pressure-Displacement Behaviour for DP20D8

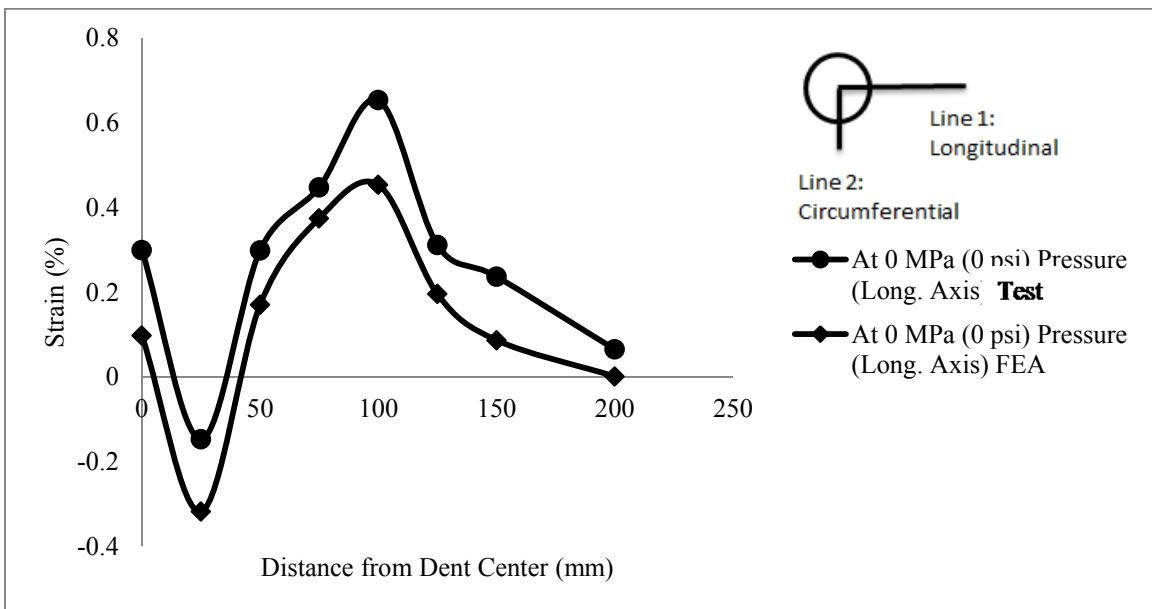Figure 6.6(a): Longitudinal Strains for DP20D8 at 20.7 MPa (3000 psi)

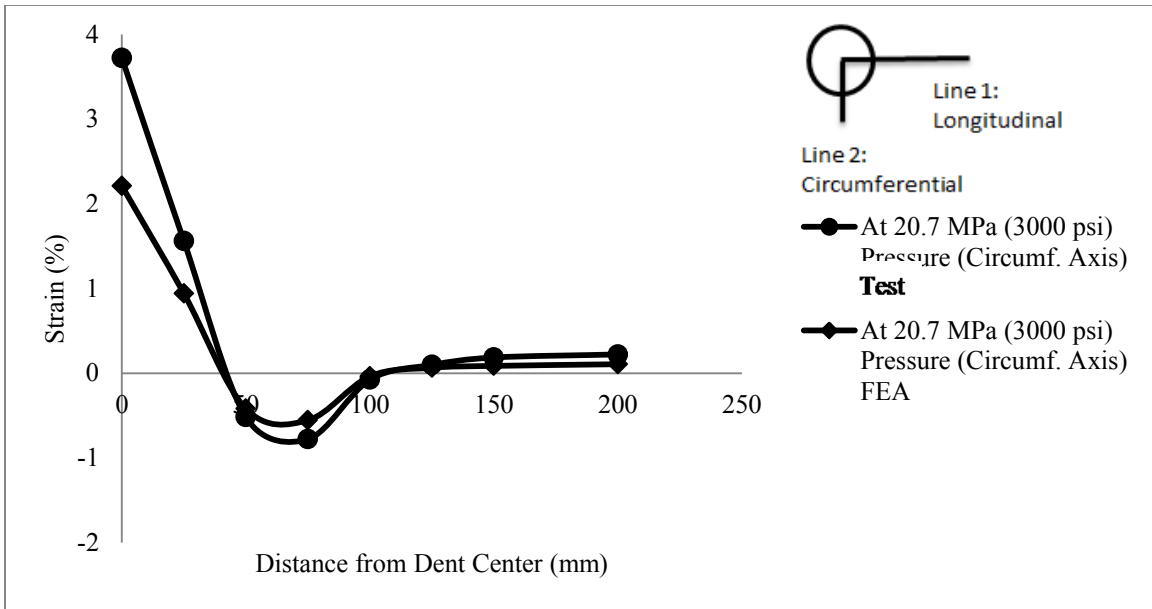Figure 6.6(b): Longitudinal Strains for DP20D8 at 0 MPa (0 psi)

89

Figure 6.6(c): Circumferential Strains for DP20D8 at 20.7 MPa (3000 psi)
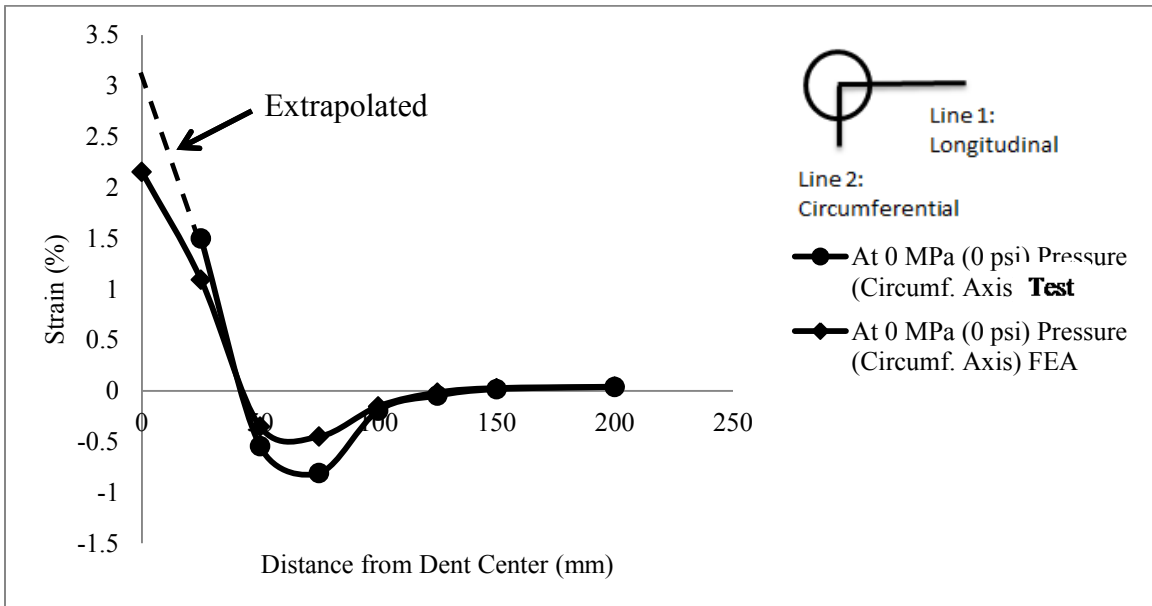

Figure 6.6(d): Circumferential Strains for DP20D8 at 0 MPa (0 psi)

Figure 6.7: FEA vs. Experimental Load-Displacement Behaviour for SP20D8
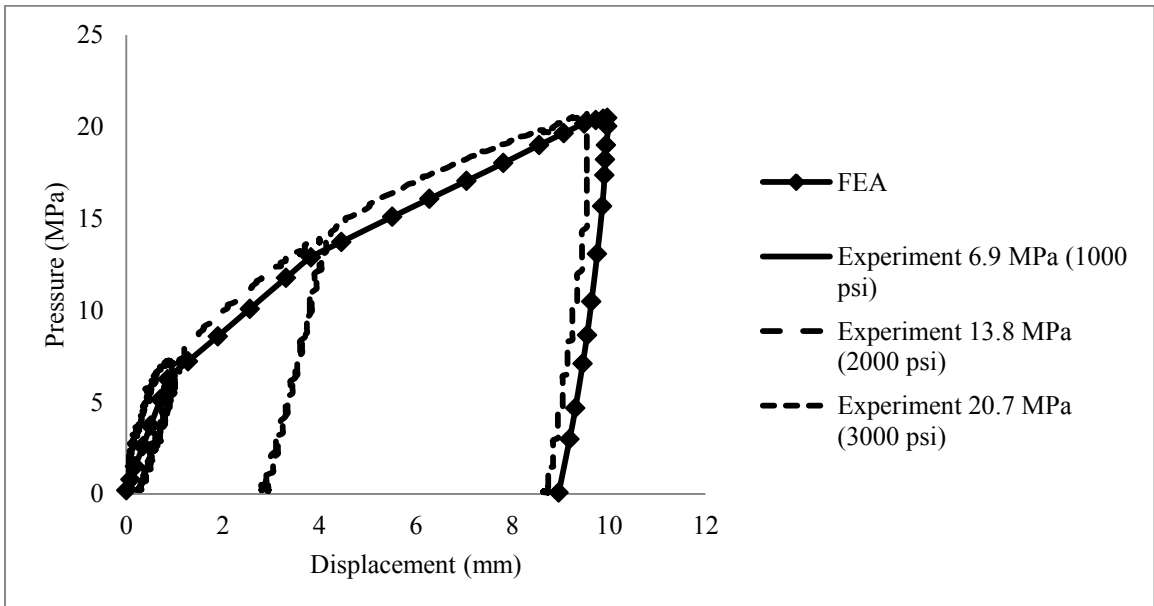
Figure 6.8: FEA vs. Experimental Pressure-Displacement Behaviour for SP20D8
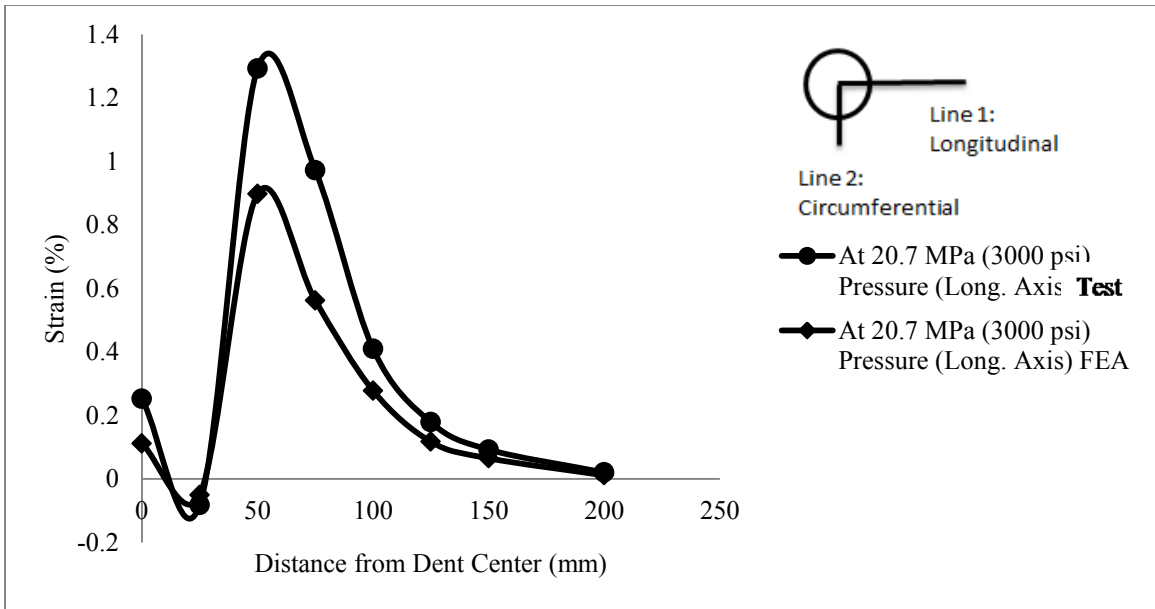
Figure 6.9(a): Longitudinal Strains for SP20D8 at 20.7 MPa (3000 psi)
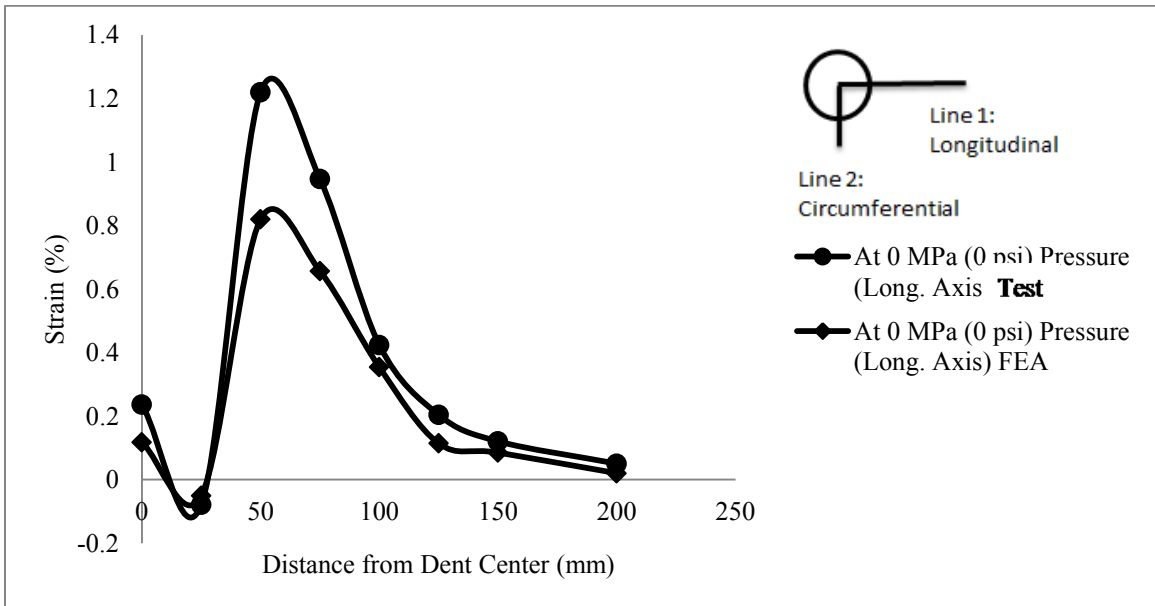
Figure 6.9(b): Longitudinal Strains for SP20D8 at 0 MPa (0 psi)
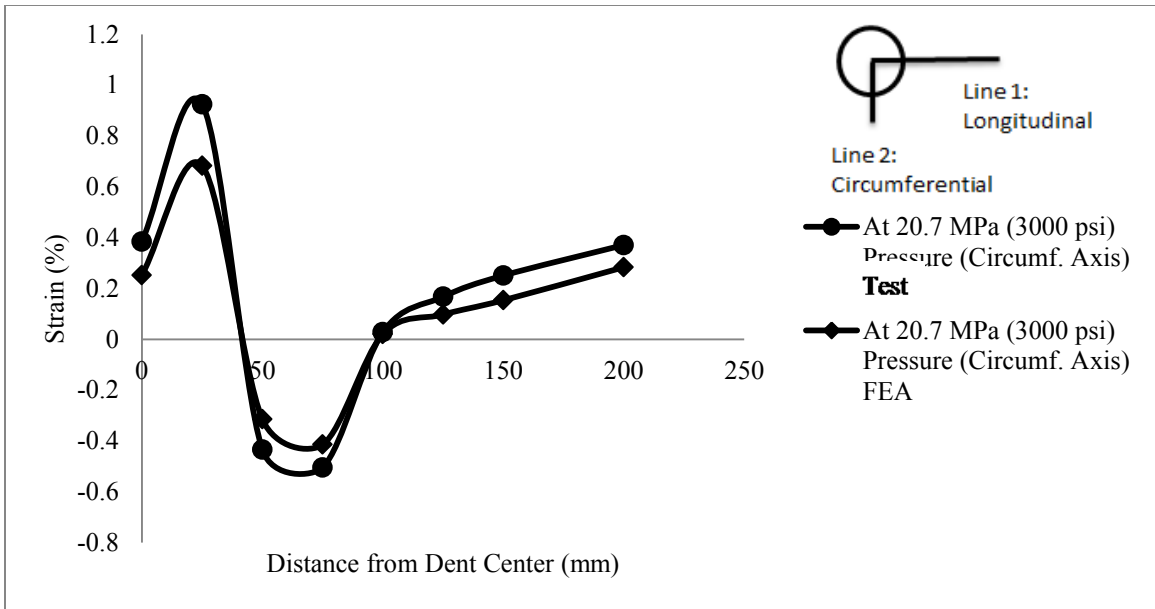
Figure 6.9(c): Circumferential Strains for SP20D8 at 20.7 MPa (3000 psi)

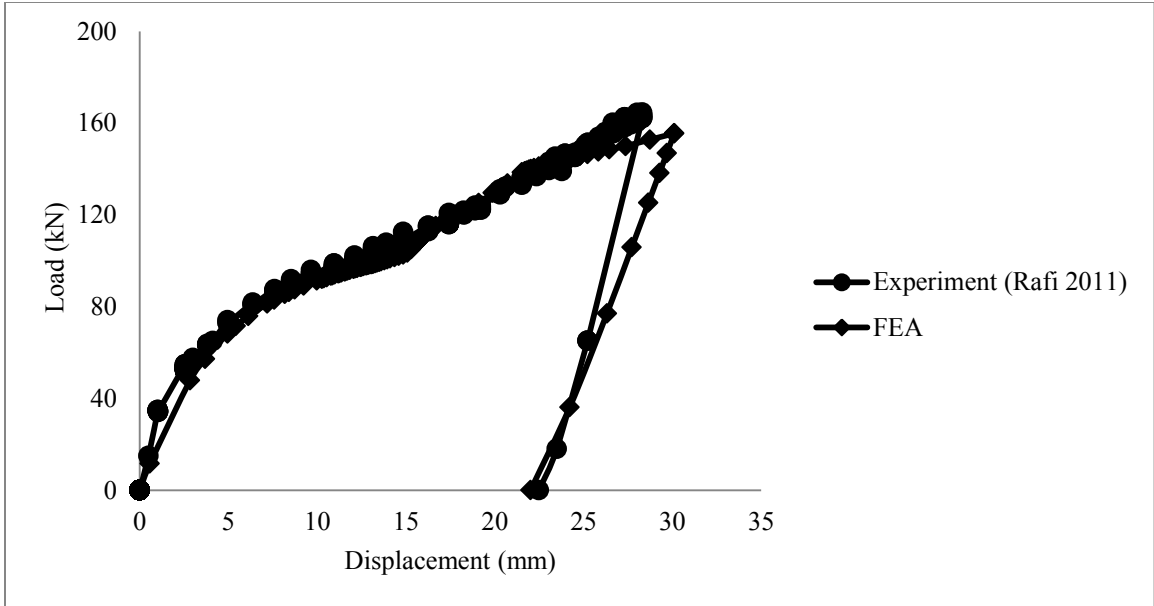Figure 6.9(d): Circumferential Strains for SP20D8 at 0 MPa (0 psi)
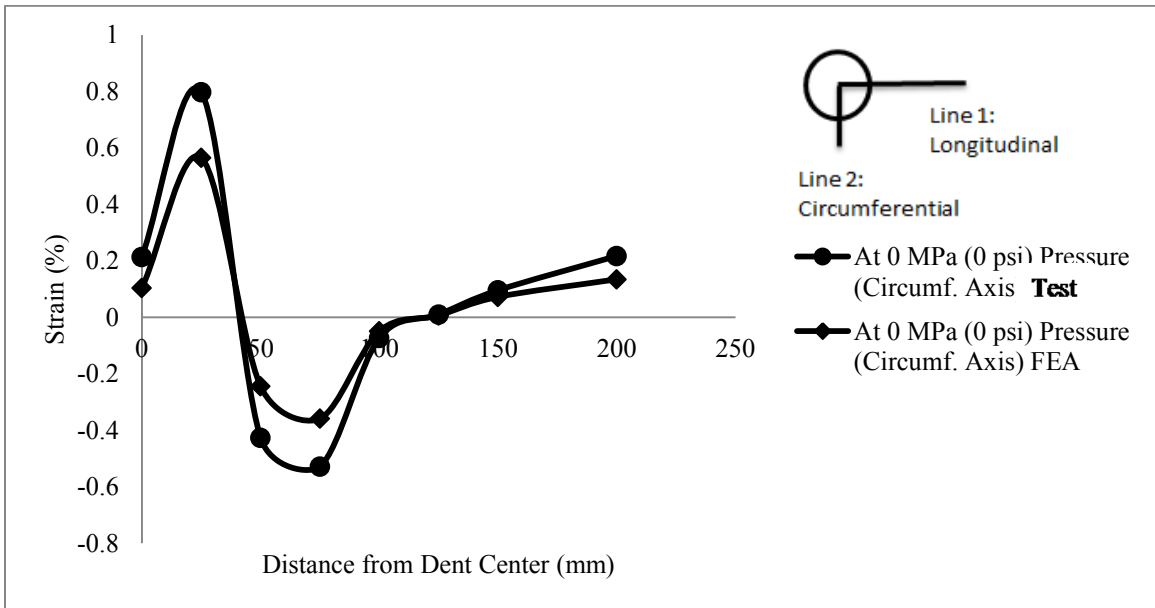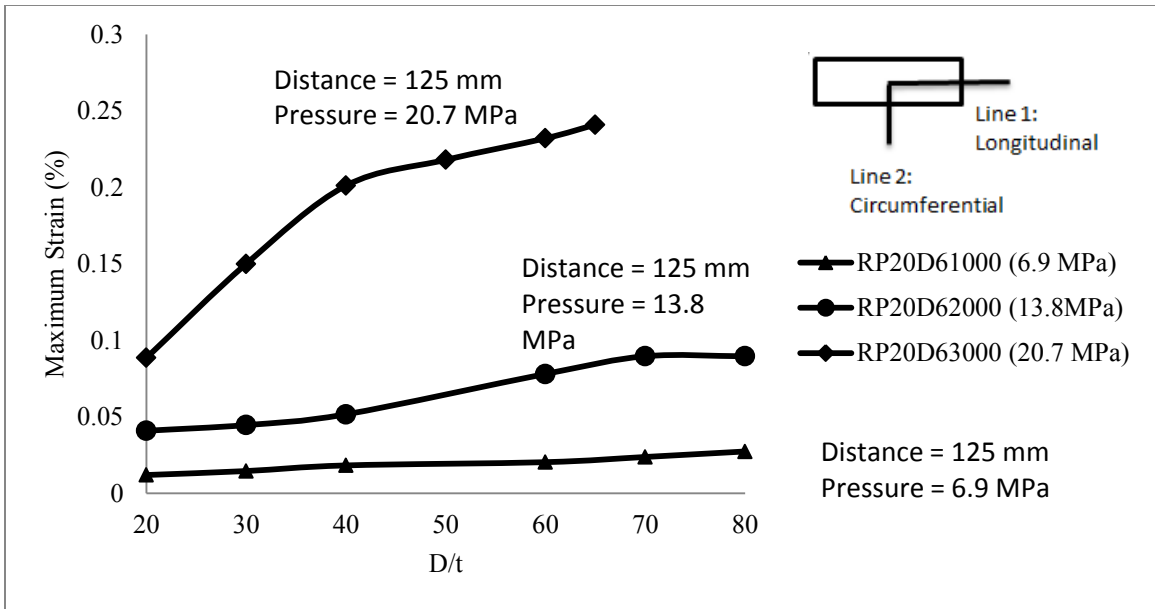
Figure 6.10: Maximum Strains for Rectangular Dent in Longitudinal Axis
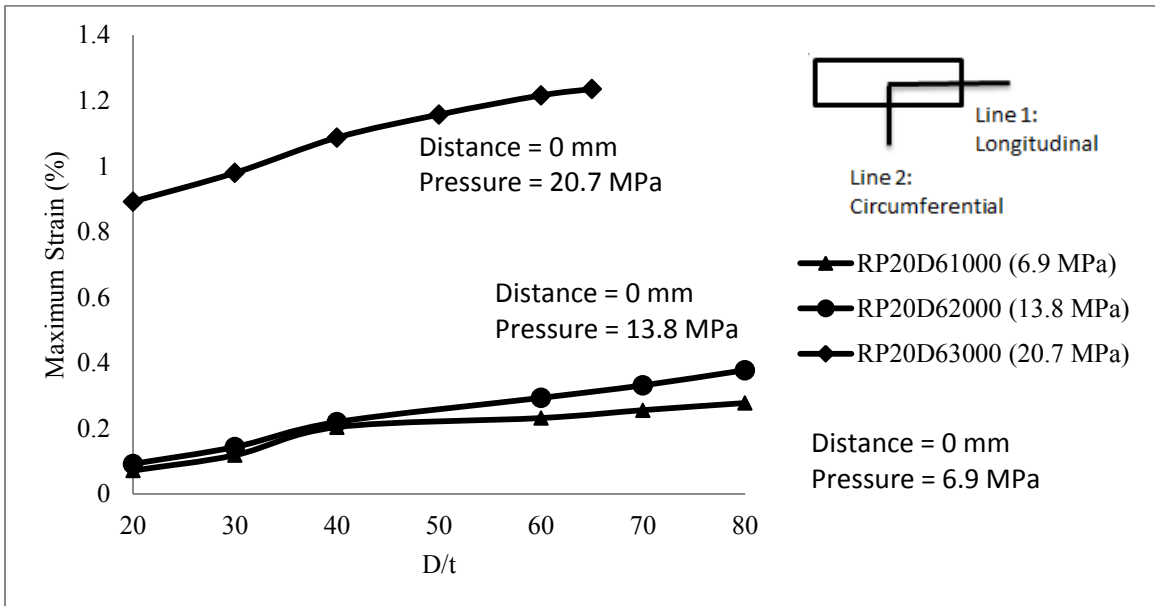
Figure 6.11: Maximum Strains for Rectangular Dent in Circumferential Axis

94
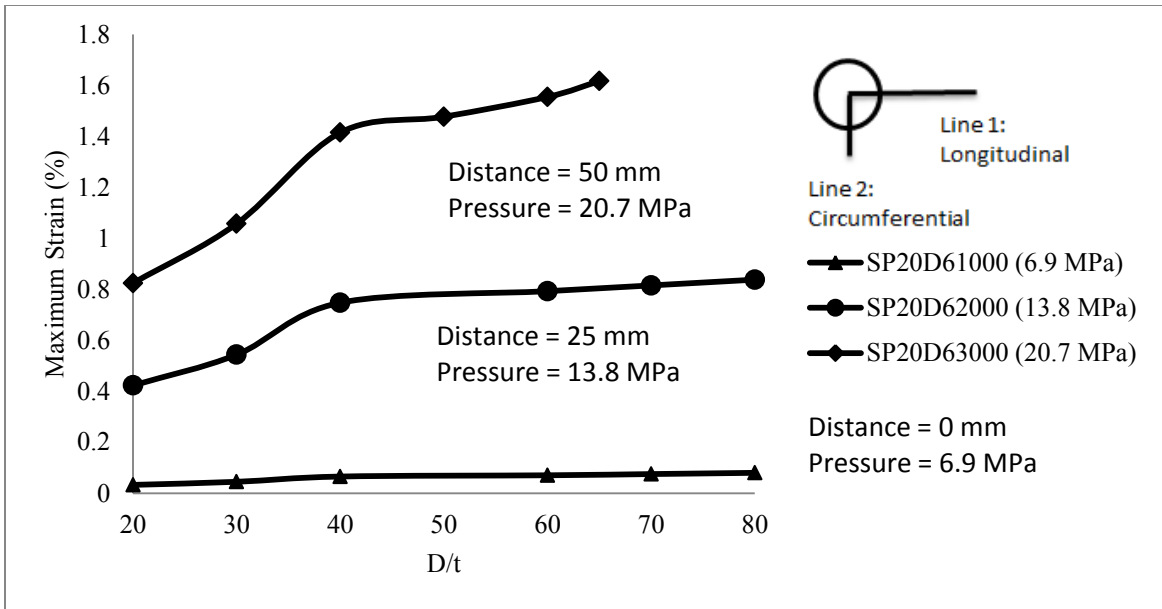
Figure 6.12: Maximum Strains for Spherical Dent in Longitudinal Axis
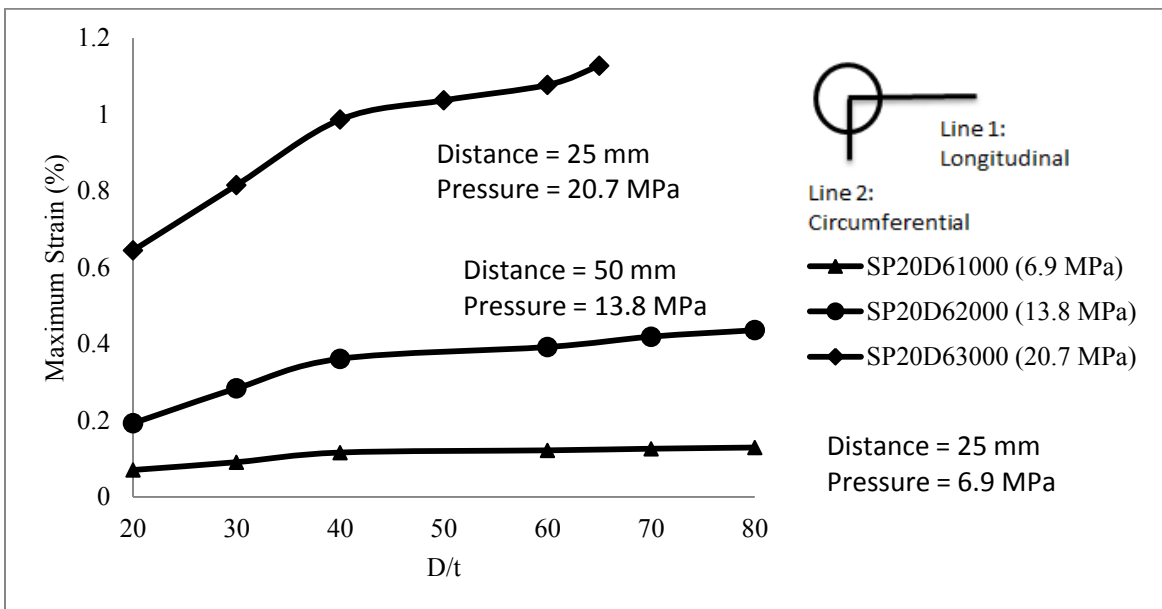
Figure 6.13: Maximum Strains for Spherical Dent in Circumferential Axis

95

CHAPTER 7

7.0 CONCLUSIONS AND RECOMMENDATIONS

7.1 Overview

This chapter is the final chapter of this thesis and presents summary of the findings of this study, the conclusions of this work, and finally the recommendations for future studies.

7.2 Summary

The main objective of this study was the following.

- Determine the strain distribution around the dented area
- Locate the position and value of the maximum strain for different types of indenters, internal pressures, and D/t ratios

In order to achieve the goals, full-scale tests were carried out. Five dented pipe specimens were tested and the test data were acquired. Finite element models using ABAQUS/Standard were created and then validated using these test data. The FE models were used to obtain other data those could not be determined from the tests. The finite element models are then used for a parametric study to better understand the the effect of the dent shape, internal pressure, and D/t on the strain distributions..

7.3 Conclusions

The following are the conclusions made based on the test and finite element analyses completed under the scope of this study.

- The pressure-displacement relationships of dented pipes vary depending on the type of the dent shape. A rectangular dent produces a higher rerounding displacement than the sphere indenter for the same pressure. However, a dome indent has a higher re-rounding than the rectangular dent as it does not contain any corners that can restrict the dent reversal to a higher value.

- The strain distributions at and near the dented region are dependent on the shape of the dent and the pressure used during indentation. The strain distribution at and near the dent region is similar for the rectangular and the dome indented pipes, However, this is not true for the sphere indented pipes although the dome and sphere indenters are closer in shape.

- The location of the maximum strain also depends on the indenting pressure. For example, the location of the maximum strain for specimen DP20D8 occurs at a distance of 100 mm from the dent center, however, that of specimen DP0D8 occurs at a distance of 75 mm from the dent center for the longitudinal axis. However, the locations of the maximum strains for the circumferential axis for both dome specimens are same (See Table 4.1 to Table 4.4).

- In general, the maximum strain locations vary between the longitudinal and the circumferential axes. For the longitudinal axis it is observed that the maximum strains occur away from the dent center, however, for the circumferential axis the maximum strain occurs close to the dent center.

- The dent shape has a significant influence on the strain values at and near the dented region. For the rectangular and dome dented pipes, the maximum strain occurs in the circumferential axis while for the sphere dented pipes the maximum strain occurs in the longitudinal axis.

- Having a large D/t ratio means that the pipe's wall thickness is very small. When this happens, the FE model becomes numerically unstable and the solution process terminates. However, further research is recommended to overcome this issue.

- As the D/t ratio increases, so do the strain values. This increase is much larger when the internal pressure is higher. This phenomenon occurs for both rectangular and spherical indented pipe specimens.

- The strain values increase as the internal pressure increases. This occurs for the rectangular and sphere indented specimens as shown in Figures 6.10 to 6.13.

- The location of the maximum strain for the rectangular dent in the longitudinal axis occurs away from the dent centre while the location of the maximum strain for the circumferential axis occur at the dent center for all internal pressures.

- The location of the maximum strain for the spherical dent in the longitudinal axis increases by 25 mm as the internal pressure increases while the location of the maximum strain for the circumferential axis has no apparent pattern.

- For the rectangular dented pipes, maximum strain values are observed in the circumferential axis while for the spherical dent, the maximum values occur in the longitudinal axis.

7.4 Recommendations for Future Studies

The study conducted provided more insight on the determination of the safety of a pipeline containing a plain dent. It also provided a way for future work to develop a guideline that could be used to evaluate the damage and determine if replacement is necessary. The following are some recommendations for future studies:

- Further research can enhance the FEM models by including different types of parameters that can in turn contribute to the development of the guideline.

- Perform more tests on sphere indented pipelines to better determine the behaviour and location of the maximum strains specifically for the circumferential axis.

- Carry out more experimental tests that include rock dents in order to better predict the effect on the pipelines.
- Conduct some constrained-dent test to be able to know the behavior of pipelines with such dents.

REFERENCES

1. Alexander, C. 1999. "Analysis of Dented Pipeline Considering Constrained and Unconstrained Dent Configurations." In 1999 Energy Sources Technology Conference & Exhibition, Sheraton Astrodome Hotel, Houston, Texas. http://www.chrisalexander.com/assetmanager/assets/1999%20Feb%20-%20Energy%20Sources%20Technology%20Conf%20Constrained%20and%20Unconstrained.pdf.

2. Alexander, C, and Kiefner, J. 1997. Final Report on Effects of Smooth and Rock Dents on Liquid Petroleum Pipelines: To the American Petroleum Institute, October 10, 1997. American Petroleum Institute.

3. American Petroleum Institute. 2007. Specification for Line Pipe, 44th Edition. 44th edition. American Petroleum Institute.

4. ASME. 2007. B31.8-2007: Gas Transmission Distribution Piping Systems. New York, NY, USA: ASME International.

5. ASTM E28.04 Subcommittee. 2013. "Test Methods for Tension Testing of Metallic Materials". ASTM International. http://enterprise.astm.org/filtrexx40.cgi?+REDLINE_PAGES/E8E8M.htm.

6. Baker, M. 2004a. "Dent Study". Delivery Order DTRS56-02-D-70036. Integrity Management Program. Office of Pipeline Safety.

7. Baker, M. 2004b. "Pipe Wrinkle Study". Delivery Order DTRS56-02-D-70036. Integrity Management Program. Office of Pipeline Safety.

8. Beller, M, Mattheck, C, and Zimmermann, J. 1991. "Stress Concentrations in Pipelines due to the Presence of Dents." In Proceedings of the First (1991) International Offshore and Polar Engineering Conference. Edinburgh, United Kingdom: The International Society of Offshore and Polar Engineers.

9. Cosham, A., and Hopkins, P. 2001. "A New Industry Document Detailing Best Practices in Pipeline Defect Assessment." In Fifth International Onshore Pipeline Conference Amsterdam, The Netherlands. http://www.penspenintegrity.com/downloads/virtual-library/industry-best-practice.pdf.

10. Cosham, A, and Hopkins, P. 2004. "The Effect of Dents in Pipelines—guidance in the Pipeline Defect Assessment Manual." International Journal of Pressure Vessels and Piping 81 (2) (February): 127–139. doi:10.1016/j.ijpvp.2003.11.004.

11. Flügge, Wilhelm. 1962. Stresses in Shells. Text Book, Springer-Verlag, Berlin, Germany.

12. Fowler, J. 1993. "Criteria For Dent Acceptability In Offshore Pipeline." In The Offshore Technology Conference, Houston, Texas, May, 1993. doi:10.4043/7311-MS. http://www.onepetro.org/mslib/servlet/onepetropreview?id=OTC-7311-MS.

13. El Sayed, A. 2013. "Oil and Gas Pipeline Design, Maintenance and Repair" Cairo University. Accessed on December 3rd, 2013. http://www.eng.cu.edu.eg/users/aelsayed/Part%2011%20Pipeline%20Rehabilitation%20and%20Repair%20Techniques.pdf.

14. Karamanos, Spyros, A., and Andreadakis, K. 2006. "Denting of Internally Pressurized Tubes under Lateral Loads." International Journal of Mechanical Sciences 48 (10) (October): 1080–1094. doi:10.1016/j.ijmecsci.2006.03.018.

15. Keating, P., and Hoffmann, R. 1997. "Fatigue Behavior of Dented Petroleum Pipelines". Technical Report DTRS56-95-C-0003. Texas A&M University: Office of Pipeline Safety.

16. Lancaster, E., and Palmer, S. 1996. "Strain Concentrations in Pressurized Dented Pipes." Proceedings of the Institution of Mechanical Engineers, Part E: Journal of Process Mechanical Engineering 210 (1) (February 1): 29–38. doi:10.1243/PIME_PROC_1996_210_290_02.

17. Lukasiewicz, S., Czyz, J., Sun, C., and Adeeb, S. 2006. "Calculation of Strains in Dents Based on High Resolution In-Line Caliper Survey" (January 1): 129–134. doi:10.1115/IPC2006-10101.

18. National Instruments Corporation. 1996. "LabVIEW® Demonstration Guide". Guide 321215A-01. Austin, TX.

19. Noronha, D., Martins, R., Jacob, B., and De Souza, E. 2010. "Procedures for the Strain Based Assessment of Pipeline Dents." International Journal of Pressure Vessels and Piping 87 (5): 254–265.

20. Ong, L., Soh, A., and Ong, J. 1992. "Experimental and Finite Element Investigation of a Local Dent on a Pressurized Pipe." The Journal of Strain Analysis for Engineering Design 27 (3) (July 1): 177–185. doi:10.1243/03093247V273177.

21. Pinheiro, B., and Pasqualino, I. 2008. "Stress Concentration Factors of Longitudinal and Transverse Plain Dents on Steel Pipelines" In the Proceedings of the 27th International Conference on Offshore Mechanics and Artic Engineering. Estoril, Portugal. ASME. doi:10.1115/OMAE2008-57836.

22. Rafi, A., 2011. "Structural Behaviour of Dented Pipelines". MASc. Thesis, Windsor: University of Windsor.

23. Rafi, A., Das, S., Ghaednia, H., Silva, J., Kania, R., Wang, R. 2012. "Revisiting ASME Strain-Based Dent Evaluation Criterion." Journal of Pressure Vessel Technology 134 (4) (July 27): 7 pages. doi:10.1115/1.4005890.

24. Rinehart, A., and Keating, B. 2007. "Stress Concentration Solution for a 2D Dent in an Internally Pressurized Cylinder." Journal of Engineering Mechanics 133 (7) (July): 792–800. doi:10.1061/(ASCE)0733-9399(2007)133:7(792).

25. Rosenfeld, M. 2001. "Proposed New Guidelines for ASME B31.8 on Assessment of Dents and Mechanical Damage". Topical Report GRI-01/0084. Des Plaines, IL: GRI.

26. Rosenfeld, M, Porter, P., and Cox, J. 1998. "Strain Estimation Using Vetco Deformation Tool Data." In International Pipeline Conference, 1:389–397.

27. Rosenfeld, M. 2002. "Factors to Consider When Evaluating Damage on Pipelines." Oil and Gas Journal 100 (37) (September 9): 9 pages.

28. Wu, Y., Zhang, P., and Wu, L. 2011. "Fatigue Life Calculation of the in-Service Dented Pipeline." Key Engineering Materials 467-469 (February): 1327–1332. doi:10.4028/www.scientific.net/KEM.467-469.1327.

VITA AUCTORIS

NAME: Jandark Oshana Jajo

PLACE OF BIRTH: Baghdad, Iraq

YEAR OF BIRTH: 1989

EDUCATION: Catholic Central High School, Windsor, ON, 2007

                          University of Windsor, B.A.Sc. Civil Engineering, Windsor, ON, 2011